THE HONG KONG
POLYTECHNIC UNIVERSITY
香港理工大學
Pao Yue-kong Library
包玉剛圖書館

Copyright Undertaking

This thesis is protected by copyright, with all rights reserved.

By reading and using the thesis, the reader understands and agrees to the following terms:

1. The reader will abide by the rules and legal ordinances governing copyright regarding the use of the thesis.

2. The reader will use the thesis for the purpose of research or private study only and not for distribution or further reproduction or any other purpose.

3. The reader agrees to indemnify and hold the University harmless from and against any loss, damage, cost, liability or expenses arising from copyright infringement or unauthorized usage.

CHARACTERIZATION OF THE OSTEOPROTECTIVE

FLAVAN-3-OLS FROM *RHIZOMA DRYNARIAE*

WONG KA CHUN

Ph.D

The Hong Kong Polytechnic University

2013

The Hong Kong Polytechnic University

Department of Applied Biology and Chemical Technology

Characterization of the Osteoprotective Flavan-3-ols from

Rhizoma Drynariae

WONG KA CHUN

A thesis submitted in partial fulfillment of the requirements

for the degree of Doctor of Philosophy

September 2012

CERTIFICATE OF ORIGINALITY

I hereby declare that this thesis is my own work and that, to the best of my knowledge and belief, it reproduces no material preciously published or written, nor material which has been accepted for the award of any other degree or diploma, except where due acknowledgement has been made in the text.

Signature

_____

WONG Ka Chun

Abstract

Rhizome of *Drynaria fortunei (Kunze) J. Sm.* (DF) is a traditional Chinese herbal medicine commonly used to manage bone disease. Recent studies suggested that flavan-3-ols are the active ingredients in DF as they could stimulate the growth of osteoblastic cells. However, the mechanisms of how flavan-3-ols act on bone remain unclear. Therefore, the present study aimed to characterize the effects of DF flavan-3-ols on bone mechanisms.

Synthetic flavan-3-ols were used in this study. Flavan-3-ols significantly increased the cell proliferation rate ($P<0.05$) of mature osteoblastic-like UMR-106 cells and these effects were blocked by estrogen receptor (ER) antagonist, ICI 182,780. Flavan-3-ols also increased the cell proliferation rate of estrogen sensitive human breast cancer MCF-7 cells significantly ($P<0.05$). Different flavan-3-ols could activate ER-α and ER-β mediated estrogen response element dependent transcription activities ($P<0.05$) differentially. Although the actions of flavan-3-ols were found to be ER mediated, there was not a direct binding between flavan-3-ols and ERs.

(-)-Epiafzelechin was selected for the further characterization as it could promote the proliferation and differentiation rate of UMR-106 cells. (-)-Epiafzelechin could increase the alkaline phosphatase activities ($P<0.05$) and extracellular matrix collagen level ($P<0.05$) but not calcium deposition in murine preosteoblastic MC3T3-E1 cells. It also significantly increased the Cbfa2/Runx2, collagen 1a1 and osteocalcin ($P<0.05$) mRNA expression in MC3T3-E1 cells. Furthermore, (-)-epiafzelechin decreased the cell viability of osteoclast precursor cells ($P<0.05$). It also decreased the number of tartrate resistance acid phosphatase (TRAP) positive

multinucleated osteoclastic cells and suppressed the TRAP activity under the induction of receptor activation of nuclear factor kappa-B ligand. These results suggested that (-)-epiafzelechin could promote osteoblasts differentiation and prevent osteoclasts maturation at the effective concentrations between 10nM and 1μM.

(-)-Epiafzelechin was further characterized in animal model. In order to determine the pharmacokinetic (PK) parameters of (-)-epiafzelechin in C57BL/6J mice model, a detection method for plasma (-)-epiafzelechin was established. The (-)-epiafzelechin in plasma samples were extracted from the plasma by liquid/liquid extraction and detected by the liquid chromatography coupled with mass spectrometric detectors. This detection method fulfilled the method validation requirements suggested by US food and drug administration and international conference on harmonization of technical requirements for registration of pharmaceuticals for human use, which could be used to quantify the (-)-epiafzelechin concentration in plasma.

The plasma concentration-time profile was used to determine the PK parameters of (-)-epiafzelechin. A single bolus intraperitoneal (i.p.) injection of (-)-epiafzelechin at 10mg/kg could rise the maximum plasma (-)-epiafzelechin concentration to 5.8mg/ml at 15 minutes after administration. From this profile, the elimination half-life of (-)-epiafzelechin was found to be 116 minutes. These results suggested that the plasma (-)-epiafzelechin level could be maintained at above 10nM for 10 hours after an i.p. injection of 10mg/kg (-)-epiafzelechin.

In summary, flavan-3-ols were found to exert estrogenic-like activities on bone cells. (-)-epiafzelechin was found to be one of the active ingredients in DF that could modulate the bone remodeling process. A bioanalytical method was successfully developed for quantifying the plasma (-)-epiafzelechin concentration. PK study indicated that (-)-epiafzelechin could be absorbed and maintained in mice plasma at the effective dose.

List of publications

1. Wong, K.C., Pang, W.Y., Wang, X.L., Mok, S.K., Lai, W.P., Chow, H.K., Leung, P.C., Yao, X.S. and Wong, M.S. (2013) "*Drynaria fortunei* derived total flavonoid fraction and isolated compounds exert oestrogen-like protective effects in bone" <u>British Journal of Nutrition</u> **10**, 1-11

2. Wong, M.S., Wong, K.C., Dong, X.L., Law, M.C. and Chan, T.H. (2012) "Flavan-3-ol isolated from rhizome of *Drynaria fortunei* (Junze) J. Sm. exerts osteoprotective effects via its actions on osteoblastogenesis and osteoclastogenesis." <u>The Journal of the Federation of American Societies for Experimental Biology</u> **26**, 373.3

3. Law, M.C., Wong, K.C., Pang, W.Y., Wong, M.S. and Chan, T.H. (2012) "Chemical synthesis and biological study of 4β-carboxymethyl-epiafzelechin acid, and osteoprotective compound from the rhizomes of *Drynaria fortunei*" <u>Medicine Chemistry Communication</u> **3(7)**, 801-806

4. Pang, W.Y., Wang, X.L., Wong, K.C., Leung, P.C., Yao, X.S. and Wong, M.S. (2012) "Total flavonoid fraction of *Rhizoma Drynaria* improves bone properties in ovariectomized mice and exerts estrogen-like activities in rat osteoblast-like (UMR-106) Cells." <u>Journal of Food and Drug Analysis</u> **20(1)**, 265-269

5. Wong, K.C., Dong, X.L., Law, M.C., Chan, T.H. and Wong, M.S. (2011) "Epiafzelechin found in *Drynaria fortunei* exerts osteoprotective effect on bone metabolism." <u>2011 International Conference on Food Factors, Taiwan</u> Poster Presentation P1-112

6. Wong, K.C., Law, M.C., Chan, T.H. and Wong, M.S. (2010) "CEA enantiomers exerts different effects on estrogen-sensitive bone and cancer cells" 2010 <u>American Society for Bone and Mineral Research Annual Meeting, ON, Canada</u> Poster Presentation MO0435

7. Wong, K.C., Law, M.C., Chan, T.H. and Wong, M.S. (2010) "A flavan-3-ol compound in *Drynaria fortunei* exerts estrogen-like activities in rat osteoblastic UMR 106 cells" <u>Progress in Nutrition</u> **12(1)**, 70-71

8. Wong, K.C., Qin, B. and Wong, M.S. (2010) "The osteoprotective effects of green tea *in vitro* study" <u>2010 Hong Kong Macau Postgraduate Symposium Chinese Medicine, Hong Kong</u> Abstract

9. Wong, K.C., Wong, M.S. (2009) "The osteoprotective effects of purified *Drynaria fortunei* compound in vitro study" <u>2009 Hong Kong Macau Postgraduate Symposium Chinese Medicine</u> Abstract

Thank you Steve, Eddy, ChongTze, Peter and all my friends in the laboratories, we have so much fun here although we are sometime frustrated by the experimental result. I cherish the time that we could think of many crazy ideas.

It would also be the great time to thank you all the technical supporting staff in ABCT and CAF for their kindly assistance.

Last but not least, I would like to express my gratitude to my beloved family members. Without their love, care and support, I would not be able to complete my study.

Kenneth Wong

Table of content

4   CHARACTERIZATION OF SELECTED FLAVAN-3-OL ON OSTEOBLASTS AND OSTEOCLASTS FUNCTIONS 98

List of Figures

List of tables

Abbreviations

[3H]E2	[^{3}H]-estradiol
ACP	Acid phosphatase
ADME	Absorption, distribution, metabolism and excretion
AUC	Area under the curve
BMD	Bone mineral density
BMP-2	Bone morphogenetic protein-2
BSP	Bone sialoprotein
CAM	Complementary and alternative treatment
Cbfa1	Core-binding factor subunit alpha-1
CI	Chemical ionization
CL	Clearance
C_{max}	Maximum concentration
Cpd A	4β-Carboxymethyl-epiafzelechin acid
Cpd B	4β-Carboxymethyl-epiafzelechin lactone
Cpd C1	(-)-epiafzelechin
Cpd C2	(+)-epiafzelechin
Cpd D1	(+)-afzelechin
Cpd D2	(-)-afzelechin
Cpd F1	(2R) 5,7-dihydroxy-2-(4-hydroxyphenyl)chroman-3-one
Cpd F2	(2S) 5,7-dihydroxy-2-(4-hydroxyphenyl)chroman-3-one
CTA	Clinical trial application
DCI	Desorption chemical ionization
DEI	Desorption electron ionization
DF	*Rhizoma Drynariae* or Rhizome of *Drynaria fortunei (Kunze) J. Smith.*
DMEM	Dulbecco's modified eagle medium
DMSO	Dimethyl sulfoxide
DXA	Dual-energy x-ray absorptiometry
E2	17β-Estradiol
EC	Epicatechin
ECM	Extracellular matrix
EGC	Epigallocatechin
EGCG	Epigallocatechin gallate

EI	Electron ionization
ERE	Estrogen response element
ERK	Extracellular signal-regulated kinase
ESI	Electrospray ionization
FBS	Fetal bovine serum
FDA	Food and drug administration
FRAX	Fracture predication algorithm
GC	Gas chromatography
HAP	Hydroxylapatite
HPLC	High performance liquid chromatography
HRT	Hormone replacement therapy
I.P.	Intraperitoneal
I.V.	Intravenous
ICH	International conference on the harmonization of technical requirements for the registration of pharmaceuticals for human Use
IND	Investigational new drug
IR	Infra-red
IT	Ion trap
LC	Liquid chromatography
LLE	Liquid/liquid extraction
LLOD	Lower limit of quantification
LOD	Limit of detection
LOQ	Limit of quantification
m/z	Mass to charge
MALDI	Matrix-assisted laser desorption/ionization
MS	Mass spectrometer
MTS	3-(4,5-dimethylthiazol-2-yl)-5- (3-carboxymethoxyphenyl)-2-(4-sulfophenyl)- 2H-tetrazolium
NCPs	Non-collagen proteins
NMR	Nuclear magnetic resonance
MSC	Mesenchymal stem cells
NOF	National osteoporosis foundation
Ob	Osteoblast
Oc	Osteoclast

OCN	Osteocalcin
OPG	Osteoprotegerin
Osx	Osterix
PBPK	Physiologically-based pharmacokinetic
PGE2	Prostaglandins E2
PK	Pharmacokinetic
PNP	Para-nitrophenol
p-NPP	p-nitrophenylphosphate
PTH	Parathyroid hormone
Q	Quadrupole
RANK	Nuclear factor kappa-B
RANKL	Nuclear factor kappa-B ligand
RBA	Receptor binding affinity
Runx2	Runt-related transcription factor 2
S/N	Signal to noise
SEM	Standard error mean
SERM	Selective estrogen-receptor modulators
SIM	Selected ion mode
SPE	Solid phase extraction
SRM	Selected reaction monitoring
$T_{1/2}$	Elimination half-life
TCM	Traditional Chinese medicine
TIC	Total ion count
T_{max}	Maximum concentration time
TOF	Time of flight
TRAP	Tartarate resistant acid phosphtase
WHO	World health organization
WLSLR	Weighting least squares linear regression

1 Introduction:

1.1   Background

1.1.1   Postmenopausal Osteoporosis

Postmenopausal osteoporosis is a skeletal disorder characterized by low bone mass and deterioration of bone architecture. It specifies the occurrence of osteoporosis in women after menopause. The cause of postmenopausal osteoporosis is mainly due to estrogen deficiency. The osteoporotic bone in osteoporosis patients cannot withstand high pressure and easily undergo fractures (Jean-Yves Reginster 2006). Wrist, spine and hip are the common fracture sites of osteoporosis patients. The consequence of spine fracture will lead to back pain while spine fracture will lead to immobility of patients. High morbidity and mortality rate are observed in patients with multiple skeletal sites fractures.

1.1.2   Prevalence of Osteoporosis

Osteoporosis mainly affects the elderly. The prevalence of osteoporosis rises from 6% in 50 year-old to 50% in 80 year-old. It is estimated that 50% of women and 20% of men over 50 year-old are suffered from osteoporosis-related fractures (Rahmani 2009). The continuous aging of population is likely to increase the incidence rate of osteoporosis all over the world. In developed countries like US, it is estimated that the population over 50 years of age will be increased by 60% between 2000 and 2025. The direct medical cost of osteoporosis in US in year 2005 is estimated at US$13.7-20.3 billion dollars and the economic burden on osteoporosis medication is still increasing (Burge, Dawson-Hughes et al. 2007).

1.1.3 Diagnosis of Postmenopausal Osteoporosis

Osteoporosis is a silent disease as the symptoms always appear after a bone fracture. The incidence rate of osteoporosis can be predicted by medical examination of bone mineral density (BMD) by dual-energy x-ray absorptiometry (DXA) on corresponding high fracture risk sites. According to the world health organization (WHO), an individual having a T-score less than -2.5 (compared with young control) is diagnosed as osteoporosis (Siris 2012). However, DXA only identifies a small component of fracture risk. In fact, the risk factors such as diseases, medicine taking, smoking, alcohol consuming, low body mass index and previous fracture history are all contributed to the risks of bone fracture. Recently, national osteoporosis foundation (NOF), WHO and University of Sheffield develop a fracture predication algorithm (FRAX) to calculate the potential fracture risk of individual. FRAX can calculate the 10 years absolute fracture risks from a questionnaire. *Siminoski* and colleagues develop another tool to predict the 10 years osteoporosis related fracture risks. Both FRAX and *Siminoski's* method are validated in clinical cohorts (Rahmani 2009).

Beside BMD, biochemical markers such as alkaline phosphatase, serum calcium, serum creatinine and type I collagen reflecting the bone turnover rate are also used to predict the prevalence of osteoporosis (Garnero 2009). Recent studies also suggested the use of cross-linked telopeptides of type I collagen N-terminal or C-terminal as a more sensitive and specific bone turnover marker. These markers are useful for evaluating the efficacy of osteoporosis therapy (Eastell and Hannon 2008). With these methods, the fracture risk can be predicted in a more convenient and accurate way.

1.1.4 Management of Postmenopausal Osteoporosis

Regular exercise, adequate calcium and vitamin D intake as well as to prevent smoking and alcohol drinking are important to prevent osteoporosis. Individuals with low BMD value reflected in T-score or high fracture risk evaluated from FRAX require the management of osteoporosis (Janis 2010; Siris 2012). Different types of therapeutic agents are available for patients with high fracture risk.

Hormone replacement therapy (HRT) replenishes the estrogen for postmenopausal women. Estrogen could inhibit the bone turnover rate by affecting the osteoclasts and osteoblasts activity under cellular level (Liu and Lebrun 2006). HRT is very effective to reduce bone fracture risk but the non-specific actions of estrogen also increase the risk of breast cancer and stroke. Therefore, HRT is continuously replacing by other therapies with fewer side effects (Glasier 2006).

Selective Estrogen-Receptor Modulators (SERMs) can also be used to manage postmenopausal osteoporosis (Avioli 1999). They selectively act as an agonist in some estrogen sensitive tissues but act as an antagonist in the others. These properties make SERM as an ideal therapeutic agent for managing osteoporosis with fewer side effects. Tamoxifen, the first generation of SERMs, could act as an agonist on liver cells, bone cells and uterine cells but act as an antagonist on breast cells (Avioli 1999). It could increase the BMD without the risk of promoting breast cancer. However, it could still stimulate the growth of endometrium cells (Dutertre and Smith 2000). Raloxifene, a second generation of SERMs, could increase BMD without stimulating the endometrium cells (Jordan and Morrow 1999). However, raloxifene is associated with venous thromboembolism. Currently, more SERMs

such as lasofoxifene, arzoxifene and bazedoxifene are being investigated for their potential osteoprotective effects and side effects on postmenopausal osteoporosis patients (de Villiers 2009; Kendler, Palacios et al. 2012).

Apart from estrogenic compounds, therapeutic agents such as bisphosophonates, calcitonin and teriparatide can also be used to manage osteoporosis. Bisphosphonates such as alendronate and risedronate are anti-resorptive drugs (Hofstetter, Gamsjaeger et al. 2012). They bind on bone surface and reduce the activities of osteoclasts. Bisphosphonates cause side effects such as gastrointestinal intolerance, esophageal ulceration and atrial fibrillation. Calcitonin is a peptide secreted by C cells of the thyroid (Silverman 2001). It could inhibit osteoclastic functions to prevent bone resorption, promote the mineralization of skeletal bone and prevent calcium loss from skeleton under calcium stress. Patient with calcitonin allergy should be avoided from this therapy. Calcitonin causes some side effects such as nausea, skin redness and flushing (Chesnut 2008). Teriparatide is a synthetic recombinant hormone with 34 amino acids of human parathyroid hormone (PTH) (Berg 2003). It could promote the bone formation. However, the cost of synthesizing this recombinant hormone is very high. In addition, some patients may suffer from nausea, headache, leg cramps and mild hypercalcemia during teriparatide treatment (Rahmani 2009).

Use of therapeutic agents can minimize the fracture risks of osteoporosis patients (Boonen, Body et al. 2005). However, the potential side effects and high treatment costs hinder the use of these treatments as the first line therapy. Recently, traditional Chinese medicine (TCM) is being explored in a complementary and alternative medicine (CAM) for managing osteoporosis. It is hope that TCM could manage osteoporosis with a lower treatment cost and fewer side effects (Yuan 2011).

1.1.5 Traditional Chinese Medicine and Osteoporosis

TCM is the medical knowledge from ancient China based on the experiences of Chinese people fight against disease over thousands of years. In the past, the medical knowledge was localized in certain area only. This limited the development of TCM in old China. In late 1950's, more Chinese medical textbooks were being published in China. They integrated the TCM theory in the health care system in China with clinical trials and began the modernization of TCM in the Chinese society (Scheid 2007).

Base on the theory from the TCM textbooks, the cause of disease is due to the imbalance of body components, Yin and Yang. Yin and Yang act opposite to each other in the human body. They explain the histological structure and physiological functions of the human body as well as the development of diseases (Yuan 2011). TCM describes diseases and treatments in a different way from western medicine. In the old TCM theory, there was not a disease called "osteoporosis". Osteoporosis was treated as a bone disease in old days. The major cause of bone disease in TCM is due to the weakness of kidney which is also known as "*kidney-deficiency*". Therefore, medicine with *kidney tonifying* properties can be used to supply essence to the kidneys and relief the bone problems (Yanquan 2003).

1.1.6 Phytoestrogen

As mentioned, HRT using estrogen is an effective treatment for osteoporosis but it does cause side effects (Dietel 2010). Therefore, people are looking for alternative osteoporosis treatments. Recent findings suggested that some polypheonic compounds found in plant could exert estrogen-like activities. These compounds are named as phytoestrogen (Vaya and Tamir 2004). Phytoestrogens are believed to have beneficial effects on estrogen deficiency condition like menopause. They could mimic estrogen response by binding to ER subtypes with different affinities (Harris, Bapat et al. 2002) and act like a natural SERM. One of the most representing phytoestrogens is soybean genistein. Genistein could reduce the risk of breast cancer, bone loss and cardiovascular disease (Dixon and Ferreira 2002). Recent findings also suggested that some *kidney tonifying* herbs contain phytoestrogens that could exert bone protective effects (Zhang 2006).

1.2 *Chinese Medicine*

1.2.1 **Rhizoma Drynariae**

Rhizoma Drynariae (DF) is the rhizome of *Drynaria fortunei* (Kunze) J. Smith. It is a common bone healing herbal medicine used in TCM with long history. The name of DF in Chinese is "Gu Sui Bu" which means healing of fractured bone. In TCM theory, DF replenishes *kidney deficiency* which could treat weak low back and knees as well as painful teeth and bleeding (Bensky 2004). DF was firstly described in *Tang* Dynasty (618-907 CE) when Emperor Li and his Queen went out for hunting (Preast 2010). It was also described in Kempo, a Japanese herbal medicine, to manage bone diseases for over thousands of years (Rister 1999). Apart from the historical records, the bone healing properties of DF have been studied extensively by different research groups recently.

Sun and et al.(2002) found that DF extract could increase alkaline phosphatase (ALP) activities in rat osteoblastic cells. DF increased the skeletal anabolic agent prostaglandins (PGE_2) and osteoclast adhesion inhibition marker acid phosphatase (ACP) activity in the alveolar mononuclear cells osteoblasts co-culture system (Sun, Lin et al. 2002). *Jeong and et al* reported that DF could increase the proliferation and differentiation rate of pre-osteoblast cells (Jeong, Lee et al. 2004). DF also increased the collagen synthesis related enzyme prolyl hydroxylase (Jeong, Lee et al. 2005). *Jeong and et al* (2004) also reported that DF could increase mineralization and the mRNA expression of bone morphogenetic protein-2 (BMP-2) and type I collagen in MC3T3-E1 cells (Jeong, Lee et al. 2004).

Previous study in our group demonstrated that the total flavanoids fraction of DF (TFDF) treatment could increase the distal femur BMD, trabecular BMD and total cross-sectional area of bone in ovariectomized (OVX) mice significantly. TFDF could also increase the cell proliferation, cell differentiation rate and the gene expression ratio of osteoprotegerin (OPG) to receptor activator of nuclear factor kappa-B ligand (RANKL) in osteoblastic-like UMR 106 cells (Pang 2012). These effects were suggested to be ER dependent which could be blocked by ER antagonist (Pang 2010).

The modern approaches to study herbal medicine involve the identification and isolation of active compounds in herbal medicine. The bioactive fraction of the herbal medicine usually contains a series of compounds with similar structures and chemical properties. They can be separated into single compound by column chromatography for further chemical identifications and biological activities characterization.

1.2.2 Chemical constitutions of DF

DF composed of different compounds such as triterpenes, flavonoids and sugars (Bensky 2004). Our previous study suggested that the active ingredients are presence in the total flavanoids fraction of DF. This fraction contains a well known bone protective compound – naringin (Pang 2010). Naringin is a well characterized flavanoid that has been studied extensively to demonstrate its protective effects on bones (Xie 2004),

Chen and et al. found that naringin could stimulate the proliferation and differentiation of pre-osteoblast MC3T3-E1 cell line (Chen, Lei et al. 2011). *Wong*

and et al. found that naringin could increase the new bone formation in collagen matrix of rabbits (Wong and Rabie 2006). Our previous study also demonstrated that naringin could improve bone properties in OVX mice as well as stimulate the growth and development of osteoblastic-like UMR-106 cells in an ER dependent manner (Pang, Wang et al. 2010). Pharmacokinetic (pK) study of naringin were also reported by *Hung and et al.* to confirm the bio-availability of naringin in rabbits plasma after oral or intravenous (i.v.) administrations (Hsiu, Huang et al. 2002). *Li and et al.* demonstrated the oral administration of DF extract to rats could rise the naringin level in rat plasma (Li Xiao-Hong 2010).

Apart from naringin, DF flavonoid fraction contains other active compounds. *Chang et al.* isolated eight bioactivity flavan-3-ols from DF through bioassay-guided separation and isolation. These compounds include **1** (-)-epiafzelechin, **2** (-)-epiafzelechin 3-O-β-D-allopyranoside, **3** (-)-epiafzelechin-3-O-(6''acetyl)-β-D-allopyranoside, **4** 4β-Carboxymethyl-(-)-epiafzelechin methyl ester, **5** 4β-Carboxymethyl-(-)-epiafzelechin sodium salt, **6** naringin, **7** (-)-epiafzelechin-(4β→8)-4βcarboxymethylepiafzelechin and **8** (-)-epiafzelechin-(4β→8, 2β→O→7)--epiafzelechin-(4β→8)-epiafzelechin. These compounds could promote the growth of osteoblast-like ROS 17/2.8 cells (Chang 2003). *Wang et al.* (2008) isolated another five flavonoid aglycones from DF including **9** naringenin, **10** kurarinone, **11** kushennol F, **12** xanthogalenol and **13** sophoraflavone G. They could increase the cell differentiation rate in UMR-106 cells (Wang, Zhen et al. 2011). Another paper from *Wang et al.* (2008) had reported other DF isolated compounds including **14** kaempferol,3-*O*-β-D-glucopyranoside-7-*O*-α-L-arabinofuranoside, **15** (2S)-5,7,3',5'-tetrahydroxy-flavonone 7-*O*-hesperidoside, **16** (2S)-5,7,3',5'-tetrahydroxy-flavonone

7-*O*-glucopyranosyl, **17** kaempferol,3-*O*-α-L-rhamnosyl-7-*O*-β-D-glucoside, **18** luteolin-7-*O*-β-D-neohesperidoside, **19** 5,7-dihydroxychromone-7-*O*-β-D-glucopyranoside, maltol glucoside, **20** 4H-1-benzopyran-4-one,7-[[2-*O*- (6-deoxy-α-L-mannopyranosyl)-β-D-glucopyranosyl]oxy]-5-hydroxy and **21** (-)-epiacatechin but lacking the biological activity data (Wang, Wang et al. 2008). *Liang and et al.* (2011) also reported the isolation of six flavan-3-ols including monomer **22** 4a-carboxymethyl-(+)-catechin methyl ester, monomer flavan-3-ol glycosides, **23** (+)-afzelechin-3-O-b-allopyranoside and **24** (+)-afzelechin-6-C-b-glucopyranoside, dimer **25** (-)-epiafzelechin-(4b β 8)-4b-carboxymethyl-(-)-epicatechin methyl ester and **26** (-)-epiafzelechin-(4b β 8)-4a-carboxymethyl-(-)epiafzelechin ethyl ester, and trimer **27** (-)-epiafzelechin-(4b β 8)-(-)-epiafzelechin-(4b β 8)-4b-carboxymethyl-(-)-epiafzelechin methyl ester (Liang, Ye et al. 2011). Again, the biological activity of these compounds was not reported.

More flavan-3-ols are being isolated from DF with newly developed separation methods. These flavan-3-ols are found to be active in bone cells. These results suggested that these flavan-3-ols might contribute to the bone protective effects of DF. However, the mechanisms of how they act on bone as well as their bioavailability in the body are still not known. A further investigation of these potential bone anabolic candidates found in DF could provide more information on how they could be used to manage postmenopausal osteoporosis. The current study of the osteoprotective effects of flavan-3-ols can be based on the knowledge of flavan-3-ols and the current understanding of bone biology.

1.2.3   Flavan-3-ols

Flavan-3-ols belong to the family of flavanoids. They share a 2-phenylbenzopyran structure (**Figure 1.1**) with hydroxyl group on B ring of carbon number 3. Beverages, fruits, vegetables, herbal medicine and dairy products contain flavan-3-ols. It is believed that the role of flavan-3-ols in plants is related to their defensive effects on bacteria, fungi and insects. Flavan-3-ols are having different beneficial effects to the human body such as anti-oxidative, anti-cancer, metal chelating activity, bone protective effects and cardiovascular system protective effects (Aron and Kennedy 2008).

1.2.3.1   <u>Tea catechins</u>

Catechins found in green tea (**Figure 1.2**) belong to the class of flavan-3-ols. Epigallocatechin gallate (EGCG), epigallocatechin (EGC), gallocatechin(GC), epicatechin(EC) and catechin(C) are the common catechins. They have long been studied in various biological studies. Recent findings suggested that catechins could promote the ALP activities and calcium deposition in primary human mesenchymal stem cell. These actions might involve the deactivation of extracellular signal-regulated kinase (ERK) (Wei, Tsai et al. 2011). *C.H. Ko and et al.* (2009) also reported that gallocatechin could stimulate ALP activities of osteoblastic like UMR-106 cell line. Another study suggested that the actions of catechins were ER dependent (Goodin, Fertuck et al. 2002). Taken the biological studies of DF and green tea flavan-3-ols together, compounds with flavan-3-ols structure are likely to exert protective effects on bones.

R3'

OR4'

HO

R6

R5

R4

R3

R5'

Structure of flavanoids

3'

2'   4'

8   B

7   5'

A   C   6'

6   3

5   4

2-phenylbenzopyrans
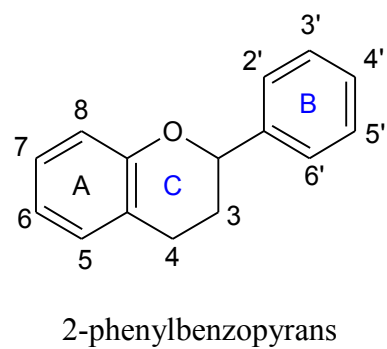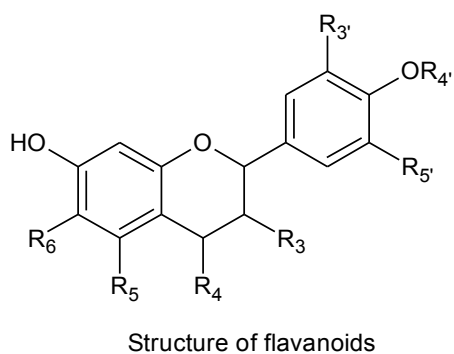
Figure 1.1 General flavanoid structure

OH

OH

HO

OH

OH

OH

(-)-Epigallocatechin

OH

OH

HO

OH

OH

OH

(+)-Gallocatechin

OH

HO

OH

OH

OH

(-)-Epicatechin

OH

HO

OH

OH

OH
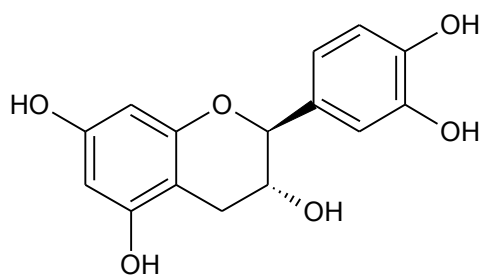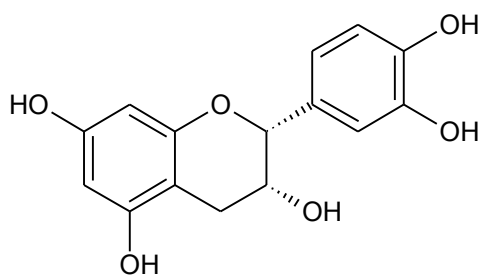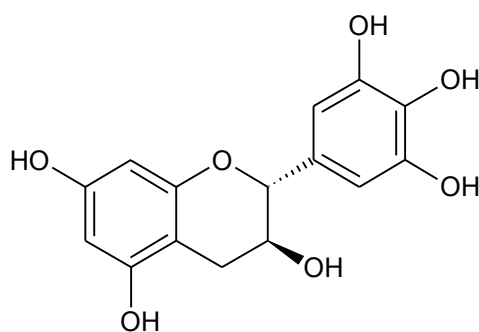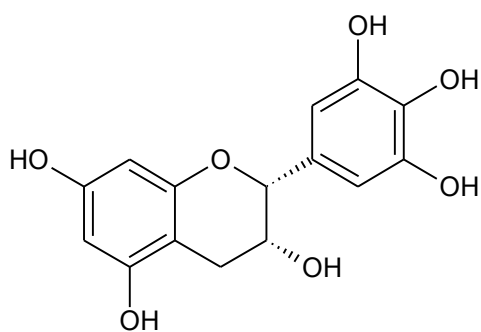
(-)-Catechin

Figure 1.2 Structures of catechin

1.2.3.2 <u>Synthetic flavan-3-ols</u>

The yield of flavan-3-ols from natural source is limited. For example, the yield of **5**
4β-Carboxymethyl-(-)-epiafzelechin sodium salt and **1** (-)-epiafzelechin are 12.5mg
and 90mg, respectively, from 6kg of DF raw herbs (Chang, Lee et al. 2003). In
addition, the isolation of natural flavan-3-ols from DF is difficult because these
compounds are having a similar structure. Their physical and chemical properties are
similar to each other. To obtain adequate amount of high purity flavan-3-ols for
biological characterization, flavan-3-ols are chemically synthesized by Prof. Chan's
research group in according to the protocol published by *Wan and Chan* (Wan and
Chan 2004). The chemical synthesis pathway of flavan-3-ols can be modified to
produce flavan-3-ol analogs for structure-activity study as well as to make it as a pro-
drug to increase the bioavailability and stability inside the body (Landis-Piwowar,
Huo et al. 2007).

Eight flavan-3-ols compounds are chemically synthesized **(Figure 1.3 & 1.4)** in according to the synthesis pathway sketched on **figure 3.1**. Their purities are verified by liquid chromatography (LC) while their structures are confirmed by infrared (IR) spectroscopy and nuclear magnetic resonance (NMR). Compound A is a racemic mixture with a similar structure to **5** 4β-Carboxymethyl-(-)-epiafzelechin sodium salt found in DF. The only difference is the replacement of sodium by hydrogen. Compound B is the precursor compound in synthesizing compound A where the functional groups in R3 and R4 formed a ring structure. Compound C1 is (-)-epiafzelechin. It is a stereospecific compound with less hydroxyl group on the R5' position when compared to epicatechin (EC). Compound D1 **(2R, 3S)** is having the same structure to compound C1 **(2R, 3R)** with different stereochemistry. The hydroxyl group at R3 of Compound F1 **(2R)** is oxidized to form a carbonyl group. Compound C2 **(2S, 3S)**, D2 **(2S, 3S)** and F2 **(2S)** are the diastereomers of C1 **(2R, 3R)**, D1 **(2R, 3S)** and F1 **(2R)**, respectively **(Figure 1.4)**. For example, the function groups of R3 and R4 position in C1 are pointing toward the paper while the function groups of R3 and R4 position of C2 are pointing outward.
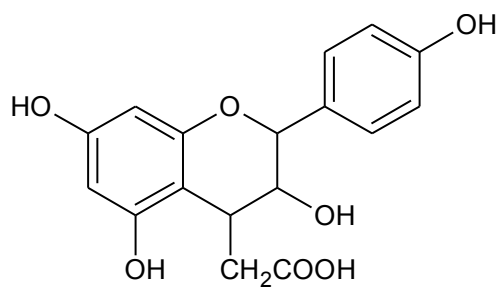
Compound A

4β-Carboxymethyl-epiafzelechin acid
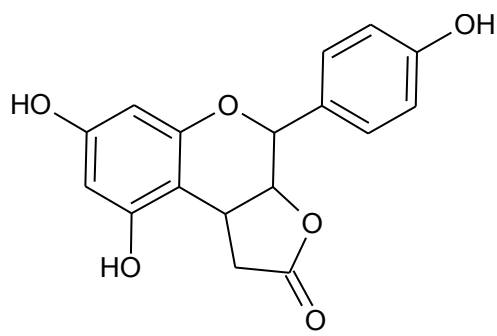
Compound B

4β-Carboxymethyl-epiafzelechin lactone
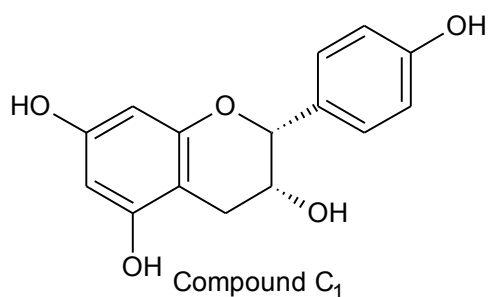
Compound C$_1$

(-)-epiafzelechin
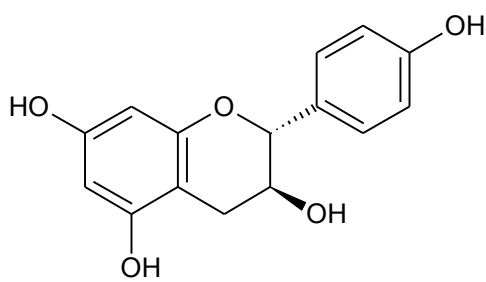
Compound D$_1$
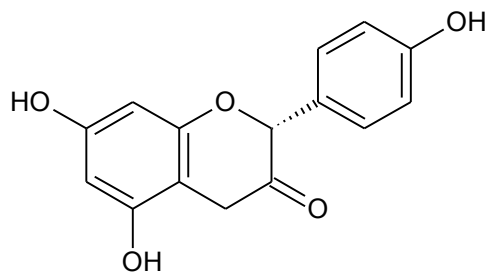
(+)-afzelechin

Compound F$_1$

(2R) 5,7-dihydroxy-2-(4-hydroxyphenyl)chroman-3-one

Figure 1.3 Structures of synthetic flavan-3-ols
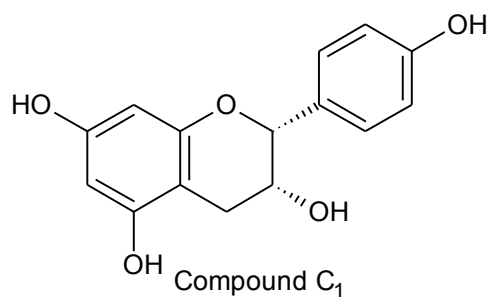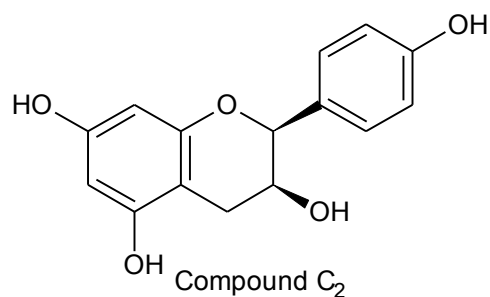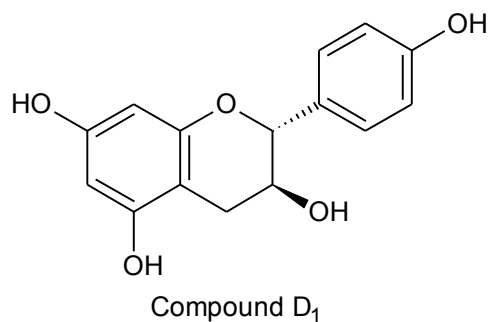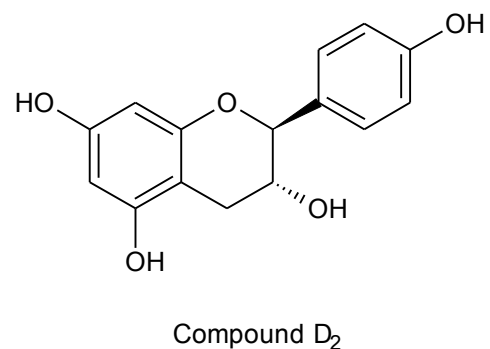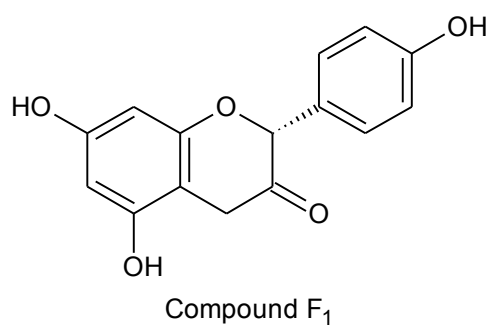
Compound C₁

(-)-epiafzelechin

Compound C₂

(+)-epiafzelechin

Compound D₁

(+)-afzelechin

Compound D₂

(-)-afzelechin

Compound F₁

(2R) 5,7-dihydroxy-2-(4-hydroxyphenyl)chroman-3-one

Compound F₂
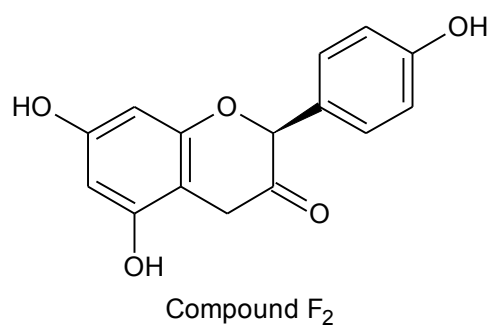
(2S) 5,7-dihydroxy-2-(4-hydroxyphenyl)chroman-3-one

Figure 1.4 Structures of flavan-3-ols diasteroisomers

1.2.4 Biological studies of flavan-3-ols

Eight synthetic flavan-3-ols with different structure or stereochemistry are used in this study. However, it is not possible to characterize all of them extensively. Therefore, it is necessary to narrow down the number of compounds by selecting a candidate for further investigation. The drug development process provides some ideas for the current study of flavan-3-ols.

1.2.4.1 Drug development

A typical drug development process includes drug discovery, preclinical development, clinical development and manufacturing (Lee 2002). A general flow of drug development is illustrated in **figure 1.5**. The current study of flavan-3-ols applies the flow of drug development mainly in the drug discovery and preclinical development stage.

Drug discovery involves the finding of a novel lead candidate from natural source or drug library with suitable pharmaceutical properties in terms of efficacy, bioavailability and toxicity studies. It highly depends on high throughput screening assays to evaluate the activities of the compounds.

Preclinical development focuses on the process research, formulation, metabolism and toxicity studies required for fulfilling the investigational new drug (IND) and clinical trial application (CTA) suggested by FDA (Lee 2002). Animal toxicology and pharmacokinetic studies provide preliminary data to determine the doses and the safety monitoring necessary for further study. A bioanalytical method development is included for the absorption, distribution, metabolism and excretion (ADME) evaluation in pharmacokinetic study.
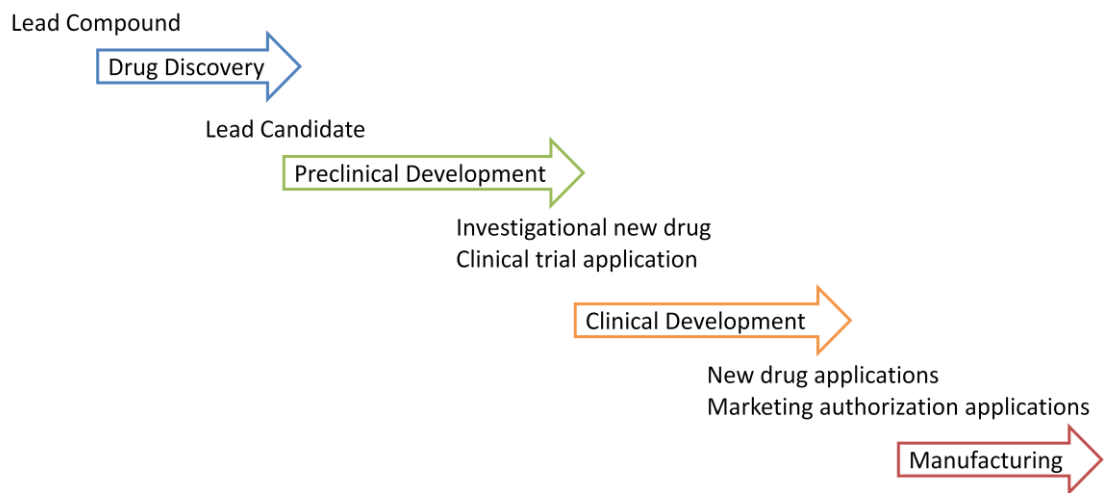
Figure 1.5 Drug development pipeline

The typical drug development contains four components, drug discovery, preclinical development, clinical development and manufacturing (adapted and modified from Courtesy of Milestone Development Services, Newtown, Pa., USA)

1.2.5 Strategies for studying flavan-3-ols

The study of flavan-3-ols can be started with a high throughput *in vitro* screening platform. This screening platform can be used to evaluate their effects on bone as well as their estrogen-like properties. The use of screening platform provides a rapid way to evaluate the biological activities of flavan-3-ols. A rat osteoblastic-like UMR-106 cell line can be used to determine the actions of flavan-3-ols on bone formation. Meanwhile, the estrogenic-like activities can be determined by using human breast carcinoma MCF-7 cell. Based on these results, one candidate will be selected for further characterization. The bone protective effects of the selected candidate can be characterized in the bone remodeling process. Murine pre-osteoblastic MC3T3-E1 cell line and murine leukemia monocyte RAW264.7 cell line can be used to evaluate the biological effects of flavan-3-ol candidate on bone formation and bone resorption, respectively. These results will be used to evaluate the *in vitro* efficacy of flavan-3-ols. The characterization of flavan-3-ols can be extended to *in vivo* study. A bioanalytical method can be developed for determining the bioavailability of selected candidate in the animal body. This detection method can be used to construct the pharmacokinetic (PK) profile of the selected candidate in animal. This PK test can provide dosing information for further *in vivo* efficacy assessment.

This study will be mainly relied on experimental biology assays performed in laboratory. Established cell lines and animal strains will be obtained from the same source to minimize the biological variation. The environmental conditions will also be controlled to reduce the influence from the external factors, and therefore a small sample size number is used in experimental biological research. In the *in vitro* part, three independent experiments (n=3) will be carried out for each assay. In the *in vivo*

part, the PK study will use a larger sample size (n=5) to minimize error from the biological variation between different animals. The results obtained will be used to estimate the true population value and therefore, the standard error mean (SEM) will be used to express the inferential error in the data presentation.

In fact, a larger sample number is always preferred in estimating the true population values which makes the prediction more precise (Cumming, Fidler et al. 2007). However, in biological assays, there should be a balance between repeating the same experiment many times with the same source of cells and carrying out another experiment with a different cell line. The effects might sometime be different from cell to cell and hence it is also worthy to explore these effects in different cells.

1.3 *Bone biology*

Bone is a hard and rigid tissue formed by inorganic salts and organic matrix. It is a part of the tissue in skeletal system which maintains the body shape, protects soft tissues, provides framework for bone marrow and transmits muscular contraction force for movement. It also acts as a mineral bank for regulating the extracellular fluid composition. Bone tissue can be adapted to the exterior environment by continuously changing in structure, mass, shape and compositions (Deng 2005). Bone can be described in anatomy and histology level.

1.3.1 Skeletal Anatomy (Organ)

Bone is composed of organic matrix (20-40%), inorganic mineral (50-70%), cellular elements (5-10%) and lipids (3%). The major composition of organic matrix is type I collagen with some types III, V and X collagens. About 10% of non-collagen proteins (NCPs) are found in the organic matrix (Deng 2005). NCPs such as bone sialoprotein (BSP) and osteocalcin (OCN) are only found in skeleton which can be used as the biochemical endpoints for detecting the bone turnover rate (Calvo, Eyre et al. 1996). Hydroxyapatite $[3Ca_3(PO_4)_2 \cdot (OH)_2]$ is the dominate compound in the inorganic mineral composite. It deposits onto the collagen fibers to provide a mechanical rigidity for high loading capacity (Hadjidakis and Androulakis 2006). Also, it contributes to the release of calcium, phosphate or magnesium ions for maintaining the mineral homeostasis of the body.

Bones are classified into cortical bone and trabecular bone. They contribute to 80% and 20% of adult skeleton, respectively. Cortical bone is compact and dense. It has a slower turnover rate. It supports and protects the body. Trabecular bone is elastic. It

has a higher turnover rate. It supports the body and fulfills the homeostatic demands of the body (Deng 2005).

1.3.2 Skeletal Histology (Tissue)

1.3.2.1 Osteoclasts

Osteoclasts are derived from granulocyte-macrophage colony-forming unit (GM-CFU). They express high level of lysosomal enzymes such as tartrate-resistant acid phosphatase (TRAP) and cathepsin K for bone resorption. The resorption process involves the binding of osteoclasts integrin protein on the surface protein of bone matrix. This cytoskeletal reorganization is activated by alpha v beta 3 integrin binding. The adhesion formed between the bone matrix and osteoclast is called podosomes. The continual assembly and disassembly of podosome facilitates the osteoclasts movement on the bone matrix. Osteoclasts digest the bone by removing the interlinking collagen and mobilizing the hydroxyapatite crystals. This process is regulated by different agents such as receptor activator of nuclear factor-κB ligand (RANKL), calcitonin, parathyroid hormone (PTH), 1,25(OH)2 vitamin D3, insulin, IGF-1, interleukin (IL) 1 and IL 6 (Kalervo Vaananen H 2006).

1.3.2.2 Osteoblasts

Osteoblasts are originated from multipotent mesenchymal stem cells (MSCs). The differentiation of osteoblasts from MSCs requires the runt-related transcription factor-2 (Runx2) and osterix (Osx). Osteoblasts are responsible for the bone matrix formation. They synthesize collagen to form osteoid and calcify osteoid to form bone matrix. Active osteoblasts express high level of ALP activity, type I collagen protein and NCPs. Osteoblasts are able to produce autocrine regulators like insulin-like

growth factors (IGF), platelet-derived growth factor (PDGF), transforming growth factor-beta (TGF-β) and bone morphogenetic proteins (BMP). They are regulated by PTH, PTH-related protein, thyroid hormone, growth hormone, insulin, progesterone, prolactin, estrogen and androgen with the expression of corresponding receptors. Osteoblasts also secret a regulator called osteoprotegerin (OPG) which could inhibit the formation of mature osteoclastic (Deng 2005).

1.3.2.3 Osteocytes

Osteocytes are the mature osteoblasts inside the bone matrix. Osteocytes have a smaller cell size and fewer proteins expression when compared with osteoblasts. They embed into the bone matrix during bone formation with losing of organelles and forming a network of thin canaliculi permeating through the bone matrix. Osteocytes are likely to response to the tissue strain and able to enhance bone remodeling activity (Klein-Nulend 2006).

1.3.3 Bone Remodeling and regulations

1.3.3.1 Bone remodeling

Bone is a living organ which undergoes remodeling throughout the life. Osteoclasts and osteoblasts form a basic multicellular unit (BMU) to resorpt mineralized old bone and form new bone in the bone remodeling process (Jilka 2003). Bone remodeling process allows the bone to adapt to the changing mechanical load and strain as well as to repair the defected microfractures. It also helps to maintain the homeostasis of calcium and phosphate in body as bone is the reservoir for storing calcium and phosphate (Deng 2005). The bone remodeling process is described and shown in **figure 1.6**.

Bone Remodeling by osteoclast and osteoblast
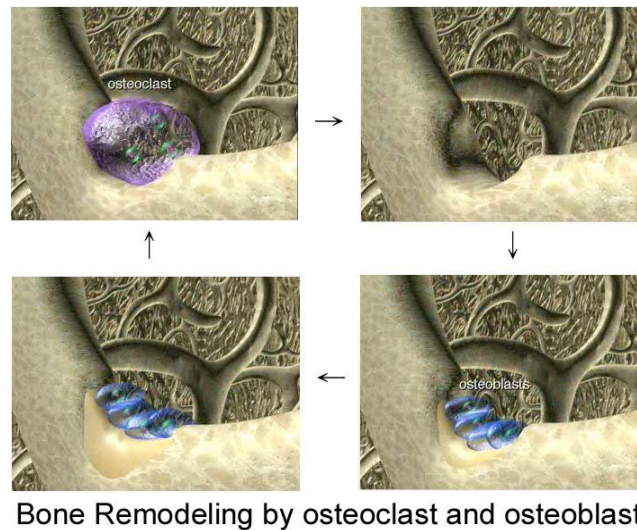
Figure 1.6 Bone remodeling process

Bone remodeling process is a three phase cycle including resorption, reversal and formation. In the resorption phase, the partially differentiated mononuclear preosteoclasts migrate to the bone surface and form multinucleated osteoclasts to resport the bone. This phase usually last for 2 weeks. Afterwards, the mononuclear cells prepare the bone formation surface and signal for osteoblasts migration. The pre-osteoblasts move to the resorption site and being differentiated in reversal phase. This phase usually last for 4 to 5 weeks. Finally, the osteoblasts form the new bone in the formation phase which last for another 4 months. (Hadjidakis and Androulakis 2006).

1.3.3.2   Regulations of Bone Remodeling

Bone remodeling is regulated by systemic and local regulations. PTH, calcitonin glucocorticoids and estrogen belong to systemic regulations while TGF-β and OPG/ RANKL belong to local regulations. Their actions are listed on **table 1-1**. Among these factors, estrogen and OPG/RANKL are highly related to the present study of the bone protective effects on flavan-3-ols.

1.3.4   Bone and estrogen

The high prevalence rate of osteoporosis in postmenopausal women strongly support the importance of estrogen in regulating bone metabolism (Pacifici 2008). In the current study, flavan-3-ols are suggested to be a phytoestrogen which could mimic the estrogen-like activities on bone. Therefore, the understanding of estrogen and it corresponding receptor is important for elucidating how bones can be stimulated by estrogen-like compounds.

1.3.4.1   Estrogen

Estrogen is a natural sex hormone found in women. There are three forms of estrogen named as estrone (E1), estradiol (E2) and estriol (E3) while E2 is the predominant form of estrogen found in human body (Chervenak 2009). Estrogen is the natural agonist of estrogen receptor and plays an important role in the reproductive system, cardiovascular system, central nervous system, and skeletal system (Nilsson, Makela et al. 2001).

Systemic Regulation of Bone Remodeling	
PTH	-induces maturation of multinucleated osteoclasts for bone resorption
Calcitonin	-decreases the mobility of osteoclasts -dissolution of mature osteoclasts into mononuclear cells
Glicocorticoids	- promotes differentiation of mesenchymal progenitors to osteoblasts - sensitizes bone cells for bone remodeling and recruits osteoclasts
Estrogen	-affects the life span of bone cells -anti-apoptotic effect on osteoblasts and osteocytes -apoptotic effect on osteoclasts -affects BMP, hormone receptors, and local regulators expression to modulate the bone remodeling process
Local Regulation of Bone Remodeling	
TGF-β	-regulates cell proliferation and differentiation of preosteoblasts and mature osteoblasts -attracts osteoblast precursor cells to resorption sites -stimulates mesenchymal cells
OPG/RANKL	-RANKL activates the multinucleate cells differentiation to form osteoclastic cells -OPG binds to RANKL and masks the effects of RANKL on osteoclasts -control by systemic regulator such as estrogen and PTH.

Table 1-1 Systemic and local regulation of bone remodeling.
Summarized from Zhang and Yao (2005); and Hadjidakis and Androulakis (2006)

1.3.4.2   <u>Estrogen receptors</u>

Estrogen receptors (ERs) with two isoforms, ERα and ERβ, are the members of nuclear receptors (NRs) family. There are six domains, A to F, in NRs and they are named from N to C-terminus of the protein. These domains are transcriptional activation domain (A/B), DNA binding domain (C), hinge region (D), ligand binding domain (E), and an unknown function domain (F) (**Figure 1.7**). Like most of the NRs, DNA binding domain is highly conservative in ER-α and ER-β with 96% amino acid identity. ER-α was found and discovered in 1958 while ER-β was recognized in 1994 (Enmark and Gustafsson 1999).

ER-α and ER-β express differentially in different tissue (Kuiper and Gustafsson 1997). ER-α is found in reproductive system, central nervous system, and skeletal system while ER-β is found in central nervous system, cardiovascular system, and immune system. It is believed that the different isoforms of ER are responsible for different biological actions in different tissues (Turner 2008).
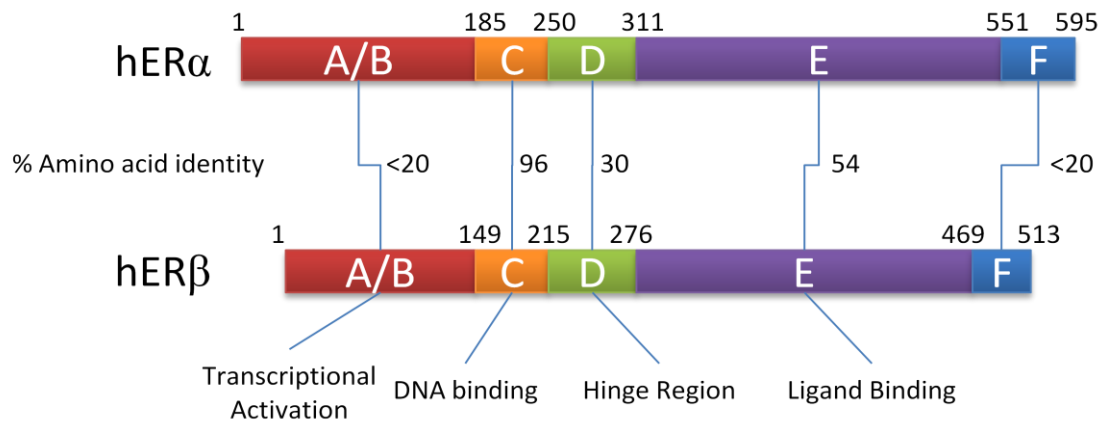
Figure 1.7 Different domains of human estrogen receptor isoforms, ER-α and ER-β

Estrogen receptors consist of different domains named as transcriptional activation domain, DNA binding domain, hinge region and ligand binding domain. Two isoforms of ER, α and β, share a similar amino acid identity in different domains (Adapted and modified from Russell T. Turner and et al. (2008)).

1.3.4.3   <u>Ligand-dependent activation of ER</u>

The classical view of activation on ER requires a direct binding of estrogenic ligand to hormone binding domain (HBD). HBD consists of 12 α-helices hydrophobic site with a three-layered anti-parallel α-helical sandwich for ligand binding. Upon binding, a reorientation of helix 12 modifies helices 3, 5, 12 and generates an activation function (AF) domain on the ligand binding domain (Brzozowski, Pike et al. 1997). This dissociates the ER from chaperones/nuclear matrix-associatied binding protein and allows ER to be dimerized. The ligand-bound ER then translocates to the nucleus and binds to estrogen responsive element (ERE) or other transcription proteins (**Figure 1.8**). The DNA binding ability of ER depends on the AF-1 and AF-2 located in A/B and E domains, respectively. This also affects the degree of transcriptional activation by ER (Maggi 2011).

1.3.4.4 Ligand-independent activation of ER

Ligand-independent activation or non-classical ER activation refers to the activation of estrogen receptor without any direct binding between ER and estrogenic ligand. Non-classical ER ligand like epidermal growth factor (EFG) (Ignar-Trowbridge, Nelson et al. 1992) and IGF-1 (Kato 1995) are able to activate ER-α via ligand-independent ER activation pathway. Ligand independent activations of ER are found to be kinases mediated and activated through post-translational modification of ER such as phosphorylation, acetylation, methylation, ubiquitylation, and sumoylation in specific amino acids (Maggi 2011). Kinases such as MAPK, PKA and p21 ras/ERK are often involved in the ER activation (**Table 1-2 & 1-3**) (Aronica and Katzenellenbogen 1993; Al-Dhaheri and Rowan 2007). A graphical illustration is shown in **figure 1.8** to illustrate the non-classical ER activation through IGF-1 receptor. Using IGF-1 receptor as an example, the IGF-1 activates Ras/Raf/MAPK cascade to phosphorylate ERK 1/2. The ERK 1/2 finally phosphorylates the ER to activate the ERE transcriptional events without any ligand binding to ER.
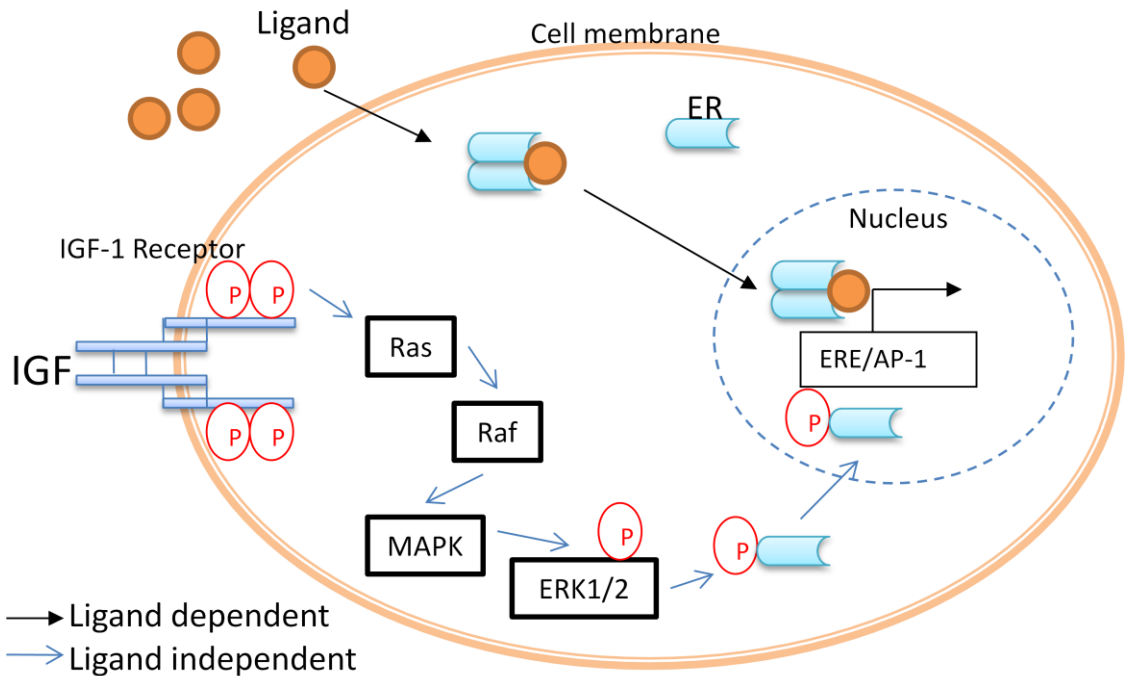
Figure 1.8 Schematic diagram of ligand-dependent and ligand-independent activation of ER
Ligand dependent activation of ER involves the direct binding of ligand to the ligand binding domain of ER. Ligand-ER complex are then translocated from the cytoplasma to the nucleus and bound to the ER responsive gene for gene activation. Ligand independent activation of ER involves activation pathways such as IGF cascade. In such case, IGF-1 receptor activates Ras/Raf/MAPK to phosphorylate ERK1/2 and finally phosphorylate the ER. Phosphorylated ER (pER) is able to activate their responsive gene without the presence of ligand-receptor complex.

	Post translation modification site(s)	Domain	Kinase	Function(s)
ERα phorsphorylation	Ser 102, 104, 106	N-terminus (AF-1)	Glycogen synthase kinase-3 (GSK3)	Transcription activation
	Ser 102, 104, 106		Cyclin A CDK2	AF-2 independent transcription activation
	Ser 104 and 106		TPA-dependent	transcription activation
	Ser 118		p42/p44 MAPK; CDK7	E2 and Tamoxifen-dependent ER activation
	Ser 118		CDK7	Ligand-dependent interaction with TFIIH/CDK7
	Ser 118			Apo-ER transcriptional activation
	Ser 118		MAPK	Recruitment of p68 helicase
	Ser 104, 106, 118		MAPK	Ligand-dependent dimerization
	Ser 104, 106, 118		MAPK	ER mRNA splicing
	Ser 104, 106, 118		Growth factors	Ligand-dependent and independent binding to p160 coactivators
	Ser 154		Unknown	Unknown
	Ser 167		Casein kinase II	Activation of unliganded receptor
	Ser 167		p90 ribosomal S6 kinase 2 (Rsk2)	Activation of unliganded ER
	Ser 167		Akt, MAPK	Ligand-independent rapid signaling
	Ser 236	DBD	PKA	ER dimerization and DNA binding
	Ser 236		PKA	Ligand-mediated receptor degradation
	Ser 305	LBD (AF-2)		Negative regulation of ER acetylation
	Ser 305		p21 kinase	Increased transactivation
	Ser 559		CK2	Transcription inhibition
	Thr 311	LBD	p38 prot kinase and MEKK	Regulation nuclear export and inhibits p160 interactions
	Tyr 52, 219		c-Abl	Transcription activation
	Tyr 537	LBD (AF-2)	src	Cell proliferation
	Tyr 537		MAPK	Hormone-independent ERA activation
ER ß phosphorylation	Ser 94, Ser 106	N-terminus (AF-1)	Erk	Ubiquitination and degradation of unliganded ERβ
	Ser 106,124		AKT	Activation unliganded receptor and SRC-1 interaction
	Ser 106,124		PKA	ERb activation
	Ser255	hinge region	AKT	Inhibits ERβ activity by inhibiting CBP interaction

Table 1-2 ER post-translational modification (Phosphorylation) (adapted from Maggie 2011)

ERα acetylation	Lysine 266; 268	hinge region	p300	Stimulates DNA-binding and ligand-dependent activity
	Lysine 299, 302, and 303		p300	Diminishes response to agonists
ER α methylation	Arg 260 [34]	hinge region		
	Lysine 302		SET7methyltransferase	ER stabilization
ER α ubiquitylation	Lysines 302-534	hinge region		Ligand-independent ubiquitination
	Residues 535 – 595 (lysine 581)			Ligand-dependent ubiquitination and receptor degradation
ER α sumoylation	Lysines 266; 268	hinge region	PIAS1 and PIAS3	Ligand-dependent activity

Table 1-3 ER post-translational modification (Acetylayion, methylation, ubiquitylation and sumoylation) (adapted from Maggie 2011)

1.3.5 OPG/RANKL

The osteoprotegerin (OPG) and receptor activation of NF-κB ligand (RANKL) play an important role on regulating bone metabolism. This regulation depends on the receptor activation of NF-κB (RANK). RANK belongs to the tumor necrosis factor (TNF) receptor family member and it can be found on the cell surface of osteoclasts (Hsu, Lacey et al. 1999). RANKL, the ligand of RANK, is found on the cell surface of osteoblasts and it is the natural agonist of RANK. In normal situation, the presence of RANKL on osteoblasts binds to the RANK on osteoclasts and activates the cells. This activation facilitates the osteoclasts maturation. Indeed, the RANK/RANKL activation of osteoclasts is further regulated by OPG. OPG belongs to the same family as RANK which is an RANKL inhibitor secreted by osteoblasts. It could bind to RANKL and prevent the activation of RANK (Simonet, Lacey et al. 1997). A graphical illustration of OPG/RANKL regulations is shown in **figure 1.9**.

The roles of OPG and RANKL in bone were demonstrated by using transgenic mice model. Osteopetrosis was observed in OPG overexpressing mice (Simonet, Lacey et al. 1997) while osteoporosis was observed in OPG deficient mice (Bucay, Sarosi et al. 1998). The deletion of RANKL encoding gene prevented the maturation of osteoclasts and caused osteopetrosis. These suggested that the OPG/RANKL regulation is important in the osteoclastogenesis. In addition, the administration of recombinant RANKL to mice could increase the calcium level in blood which is the evidence of high osteoclastic activity (Lacey DL 1998). RANKL was also found to induce the maturation of an *in vitro* osteoclast precursor cells RAW264.7 to mature multinucleated osteoclastic cells (Cuetara, Crotti et al. 2006).
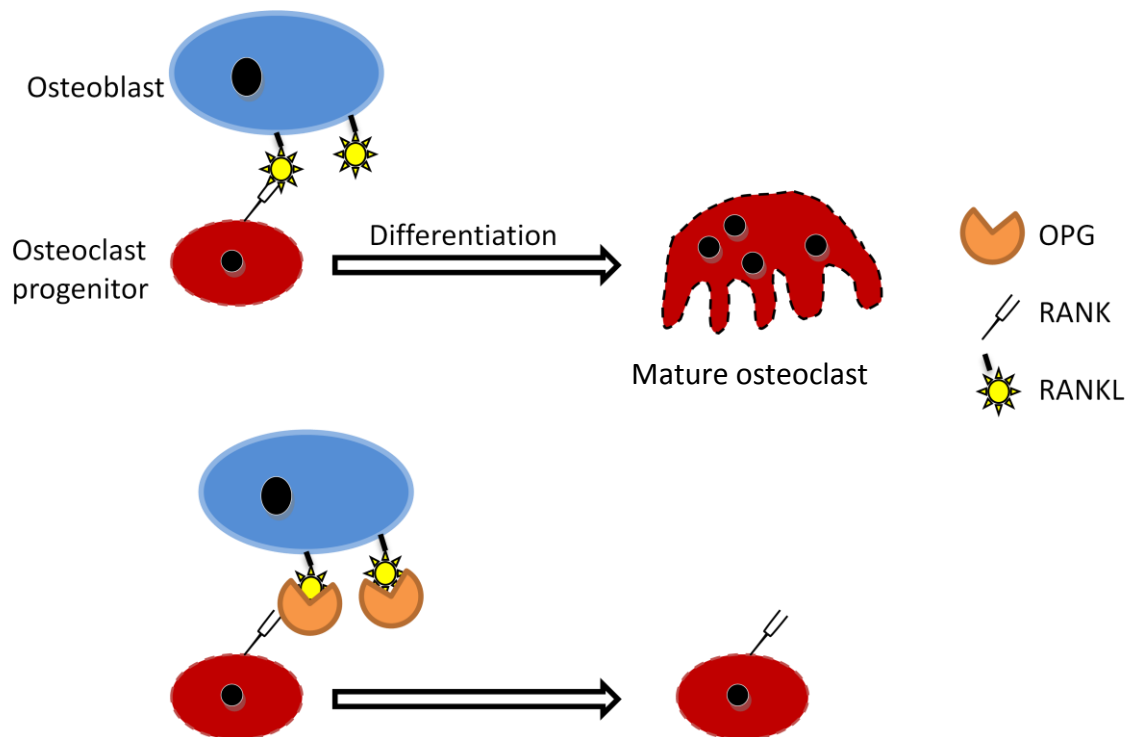
Figure 1.9 OPG/RANKL regulations between osteoblasts and osteoclasts
Osteoblasts express RANKL on cell surface and bind to the RANK on osteoclast progenitor. This facilitates the maturation of progenitor cell to mature osteoclasts. In contrast, the presence of OPG binds on the RANKL to prevent the binding of RANKL to RANK. This prevents the maturation of osteoclast progenitor.

1.4 *Pharmacokinetic*

Pharmacokinetic (PK) describes the absorption, distribution, metabolism and elimination (ADME) of the drug in the body (Bayliss 2000). It monitors the drug concentration in plasma as well as the target organs at different time interval after drug administration. These information can be fitted into a pharmacokinetic modeling to predict for the drug disposition throughout the body (Bischoff 1987). PK is useful for designing and evaluating the dosage and drug formulation. Apart from PK study, pharmacodynamic study is sometime correlated to PK results and used to describe the concentration-action of drug which is useful to optimize the dosage of drug with maximal therapeutic effects and minimal adverse effects (Hedaya 2012).

The ADME of flavan-3-ols could affect their pharmacological behavior in the animal body. Different studies have indicated that the ingestion of green tea could raise the green tea flavan-3-ols in animal plasma (Chu, Wang et al. 2006; Del Rio, Calani et al. 2010). However, there is not any previous study describe the bioavailability of DF flavan-3-ols in animal body. Although the structure of green tea flavan-3-ols and DF flavan-3-ols are similar, their bioavailability might not be the same. Therefore, a PK study will be useful to investigate the PK behavior of DF flavan-3-ols in animal body. This can be used to predict the dose and dosage interval for use in the further *in vivo* efficacy study.

1.4.1 Pharmacokinetic modeling for analysis

PK modeling predicts the drug behavior inside the body. Different PK models are developed from the same foundation as physic or chemistry. However, biological modeling tends to be more complex because it contains many components (Bonate 2006). There are three common PK approaches and they are based on different assumptions which are suitable for use in different scenarios.

Noncompartmental approach is the simplest PK study without making any assumption. Parameters like the maximum blood drug concentration, the time for reaching the maximum blood drug concentration and the area under the plasma concentration-time curve are used to direct compare between two different drug products for the same active drug. It can be used to study bioequivalence of drugs (Hedaya 2012).

Compartment model describes the body into different compartments. This model is further divided into one compartment or multiple compartments depending on the drug distribution rate to different organ. One compartment model can be used to describe the drugs with a short distribution time throughout the whole body. Multiple compartments can be used to describe the drug with different distribution time to different organs (Hedaya 2012). Compartment modeling can be used to predict the blood concentration of drug in different time points from the drug concentration-time plot (Smith 1987).

Physiological model likes multiple compartments model divides the body into different compartments by physiological organs or tissues. The uptake and disposition of drug in the different compartments can be described by this modeling. Currently, the physiologically-based pharmacokinetic (PBPK) combines *in vitro* and *in vivo* information such as organ size, blood flow, drug uptake rate and drug elimination rate to build up the PBPK model. It can be used to describe the active site of drug and toxicity of drug in specific organ (Loizou 2011). This model can also be used to predict the change in drug pharmacokinetic behavior of drug upon different physiological changes in the body. This is the most complicated modeling among these three approaches.

1.4.2 Administration routes

Intravenous (I.V.) injection administrates the drug into the vein of animal directly. It is the most common administration route for studying pharmacokinetic (Chen 1997; Wang 2010). This allows direct observation of the drug interactions in the body. The concentration of drug in blood reaches the maximum drug concentration instantly without delay. Intraperitoneal (I.P.) injection administrates the drug to the peritoneum of animal. This form of injection is mainly used in animal studies because of the ease of administration for small animal like rat and mouse. Oral administration is the most common way for drug administration for drug owing to the ease of application in human subjects (Hedaya 2012). Different administration routes would give rise to different absorption pattern which can be observed in the drug concentration-time plot.

1.4.3   Pharmacokinetic parameters

In a PK study, different metrics are used to describe the drug behavior. The common parameters are listed on the **table 1-4** (PHARMACOKINETICS 2004). Dose is the amount of drug administrated into the subject. The administration of drug can be through i.v., oral or other forms of injection. After administration, the drug concentration in plasma or serum can be detected. With the drug plasma or serum concentrations in different time intervals, the drug concentration-time curve can be constructed. Parameters such as area under the curve (AUC), clearance (CL), maximum concentration (C_{max}), maximum concentration time (T_{max}) and elimination half-life ($T_{1/2}$) can be found from this curve. AUC describes the total exposure of drug to the body. CL is the rate of the body to remove the drug in blood, plasma or serum. C_{max} is the maximum level of drug concentration after administration while T_{max} is the time for reaching C_{max}. The T_{max} is at time zero by i.v. injection while a time delay can be observed in other forms of administration. Elimination half-life ($T_{1/2}$) is the time for halving C_{max}. $T_{1/2}$ can be further divided into distribution (α) and elimination (β) phase in compartmental modeling. $T_{1/2,\ \alpha}$ is a rapid process mainly due to the rapid distribution of drug to different body compartment while $T_{1/2,\ \beta}$ is a slower process mainly due to the metabolism and excretion.

	Symbol:	Unit	Definition:
Dose	D	mg	Dose administrated
Concentration	C	mg/ml	Concentration in serum or plasma
Area under the curve	AUC	mg/ml/min	Area under the concentration-time curve it is usually to describe the exposure of drug
Clearance	CL	L/h	Total plasma, serum or blood clearance of drug
Maximum concentration	C_{max}	mg/ml	Peak plasma concentration after drug administration
Maximum concentration time	T_{max}	min	Time to reach peak plasma concentration after drug administration
Elimination half-life	$T_{1/2}$	min	Time required for the drug to reach half of the Cmax;
Alpha, beta phase	α, β	-	Exponents of the polyexponential equation for compartmental modeling; α: distribution phase; and β elimination phase

Table 1-4 Common pharmacokinetic parameters (Adapted from AGAH working group Pharmacokinetics (2004))

1.4.4 Bioanalytical methods

The plasma drug concentration is the common parameter for use in pharmacokinetic study. It can be determined by validated bioanalytical method with optimized extraction, separation and detection procedures.

1.4.4.1 Extraction

The analyte in the plasma is usually determined after the removal of proteins in plasma by extraction process. A successful extraction procedure should be able to extract the analyte with high recovery rate and low protein contamination (Chu, Wang et al. 2004). Liquid/liquid extraction (LLE) and solid phase extraction (SPE) are commonly used to extract the analyte from plasma.

LLE uses an immiscible solvent to extract the analyte and precipitate the proteins. Solvent such as acetonitrile and methanol are commonly used in LLE (Lloyd R. Snyder 2010). The extraction solvent can be air dried to yield the concentrated analyte for further analysis. SPE is an extraction method using the technology of chromatography. The analyte in biological matrix passes through the stationary phase in the SPE column (C8 or C18) and binds to the column. The impurities with non-specific binding can be washed away by suitable washing buffer without removing the analyte. After removing the impurities, the analyte can be eluted from the column by elution buffer for further analysis. Different types of SPE columns are commercially available for analytes with different properties. SPE offers an efficient way in extraction but the high running cost is the major concern.

1.4.4.2 Separation

High performance liquid chromatography (HPLC) is a liquid chromatography (LC) that separates the chemical mixture under high pressure. It can separate a wide range of compounds such as amino acids, nucleic acids and carbohydrates (McMaster 1994). The separation of LC is due to the different affinities between the adsorbent surface on the column and the analytes. This involves a series of molecular behavior and interactions between the media and the analyte such as molecular diffusion and dynamic transfer. The separation theory of LC can be further divided into kinetic and thermodynamic aspects. These two aspects affect the band broadening and analyte retention in the column respectively. A successful separation in HPLC requires the optimization of all these factors (Kazakevich 2007). After separation, a suitable detection method can be used to quantify the amount of analytes.

1.4.4.3 Bioanalyte Detectors

HPLC is always equipped with an inline detector for monitoring or detecting purposes. UV detector is the most common detector used to detect the UV absorption properties of analyte. UV detector is a basic and powerful analytical tool for many laboratories because of the low investment cost and ease of operation. However, UV detector cannot distinguish between analyte and biological matrix interference unless the matrix containing a large amount of analyte. This lowered the sensitivity of UV detector. Therefore, other detectors such as fluorescence detection (Ho, Lee et al. 1995) Coulochem electrode array detector (Chen, Lee et al. 1997) and mass spectrometer (MS) (McMASTER 2005) are coupled with HPLC to increase the sensitivity and specificity in bioanalyte detection.

1.4.5 Mass spectrometer

Mass spectrometer (MS) determines the mass to charge (m/z) ratio of an ionized molecule. In the basic principle of MS, the compound is firstly ionized by heat or electron to yield the ionized molecule. The charged ion is deflected by a magnetic field in the vacuum and reached the detector for mass analysis. An ion with heavier mass and fewer charges deflect with a smaller degree and vice versa. The deflection angle of an ion represents different m/z ratio. The basic principle of mass spectrometry is illustrated in **figure 1.10**.

There are four components in modern MS equipments. They are ionizer, mass analyzer, detector and data processor. LC may sometime be coupled with the MS for separating the analyte before ionizing and mass analyzing. The schematic diagram of a typical LC-MS system is illustrated on **figure 1.11**. With the more advance in MS design, more ionization modes and mass analyzer were developed. They can be either used alone or combined with each other for different analytical purposes. In the current study, the MS must be able to couple with an LC for continuous monitoring the bioanalyte. Hence, the basic prinicple of different ionizers and mass analyzers will be useful during the machine selection process.
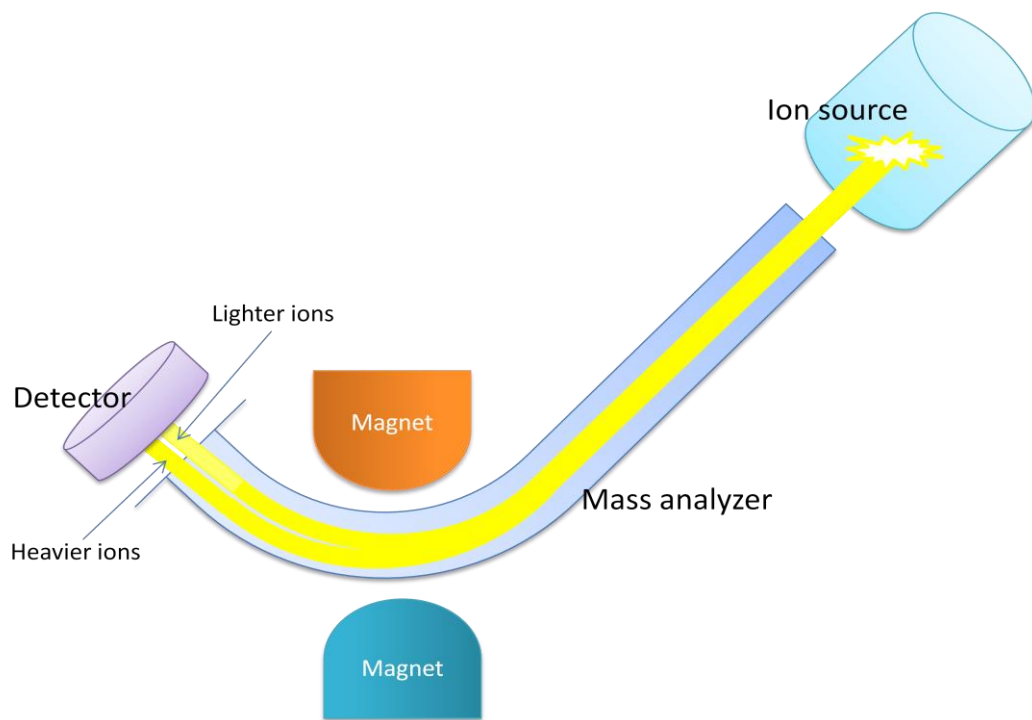
Figure 1.10 Basic principle of mass spectrometry
Ions pass through the vacuum tube and deflect by the magnetic field. Those heavier
ions will be deflected by a smaller angle while the lighter ions will be deflected by a
larger angle to hit the detector. This distinguished the mass of ions by measuring the
bending angle of ions track.
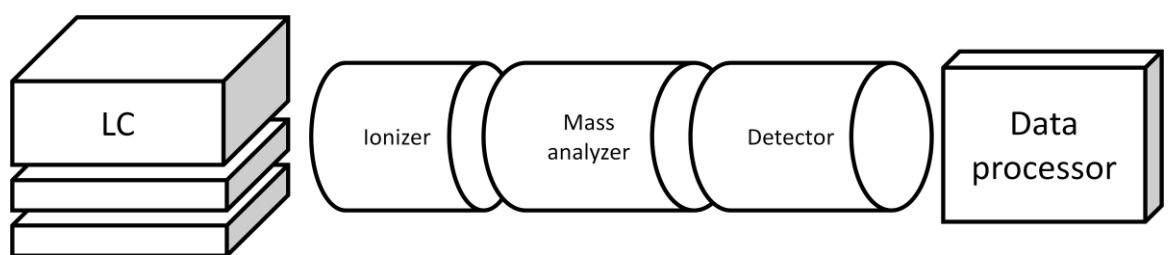
Figure 1.11 Symmetric diagrams of LC/MS components
A typical MS composes of ionizer, mass analyzer, detector and data processor. LC is
sometime linked to the ionizer for separating the analyte in the matrix.

1.4.5.1 <u>Ionization mode</u>

<u>Electron ionization (EI)</u> ionizes the sample by accelerated electron. Only gaseous sample or sample with high vapor pressure can be ionized by EI. A major concern of EI is the high energy accelerated electrons could generate different radical cations fragments from the sample. Hence, the information from original structure might be lost during the ionization process (Gross 2011). To minimize the fragmentation problem, <u>chemical ionization (CI)</u> can be used. CI ionizes the sample by reagent gas to prevent fragmentation. However, both EI and CI are not suitable for low vapor pressure liquid. <u>Desorption electron ionization (DEI)</u> and <u>desorption chemical ionization (DCI)</u> are the improvement of EI and CI by heating the liquid sample rapidly to prevent the sample undergo thermal degradation (Gross 2011). However, the ionization is not continuous and they are not suitable for couple with LC.

<u>Matrix-assisted laser desorption/ionization (MALDI)</u> ionizes the sample by laser. The high energy laser ionizes the peripheral matrix molecule and causes proton transfer to the analyte. This is a soft ionization technique that can preserve the structure of the sample molecule (Cole 2010). However, the sample has to be immobilized on the solid matrix which cannot monitor the analyte from LC continuously. In addition, the angle of incident of the laser to the matrix also affects the ionization degree of analyte which might cause deviation on quantifying the analyte.

Electrospray ionization (ESI) ionizes the sample directly from liquid phase to gas phase by stream of inert gas under high potential difference. The liquid passes through a needle and sprays through a high potential difference electrode (Johnstone 2003). The ion formation mechanism is shown in **Figure 1.12**. It simultaneously ionizes the analyte from high flow rate of liquid inlet which makes it favorable to couple with LC for real time ionizing. In addition, ESI is a soft ionization technique which preserves the structure of analyte (Cole 2010).
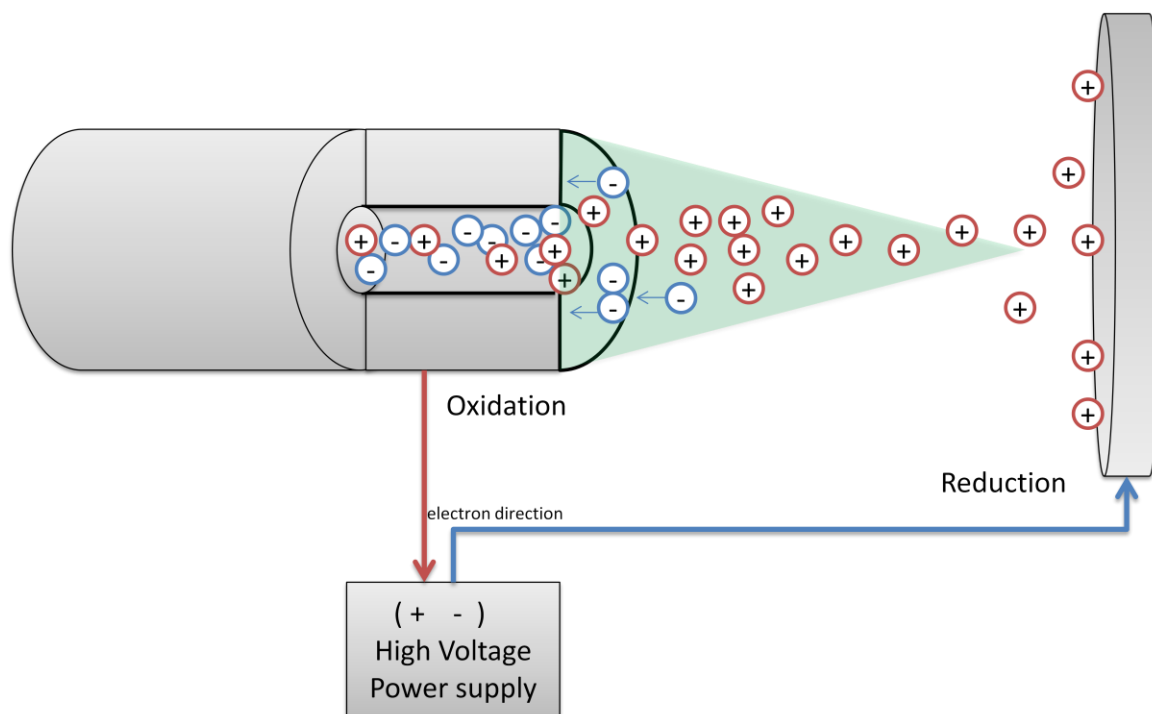
Figure 1.12 Ions formation in ESI operated in positive mode (+ESI)
The analytes pass through the capillary to a high electric field region and forming a taylon cone (Green zone). The ions with positive charges are attracted by the reduction plate and generate a cloud of positive ions.

1.4.5.2 <u>Mass analyzer</u>

<u>Quadrupole (Q)</u> consists of four cylindrically shaped rod electrodes arranged on the x-y plan (**Figure 1.13**). Ions can pass through the z plan from the ion source to the detector. A direct current and radio frequency (dc/Rf) voltages are adjusted and applied to the rods for m/z ion selection. An unstable ion will deflect to the y plan and escape without passing through the detector end of quadrupole while a stable ion will travel through the quadrupole and reach the detector. This acts as a mass selector to select the desired stable ion in selected ion mode (SIM). Quadrupole such as a triple quadrupole (QqQ) linked three quadrupole together to perform tandem MS. The first Q is used to select the parent ions. The ions pass through the second Q will undergo fragmentation by the collusion gas. The fragmentized ions will pass through the third Q for daughter ions selection. Tandem MS operates in selected reaction monitoring (SRM) can be used to monitor the parent and daughter ion from the analyte which gives a higher specificity of ions monitoring (McMASTER 2005).

<u>Time of Flight (TOF)</u> distinguishes the m/z ratio of an ion by the travel time through the vacuum. Ions with low m/z ratio travel faster and reach the detector in a shorter time and vice versa. TOF is always coupled with pulsed ionization source such as MALDI to detect large biological molecule such as proteins (Cole 2010) with high sensitivity and mass accuracy. TOF can also be used with continuous ion source by building a hybrid system such as LC/ESI-Q/TOF/MS/MS for a faster and more accurate ions detection (Neffling, Spoof et al. 2010).

Ion trap (IT) analyzer is similar to quadrupole. It uses the dc/Rf voltage to trap the ion molecules within the analyzer. 3D ion trap and linear ion trap are commonly found in the ion trap mass spectrometer. Unlike quadrupole, IT traps the desired ion by adjusting the dc/Rf. The desired ions are stably held in the ion trap until ejection. These ions can also be fragmentized by introducing the damping gas to the chamber to facilitate a tandem in time MS (Douglas, Frank et al. 2005). This is particular useful for analyzing the precursor ion and daughter ion by using a single mass analyzer with lower investment cost (McMASTER 2005).

1.4.5.3   Quantification

The combination of LC/ESI-QqQ is commonly used to quantify the analyte. ESI continuously ionizes the analyte from LC and these ions can be detected by QqQ using SRM mode. The total ion count (TIC) from SRM is positively correlated to the quantity of analyte. The affordable price of this combination is also an advantage when compared with other LC/MS systems (Cole 2010).
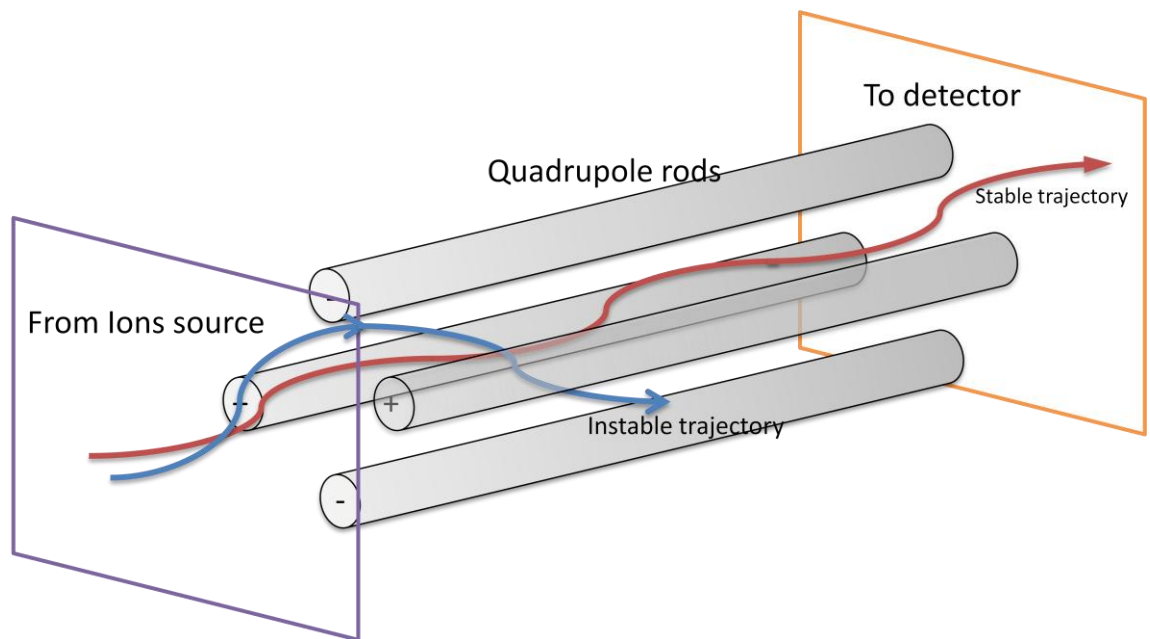
Figure 1.13 Schematic diagram of a quadrupole mass analyzer
Two ions with different m/z ratio pass through the quadrupole. The quadrupole select the ion m/z ratio by dc/Rf on the rods. The ion with stable trajectory (Red) passes through the quadrupole and reaches the detector while the ion with unstable trajectory (Blue) hits on the rods and leads to signal loss.

1.4.6 Bioanalytical Method Validation

Method validation is an important procedure in developing an analytical method. It ensures the quality and reliability of the results for analytical applications. For the pharmaceutical analysis, the method validation is a critical step to ensure the safe and efficient use of newly developed drugs in human body. Different countries might have different regulations for the pharmaceutical analysis. Therefore, the International conference on the harmonization of technical requirements for the registration of pharmaceuticals for human use (ICH) was established in 1990 to harmonize the terms, definitions and the basic requirements of new drug submission between Europe, USA and Japan. ICH has offered a guideline "Validation of Analytical Procedures: Text and Methodology" (2005). This guideline presents the considerations during the validation of analytical procedures.

The US food and drug administration (FDA) also provides guidelines on method validation for pharmaceutical analysis (Ermer 2005). The FDA guideline "Guidance for Industry: Bioanalytical Method Validation" (2001) is applicable to bioanalytical method using gas chromatography (GC), high pressure liquid chromatography (HPLC) and combined mass spectrometric (MS) analysis like GC-MS, LC-MS for quantification of drugs or metabolites in human clinical pharmacology, bioavailability and bioequivalence studies or non-human pharmacology, toxicology and preclinical studies. Documentation is also recommended in this guideline to ensure the performance of the method can meet the standard of analytical applications. This document is also useful for establishing a standard method validation in different laboratories.

The guidelines from ICH and FDA are both important reference material for developing bioanalytical method (Ermer 2005). They describe the method validation requirements for the detection of the chemical in a complex biological matrix by bioanalytical methods. A method validation consists of different components including accuracy, precision, selectivity, sensitivity, reproducibility, and stability which have been described in both guidance from ICH and FDA. A recommendation of the method validation from ICH and FDA is summarized on **table 1-5**.

1.4.6.1   <u>Selectivity</u>

The selectivity is the ability to assess unequivocally the analyte in the presence of components which is expected to be present. The ability of method to differentiate the interference and target analyte determines the selectivity of method. The selectivity can be improved by sample separation like extraction, precipitation and adsorption as well as using a more specific detection method. In ICH guideline, the term identification is used to describe the selectivity. The identification can be simply determined by comparing two samples with and without the analyte. The FDA suggests to including six sources of blank samples to compare with spiked samples at the concentration of limited of quantification (LLOQ). This ensures different sources of blank samples do not contain interference in a specific detection method (Vessman 1996).

1.4.6.2   <u>Accuracy</u>

The accuracy is described as the closeness between the true value and the value founded by a method. There are different ways to determine the accuracy such as using reference standard, inferring from the result of precision, determining the

linearity and specificity as well as comparing the results to well-characterized procedures. FDA suggests to use at least three concentrations with three replicates for each concentration to conduct the accuracy test in the validation process (Ermer 2005).

1.4.6.3 Precision

The precision is described as the closeness of measurements obtained from multiple aliquots of a single homogeneous biological matrix. The precision is sometime described as the repeatability. It can be further divided into within-run and intra-batch precision. Intra-laboratory precision is described as the reproducibility involves different analysts, equipments, reagents and laboratories. ICH (2005) suggests to use at least three concentrations with three replicates for each concentration to conduct the precision test in the validation process

1.4.6.4 Recovery

The recovery is described as the detector response obtained from the amount of analyte extracted from the biological matrix and compared to the detector response obtained from the standard without undergoing extraction. Recovery is frequently found in bioanalytical method involving biological matrix. FDA (2001) suggests to including three concentrations for calculating the recovery rate in a single analyte.

1.4.6.5 Calibration/standard curve

The calibration/standard curve or the linearity is the relationship between instrument response and analyte concentration within a given range. It is recommended to have at least five concentrations to construct the curve. The correlation coefficient, y-intercept, slope of the regression line, residual sum of squares and the data plot are

useful for evaluating the linearity. The range can be adjusted to meet the requirement of linearity. The range describes the upper and lower concentrations of analyte in the sample which fulfills the precision, accuracy and linearity. This curve can be further used to determine the unknown concentrations of the samples.

1.4.6.6   Detection and quantification Limit

The detection limit is the lowest amount of analyte in a sample can be detected but not necessarily to quantify while the quantification limit is the lowest concentration of analyte in a sample can be quantified with certain precision and accuracy. Signal-to-noise (S/N) ratio determine the limits of quantification (LOQ) and limit of detection (LOD). LOD and LOQ are defined as S/N = 3 and S/N = 10, respectively. FDA (2001) suggests to including LLOQ (S/N = 5) in the method validation.

1.4.6.7   Stability

Stability or robustness is referred to the stability of analyte in a biological fluid. It can be affected by the storage conditions, the chemical properties of analyte and matrix as well as the container system. The extraction process and separation process can also affect the stability. The guideline in FDA (2001) has mentioned freeze and thaw stability, short-term temperature stability, long-term stability, stock solution stability and post-preparative stability of analyte.

	ICH	FDA
Selectivity / specificity	Not specify	Biological matrix obtained from six source
Accuracy	Inferred from precision, linearity and specificity	Minimum three concentrations in working range. The mean value should be within 15% of the actual value , 20% of the actual for LLOQ
Precision	A minimum 9 determinations coverage of the specified range for the procedure	Minimum three concentrations in working range. The coefficient of variation (CV) should be within 15% and 20% for LLOQ
Recovery	Not specify	Three concentrations in the range. Not necessary to be 100%.
Linearity	Minimum of five concentrations is recommended	Six to eight non-zero sample in workable range includes LLOQ
Limit of Quantification	S/N =9:1	LLOQ: S/N = 4:1
Limit of Detection	S/N =2:1	Not specify
Stability / Robustness	Not specify	Freeze and Thaw Stability Short-Term Temperature Stability Long-Term Stability Stock Solution Stability Post-Preparative Stability

Table 1-5 The recommendations of method validation from ICH (2005) and FDA (2001)

2 Hypothesis, Objectives and Significance

2.1   Hypothesis:

The osteoprotective effects of traditional Chinese medicine *Rhizome Drynariae* (DF) were demonstrated in our previous studies (Yin 2007). Naringin, a phytoestrogen, found to be one of the active compounds in DF, could exert bone protective effect through modulating the estrogen receptors (Pang WY 2010). Bio-assay guided separation of DF further isolated a series of flavan-3-ol compounds that could stimulate the growth of osteoblastic cells (Chang, Lee et al. 2003). Because of the structure similarity between naringin and flavan-3-ols, we hypothesized that flavan-3-ol compounds could exert bone protective effect through modulating estrogen receptors. Bone protective agents are suggested to act on osteoblasts and osteoclasts to regulate the bone remodeling process. Hence, we also hypothesized that flavan-3-ols could protect the bone through promoting osteoblastogenesis and reducing osteoclastogenesis.

Osteoporotic ovariectomized (OVX) *in vivo* animal models are commonly used to study osteoporosis. The current study of bone protective effects extended to the *in vivo* study. Therefore, we hypothesized flavan-3-ols could maintain at an effective concentration in the animal plasma to prevent the bone loss in osteoporotic animal models.

2.2 Objectives:

This study aims to characterize the bone protect effects of DF flavan-3-ols. The specific aims of this study are:

1. To correlate the structure and biological activities of different DF flavan-3-ols by estrogen sensitive cells

2. To determine the estrogenic-like activity of DF flavan-3-ols

3. To select a representing flavan-3-ol for further characterization

4. To determine the direct effect of a flavan-3-ol candidate on osteoblastogenesis and osteoclastogenesis

5. To establish a bioanalytical detection method for flavan-3-ol candidate

6. To obtain the dosage information of flavan-3-ol candidate in animals by pharmacokinetic study

2.3   Significance:

Bioactive flavan-3-ols were isolated and separated from DF by modern experimental approach (Chang, Lee et al. 2003; Liang, Ye et al. 2011). However, there are limited studies on how DF flavan-3-ols act against bone loss. Therefore, we are interested in investigating how DF flavan-3-ols act on bone remodeling process as well as their pharmacokinetic behavior in animal. It is hope that the current study could link up the relationship between flavan-3-ols and bone protective effects by studying them in different biological models. In addition, this study might also provide more evidence for the use of flavan-3-ols rich DF in managing osteoporosis.

3   Screening of synthesized flavan-3-ols compounds

3.1 Introduction

Rhizome of *Drynaria fortunei (Kunze) J. Sm.* (DF), a Chinese herbal medicine, has been used to mange bone disease for many years. Recent findings suggested DF could exert bone protective effects. The bioassay guided separation of DF extracted, isolated and identified different active flavanoids in DF. Naringin was found to be one of the active compounds in DF and had been well characterized in different bone models. It could promote the proliferation and osteogenic differentiation of human bone mesenchymal stem cell (Zhang, Dai et al. 2009) and improve bone properties in ovariectomized mice (Pang, Wang et al. 2010). Recent research also suggested that naringenin, the structure of narginin without the neohesperidose group, could inhibit osteoclastogenesis (La, Tanabe et al. 2009) and exert estrogen-like activity (Vaya and Tamir 2004). Indeed, flavan-3-ols in DF were also found to have anabolic effects in bone cells (Chang, Lee et al. 2003). However, their effects on bones were not studied intensively. Hence, the current study helps to increase our understanding of the effects of these compounds on bones.

The potential osteoprotective effects of flavan-3-ols in DF were demonstrated by the cell proliferation rate in osteoblastic cells (Chang, Lee et al. 2003). These results suggested that different structures of flavan-3-ols have different potency on stimulating the growth of bone cells and aroused our interest to study the structure-activity relationships of these compounds on bone cells. Owing to difficulties in isolating flavan-3-ols from DF, the flavan-3-ols monomers were chemically synthesized for bioactivity screening. The synthesis pathways were adopted from the protocol for synthesizing the afzelechin and epiafzelechin (Wan and Chan 2004). Because the chemical structure of flavan-3-ols are similar to those of tea catechins,

therefore, a parallel study of (-)-epigallocatechin, (+)-gallocatechin, (-)-epicatechin and (-)-catechin were also included for comparison.

The design of assays in the current study was based on the potential estrogen-like activities of flavan-3-ols. A steroid hormone free environment was employed throughout the screening procedure to simulate the estrogen deficiency environment. Rat osteoblastic like UMR-106 cells were used to evaluate the bone protective effects of flavan-3-ols. In addition, a common estrogen receptor antagonist ICI 182,780 was also added to the culture to see if it could abolish the estrogenic-like effects of flavan-3-ols. ICI 182,780 is an analog to estrogen with high binding affinity to ER-α and ER-β (Wakeling, Dukes et al. 1991). It is an effective antagonist which can block the ER-dependent proliferative actions (Howell, Osborne et al. 2000). To further confirm the estrogenic-like activities of these compounds, an ER-α positive human breast carcinoma cell line MCF-7 was used. MCF-7 is a popular cell model used to study ER-α signaling pathway (Chen, Huang et al. 2003; Lau, Chen et al. 2009). The stimulation of MCF-7 cell is an evidence to support that these compounds exert estrogen-like activity.

The classical view of estrogenic activity refers to the direct binding between ER and estrogen to form a ligand-ER complex. The binding of this complex to the DNA activates the downstream genomic pathway such as estrogen response element (ERE). The binding affinity between the ligand and estrogen receptors is undoubtedly, an important event for investigating the estrogenic properties of the flavan-3-ols. As there are two ER subtypes, the involvement of classical ER activation was determined by radioligand competitive assay in ER-α and ER-β individually to determine if flavan-3-ols could active ER through the direct binding to any of the

ERs. Besides direct binding, some phytoestrogens could activate the ligand-independent activation of ER such as phosphorylating the serine 118 of ER-α (Pang, Wang et al. 2010). But the complex experimental procedures of measuring ER-α phosphorylation is not suitable to be used as a rapid screening platform to determine the estrogenic properties in this study. Apart from the upstream ER activation, the activation of ERE in downstream was used to determine the estrogenic properties of the flavan-3-ols. ERE is a specific ER responsive region in DNA that could be activated by ligand-ER complex. A luciferase-linked ERE plasmid was transfected to a cell model and used to determining the activation of ERE promoter by the flavan-3-ols. The ER competitive binding assay and ERE-linked luciferase assay has been used to demonstrate the estrogenic properties of tea catechins which can also be used to assess the estrogenic properties of flavan3-ols (Goodin, Fertuck et al. 2002).

Different structures of flavan-3-ols were used in this study because the difference in functional groups might affect their biological activities. In addition, both racemic mixture and stereospecific flavan-3-ols were used in this study to evaluate if there are any biologically differences between each others. The current study employed different cell models and ER-mediated assays to characterize the flavan-3-ols. These results are important for used to select a potential flavan-3-ol candidate for further investigation.

3.2 Methodology

3.2.1 Synthesis of flavan-3-ols

The synthetic pathway of flavan-3-ols is illustrated in **figure 3.1**. Before starting the biological study, all synthetic flavan-3-ols were verified by analytical technique such as NMR, MS and IR. This ensured the synthetic flavan-3-ols are meeting the quality standard to be used in biological assay (Wan and Chan 2004; Chan 2012).

3.2.2 Culture of rat osteoblastic-like UMR-106 cell line and human breast carcinoma MCF-7 cell line

UMR-106 cells (ATCC No. CRL-1661) and MCF-7 cells (ATCC No. HTB-22) were cultured in high glucose Dulbecco's modified eagle medium (DMEM) with 10% fetal bovine serum (FBS), 100 U/ml penicillin and 100μg/ml streptomycin (Invitrogen, Carlsbad, CA). The environment was controlled at 37 ^{o}C, 95% humidity and 5% of CO_2. Cells were sub-cultured every 4-5 days. To remove background hormone for different experiments, assay medium (phenol-red free DMEM with 1% charcoal-stripped FBS, 100 U/ml penicillin and 100μg/ml streptomycin) was used upon 70% cells confluence. After assay medium was changed for 24 hours, cells were treated with different compounds, 17β-estradiol (Sigma, St. Louis, MO, USA) and its vehicle.
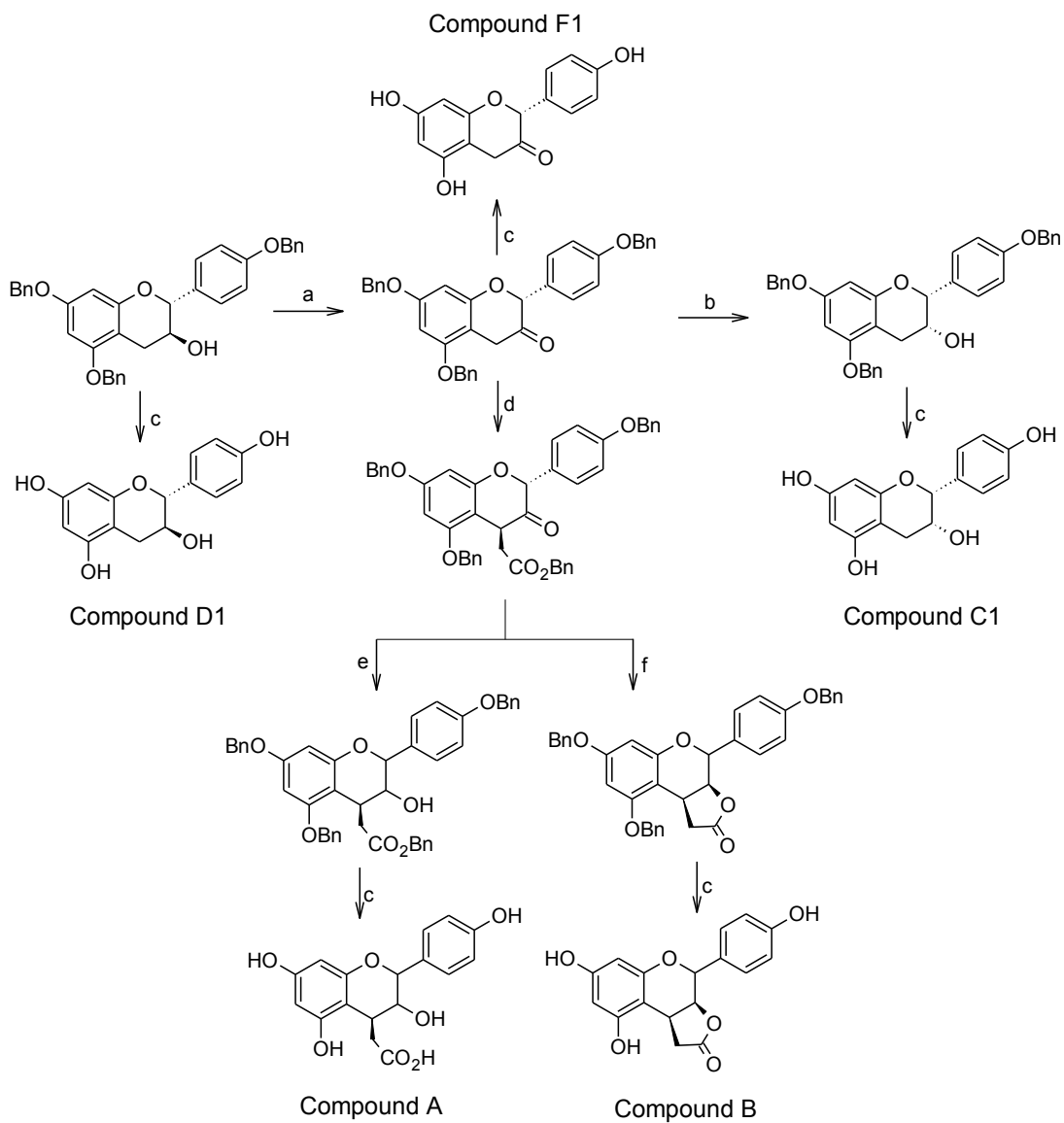
Figure 3.1 Synthetic pathway of flavan-3-ols
(a)Dess-Martin periodinane/CH2Cl2, rt; (b)L-Selectride/THF,-78°C-rt; (c) H_2, Pd(OH)$_2$, THF, MeOH; (d) NaOH/BrCH$_2$CO$_2$Bn,THF,70°C, O.N.; (e) L-Selectride/THF, rt; and (f) NaBH$_4$, THF, rt.

3.2.3 Cell Proliferation Assay

5×10^3 cells were seeded in each well of 96-well microtiter plate. Upon 70% confluence, the medium was changed to assay medium and incubated for another 24 hours. Afterward, cells were treated with flavan-3-ols compound at 10^{-14} to 10^{-6} M, 17β-estradiol at 10^{-8} M and its vehicle for 24 hours in UMR-106 cells and 48 hours in MCF-7 cells. The cell viability were determined by MTS assay using (3-(4,5-dimethylthiazol-2-yl)-5-   (3-carboxymethoxyphenyl)-2-(4-sulfophenyl)-   2H-tetrazolium) (Promega, USA) and incubated at 37°C for one hour. The optical densities at 490nm were recorded by spectrophotometric plate reader at the end of incubation (Bio-Rad model 550, Japan).

3.2.4 Alkaline Phosphatase (ALP) Activitiy Assay

5×10^3 cells were seeded in each well of 96-well microtiter plate. Upon 70% confluence, the medium was changed to assay medium and incubated for another 24 hours. Afterward, cells were treated with flavan-3-ols compound at 10^{-14} to 10^{-6} M, 17β-estradiol at 10^{-8} M and its vehicle for 24 hours. ALP activity was measured by the rate of hydrolysis of *p*-nitrophenylphosphate (*p*-NPP) to *p*-nitrophenol. Substrate *p*-NPP at 10mM was added in each well and incubated at $37\ ^{o}$C. After 30 minutes, the optical densities at 405nm were recorded by spectrophotometric plate reader (Bio-Rad model 550, Japan). In addition, protein concentrations were determined by Bradford protein assay (Bio-rad) to normalize the protein content in each sample. Ten minutes after adding Bradford reagent, the optical densities at 405nm were recorded by spectrophotometric plate reader (Bio-Rad model 550, Japan).

3.2.5 Transient transfection of UMR-106 cells for ER-α and ER-β-mediated Estrogen Response Element (ERE) luciferase assay

UMR-106 cells were grown in 24-well plates with cell density 2.5×10^4 cells per well. Upon 70% confluence, medium was changed to assay medium. Twenty four hours later, an ERE-containing luciferase reporter plasmid (0.4μg), ERα or ERβ expression construct plasmid (0.4μg), together with inactive control plasmid pRL-TK (0.1μg) were co-transfected to the cells by Lipofectamine^{TM} 2000 reagent (Invitrogen, Carlsbad, CA). Flavan-3-ols compound at 10^{-14} to 10^{-6} M, 17β-estradiol at 10^{-8} M and its vehicle were added after 6 hours of transfection. After 24 hours, the cells were collected by passive lysis buffer. The luciferase activities of the cell lysates were measured by Dual-luciferase$^®$ reporter assay system (Promega, Madison, WI, USA) and the signal was detected by GloMax20/20 single tube luminometer (Promega, USA). The *firefly* luciferase represents the ERE activity while the *Renilla* luciferase represents the normalization pRL-TK expression.

3.2.6 Estrogen receptors competitive binding assay

Radio-inert flavan-3-ols and 17β-estradiol were competed with [^{3}H]-estradiol for the binding sites in recombinant full length human ER α or β protein. [^{3}H]-E$_2$ at 10^{-8}M (~70Ci/mmol) (Perkin Elmer), flavan-3-ols at 10^{-11} to 10^{-6}M and recombinant ER protein (Pan Vera/Invitrogen Corp, USA) at 1nM were co-incubated in a 96 well filtration plate (Millipore) with ER binding assay buffer (50mM Tris, 10% glycerol, pH 8.0, 0.3mg/ml BSA, 7% (v/v) DMSO) overnight at 4°C. Hydroxylapatite (HAP) (Bio-rad) slurry was then added to each well to absorb the proteins. The plate was kept in ice bath and shake for 15 minutes. A vacuum was applied to the filter plate by microplate manifold system (Millipore) to remove the solvent. The protein bound HAP retained on the filter plate was then washed twice by HAP washing buffer (0.05M Tris, pH 7.3). Finally, the HAP was re-suspended by HAP washing buffer and transferred to a scintillantion counting vials with 2 ml scintillant fluid. The vials were counted in a liquid scintillantion counter LS6500 (Beckman Coulter) for the radioactivity counting (DPM). E$_2$ standard curve was constructed by using E$_2$ at 10^{-11} to 10^{-5}M while nonspecific E$_2$ binding was measured by using 1000-fold molar excess of radio-inert E$_2$.

3.2.7 Statistical Analysis

Results are reported as mean ± standard error mean (SEM). Significant differences between different groups of means were evaluated by student t-test in confidence level at 95% ($P<0.05$)

3.3 Results

3.3.1 Effects of flavan-3-ols on the cell proliferation of UMR-106 cells

All flavan-3-ols could promote the growth of osteoblastic cells. Compound A and B promoted the growth of cells in a dose dependent manner **(Figure 3.2)**. Compound A, B, D and F exerted their maximum effects at 10^{-8}M by 52% ($P<0.001$ vs. Ctrl), 34% ($P<0.001$ vs. Ctrl), 56% ($P<0.01$ vs. Ctrl) and 37% ($P<0.001$ vs. Ctrl) in the cell proliferation rate, respectively. Compound C exerted their maximum effects at 10^{-14}M by increasing 36% ($P<0.01$ vs. Ctrl) in the cell proliferation rate. An inhibitory effect was observed at 10^{-6}M of compound F on the cell proliferation rate.

3.3.2 Effects of catechins on the cell proliferation of UMR-106 cells

All catechins could promote the growth of osteoblastic cells **(Figure3.3)**. (-)-Epigallocatechin, (+)-gallocatechin and (-)catechin exerted their maximum effects at 10^{-10}M by 29% ($P<0.001$ vs. Ctrl), 27% ($P<0.001$ vs. Ctrl) and 30% ($P<0.001$ vs. Ctrl) in the cell proliferation rate, respectively. (-)-Epicatechin exerted its maximum effects at 10^{-8}M by 26% ($P<0.001$ vs. Ctrl) in the cell proliferation rate.
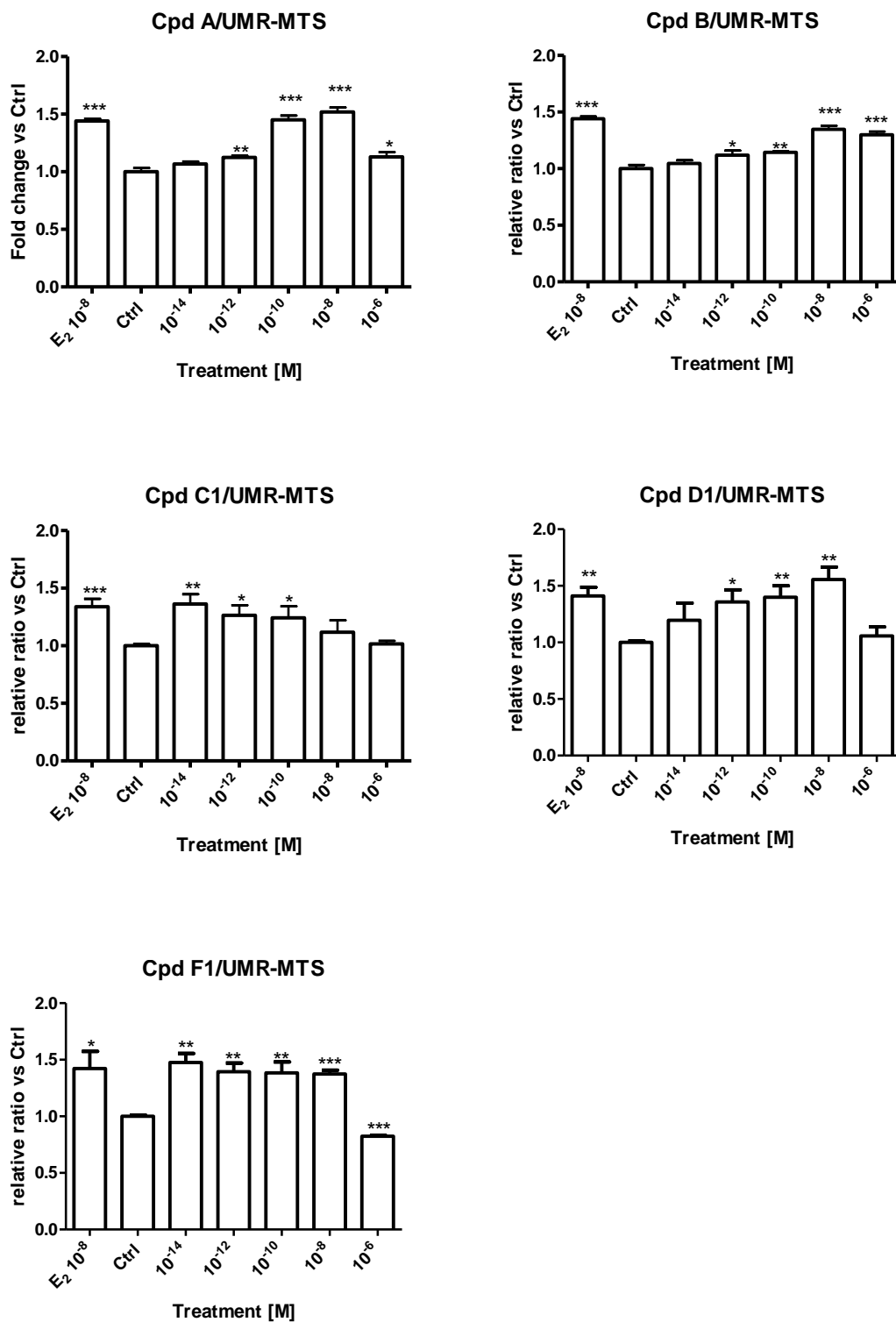
Figure 3.2 Effects of different flavan-3-ols on the proliferation of UMR-106 cells
MTS assay was performed after cells were treated with 10^{-8}M of E_2, 10^{-14} to 10^{-6}M of compound A, B, C1, D1, F1 and its vehicle (1% DMSO v/v) for 24 hours. The bars represent mean ± SEM value with n=3. *$P<0.05$, **$P<0.01$ and ***$P<0.001$ versus control.
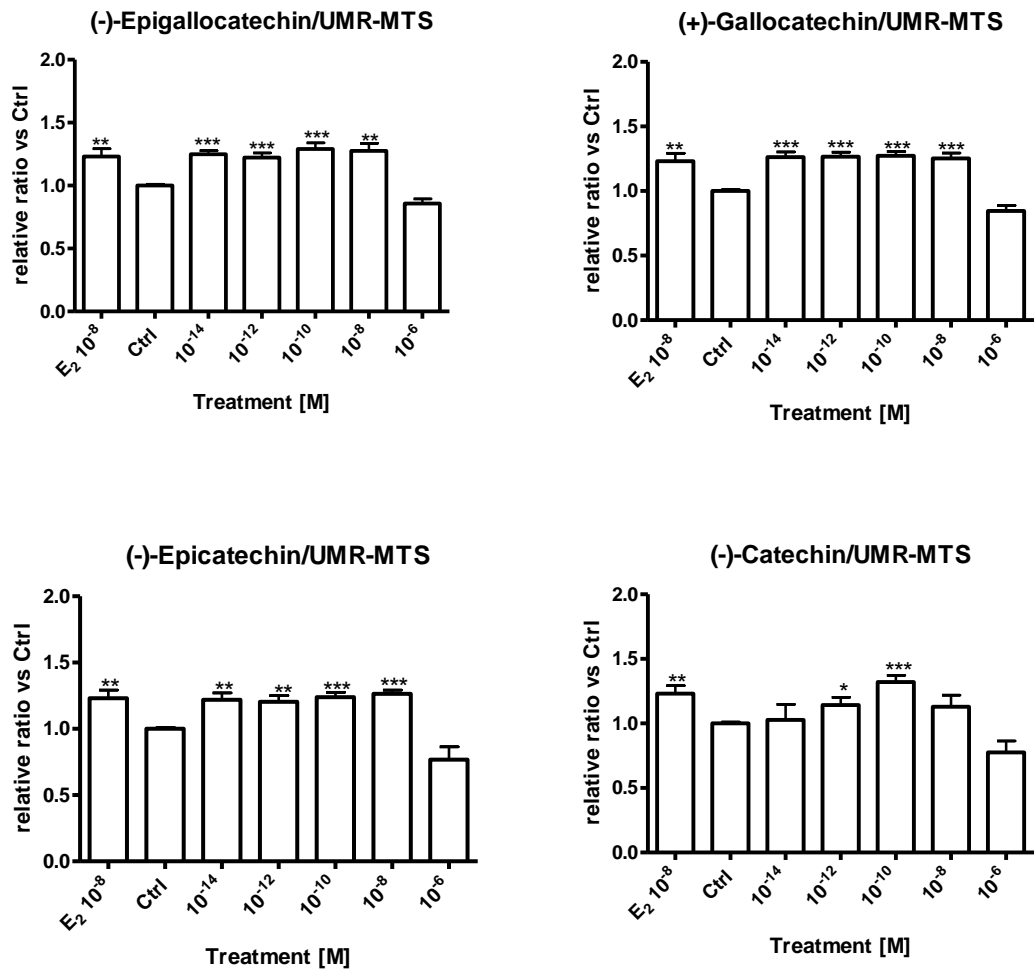
Figure 3.3 Effects of different catechins on the proliferation of UMR-106 cells
MTS assay was performed after cells were treated with 10^{-8}M of E_2, 10^{-14} to 10^{-6}M of compound A, B, C1, D1, F1 and its vehicle (1% DMSO v/v) for 24 hours. The bars represent mean ± SEM value with n=3. *$P<0.05$, **$P<0.01$ and ***$P<0.001$ versus control.

3.3.3 Effect of flavan-3-ols on the cell proliferation of MCF-7 cells

All flavan-3-ols could promote the growth of MCF-7 cells **(Figure 3.4)**. Compound A and D exerted their maximum effects at 10^{-14}M by 57% ($P<0.001$ vs. Ctrl) and 27% ($P<0.01$ vs. Ctrl) in the cell proliferation rate of MCF-7, respectively. Compound B and F exerted their maximum effects at 10^{-12}M by increasing 49% ($P<0.001$ vs. Ctrl) and 36% ($P<0.01$ vs. Ctrl) in the cell proliferation rate of MCF-7 cells, respectively. Compound C increased the cell proliferation at 10^{-8}M by 37% ($P<0.001$ vs. Ctrl). An inhibitory effect was observed at 10^{-6}M of all flavan-3-ols on the cell proliferation.

3.3.4 Effect of catechins on the cell proliferation of MCF-7 cells

All catechins could promote the growth of MCF-7 cells in a dose dependent manner **(Figure 3.5)**. (-)-Epigallocatechin exerted its maximum effects at 10^{-14}M by 54% ($P<0.001$ vs. Ctrl) in the cell proliferation rate of MCF-7. (+)-Gallocatechin, (-)-epicatechin and (-)-catechin exerted their maximum effects at 10^{-12}M by 20% ($P<0.001$ vs. Ctrl), 25% ($P<0.001$ vs. Ctrl) and 35% ($P<0.001$ vs. Ctrl) in the cell proliferation rate, respectively
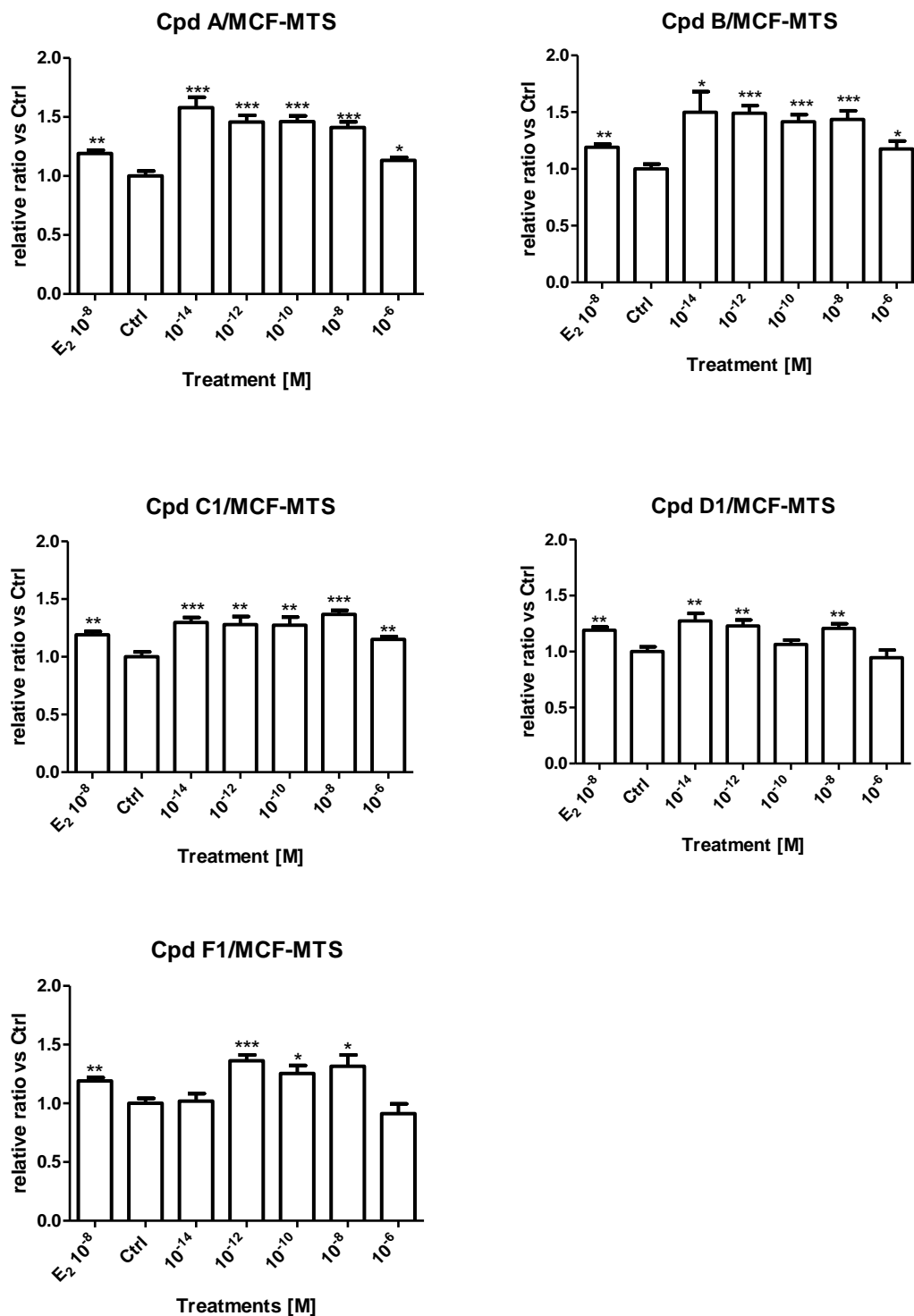
Figure 3.4 Effects of different flavan-3-ols on the proliferation of MCF-7 cells
MTS assay was performed after cells were treated with 10^{-8}M of E_2, 10^{-14} to 10^{-6}M of compound A, B, C1, D1, F1 and its vehicle (1% DMSO v/v) for 48 hours. The bars represent mean ± SEM value with n=3. *$P<0.05$, **$P<0.01$ and ***$P<0.001$ versus control.
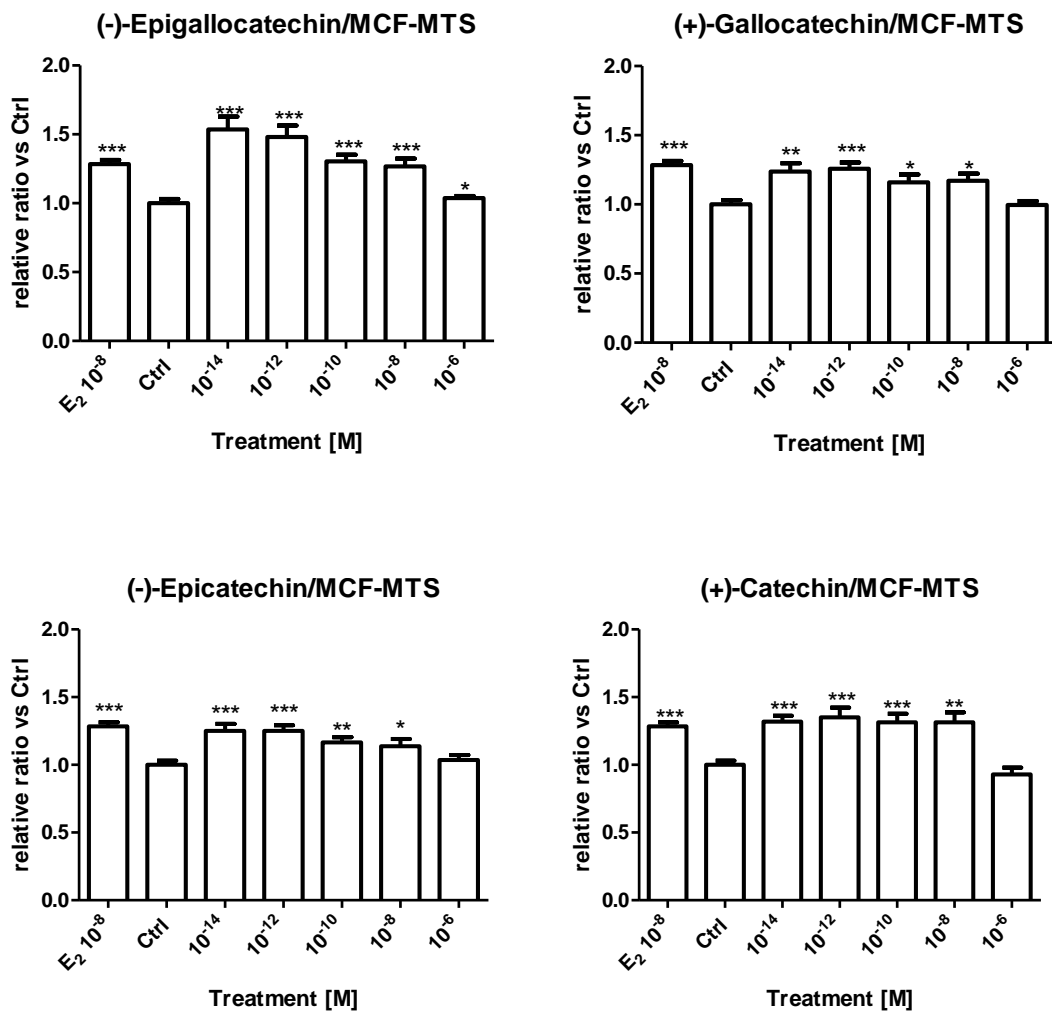
Figure 3.5 Effects of different catechins on the proliferation of MCF-7 cells
MTS assay was performed after cells were treated with 10^{-8}M of E_2, 10^{-14} to 10^{-6}M of compound A, B, C1, D1, F1 and its vehicle (1% DMSO v/v) for **48** hours. The bars represent mean ± SEM value with n=3. *$P<0.05$, **$P<0.01$ and ***$P<0.001$ versus control.

3.3.5   Estrogen receptor dependency of flavan-3-ols on UMR-106 cells

The proliferative effects of flavan-3-ols could be abolished by co-incubation of UMR 106 cells with ER antagonist, ICI 182780 **(Figure 3.6)**. The promotional effect of osteoblastic cells growth in E2 at 10^{-8}M was inhibited by 47% ($P<0.001$ vs. same group with blocker) in the presence of blocker. This effect was also observed in all tested flavan-3-ols. The presence of blockers could diminish the proliferative effect by 36% ($P<0.001$), 30% ($P<0.001$), 27% ($P<0.05$) and 39% ($P<0.01$) in compound A, B, C and D, respectively. The inhibitory effect by ICI blocker was only 14 % in compound F which could not reach a statistical significance.
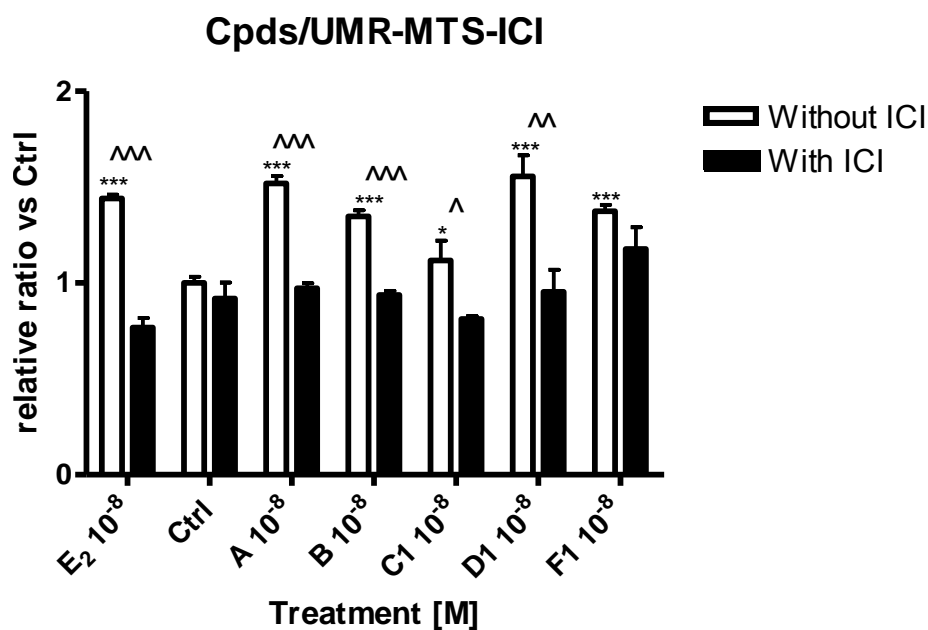
Figure 3.6 Estrogen dependency of different flavan-3-ols on the proliferation of UMR-106 cells

MTS assay was performed after cells were treated with 10^{-8}M of E_2, 10^{-14} to 10^{-6}M of compound A, B, C1, D1, F1 and its vehicle (1% DMSO v/v) for 24 hours. A duplicate set of treatment groups were co-treated with ER antagonist at 10^{-7}M. The bars represent mean ± SEM value with n=3. *$P<0.05$, **$P<0.01$ and ***$P<0.001$ versus control and ^$P<0.05$, ^^$P<0.01$ and ^^^$P<0.001$ versus treatment group with and without ER antagonist ICI182780.

3.3.6 Effect of different stereospecific flavan-3-ols on the proliferation of UMR-106 cells

Different stereospecific flavan-3-ols exerted different effects on the growth of osteoblastic cells **(Figure 3.9)**. Compound C1, C2 and D1 exerted their maximum effects on cell proliferation rate at 10^{-14}M by 31% ($P< 0.05$ vs. Ctrl), 19% ($P<0.05$ vs. Ctrl) and 14% ($P< 0.05$ vs. Ctrl), respectively. Compound D1 exerted the maximum proliferative effect at 10^{-8}M by 8% ($P<0.05$ vs. Ctrl). Compound F1 and F2 appeared to slightly increase the cell proliferation rate but the changes did not reach statistical significance.

3.3.7 Effect of different stereospecific flavan-3-ols on the alkaline phosphates activity of UMR-106 cells

Different stereospecific flavan-3-ols exerted differential effects on the ALP activities of osteoblastic cells **(Figure 3.8)**. Only compound C1 could stimulate the ALP activity at 10^{-12}M by 6% ($P< 0.05$). Other compounds did not alter ALP activities in UMR-106 cells.
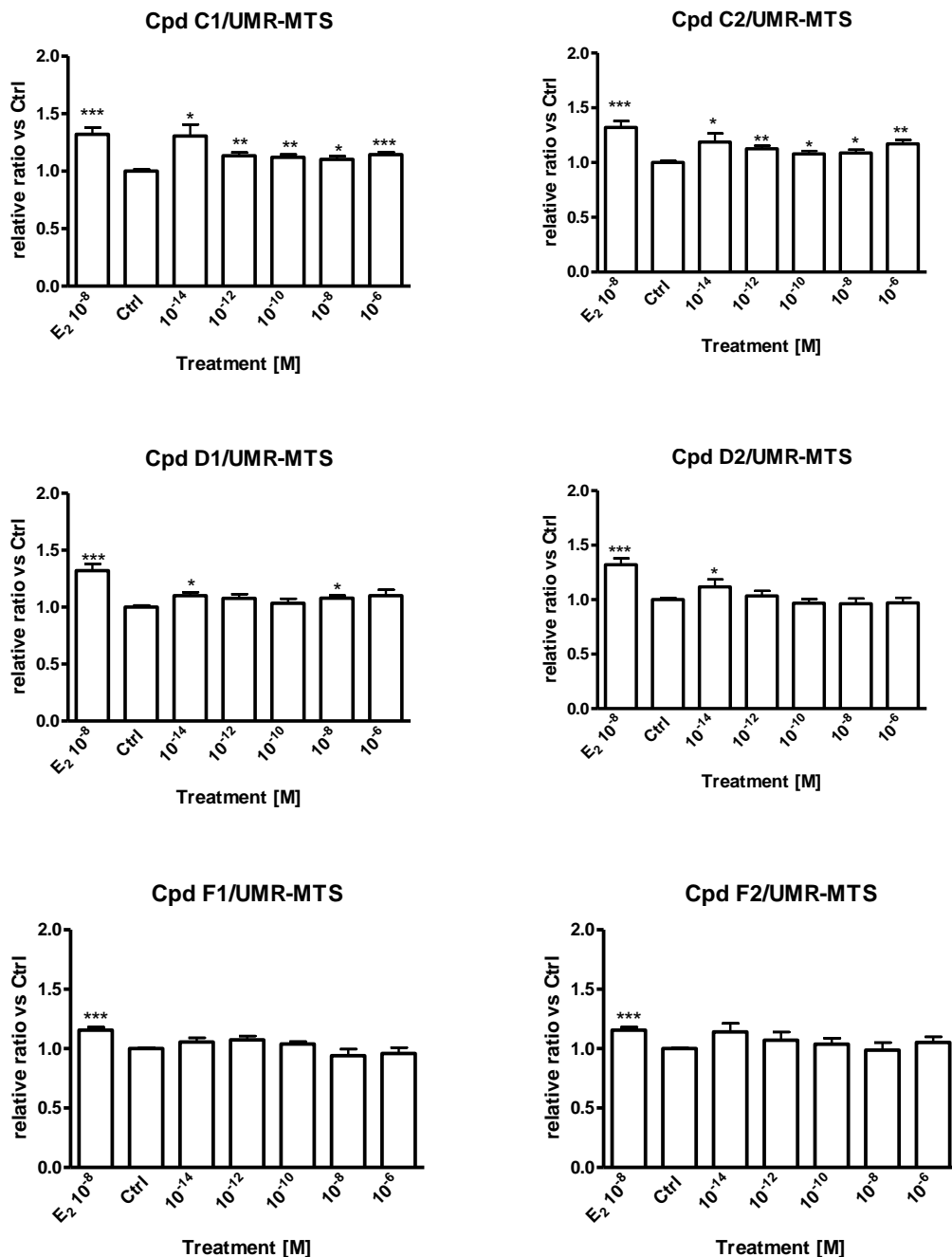
Figure 3.7 Effect of different stereospecific flavan-3-ols on the proliferation of UMR-106 cells

MTS assay was performed after cells were treated with 10^{-8}M of E_2, 10^{-14} to 10^{-6}M of compound C1, C2, D1, D2, F1, F2 and its vehicle (1% EtOH v/v) for **24** hours. The bars represent mean ± SEM value with n=3. *$P<0.05$, **$P<0.01$ and ***$P<0.001$ versus control.
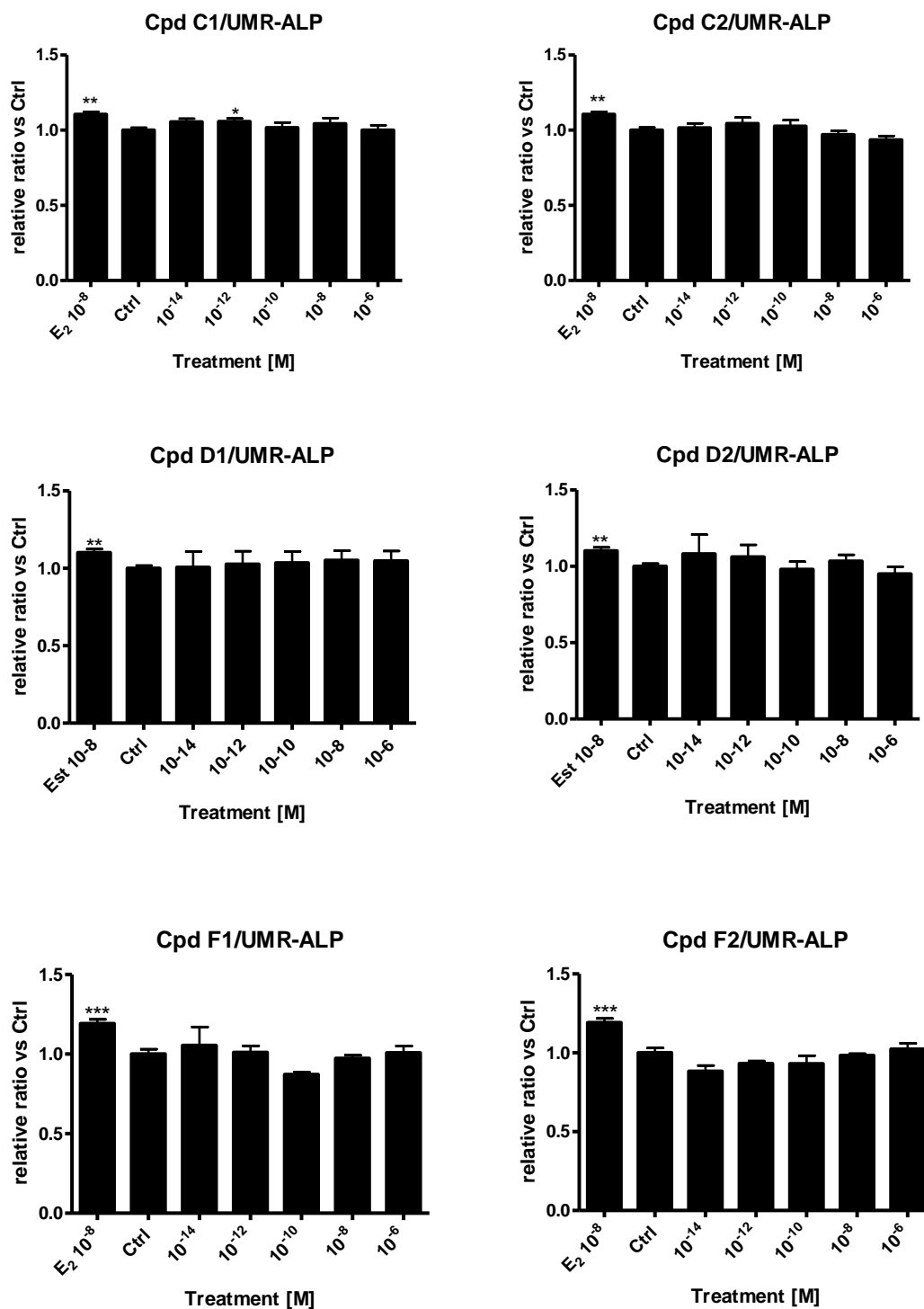
Figure 3.8 Effect of different stereospecific flavan-3-ols on the alkaline phosphates activity of UMR-106 cells

ALP assay was performed after cells were treated with 10^{-8}M of E_2, 10^{-14} to 10^{-6}M of compound C1, C2, D1, D2, F1, F2 and its vehicle (1% EtOH v/v) for **24** hours. The bars represent mean ± SEM value with n=3. *$P<0.05$, **$P<0.01$ and ***$P<0.001$ versus control.

3.3.8 The activation of estrogen receptor alpha and beta mediated estrogen response element by different stereospecific flavan-3-ols on UMR-106 cells

Compound C1 only significantly increased the ER-α mediated ERE luciferase activity at 10^{-14}M ($P<0.05$ vs Ctrl). Compound C2 increased both ER-α and ER-β mediated ERE luciferase activities at the concentration of 10^{-14} to 10^{-6}M. A peak was observed in 10^{-10}M for both subtypes of ER mediated ERE luciferase activities ($P<0.001$ vs Ctrl). Compound D1 and D2 increased both ER-α and ER-β mediated ERE luciferase activities at concentrations between 10^{-12} and 10^{-6}M. Compound F1 only significantly increased the ER-β mediated ERE luciferase activity at 10^{-6}M ($P<0.01$ vs Ctrl) but not ER-α. Compound F2 significantly increased the ER-α and ER-β mediated ERE luciferase activities at 10^{-6}M ($P<0.05$ vs Ctrl for ER-α and $P<0.01$ vs Ctrl for ER- β).
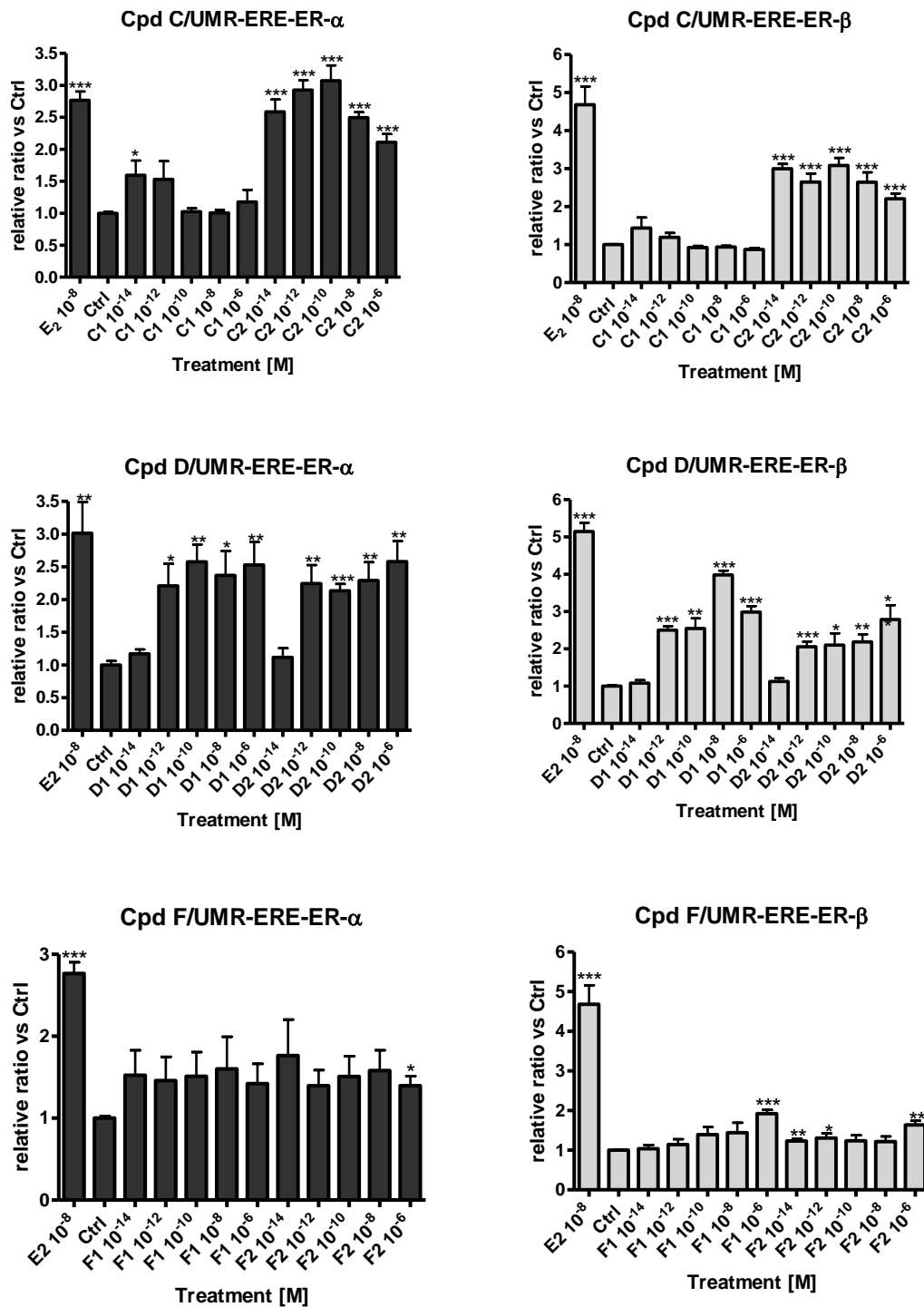
Figure 3.9 The activation of estrogen receptor alpha and beta mediated estrogen response element by different stereospecific flavan-3-ols compounds

UMR-106 cells were co-transfected with plasmid expressing human ERα or ERβ, ERE-luciferase reporter, TK plasmids and treated with 10^{-8}M of E$_2$, 10^{-14} to 10^{-6}M of compound C1, C2, D1, D2, F1, F2 and its vehicle (1% EtOH v/v) for 24 hours. The bars represent mean ± SEM value with n=3. *$P<0.05$, **$P<0.01$ and ***$P<0.001$ versus control.

3.3.9 The binding affinity of different flavan-3-ols on estrogen receptor alpha and beta

E2 was able to compete with [3H]E2 for the ligand binding sites in both ER-α and ER-β. At low concentration (10^{-11}M) of E2, a high [3H]E2 binding was found in both ER subtypes. A further increase in radioinert E2 started to compete with the [3H]E2 and displace them from ligand binding site of ER gradually. At concentration of 10^{-5}M, most [3H]E2 were displaced from the ligand binding site. The %[3H]E2 binding could not reach zero because of the non-specific binding. The signal was not removed even increasing the E2 concentration to 10^{-4}M. E2 displaced [3H]E2 from the ligand binding site of ER-α and ER-β and formed a sigmoid curve. The IC50 of E2 on ER-α and ER-β are 2.0 x 10^{-8}M and 1.3 x 10^{-8}M, respectively. All flavan-3-ols compound did not displace the ER-α or ER-β bounded [3H]E2 at the concentration between 10^{-12} and 10^{-6}. Only compound F1 and F2 shown a [3H]E2 displacement in ER-β at concentration 10^{-6} but not the others.
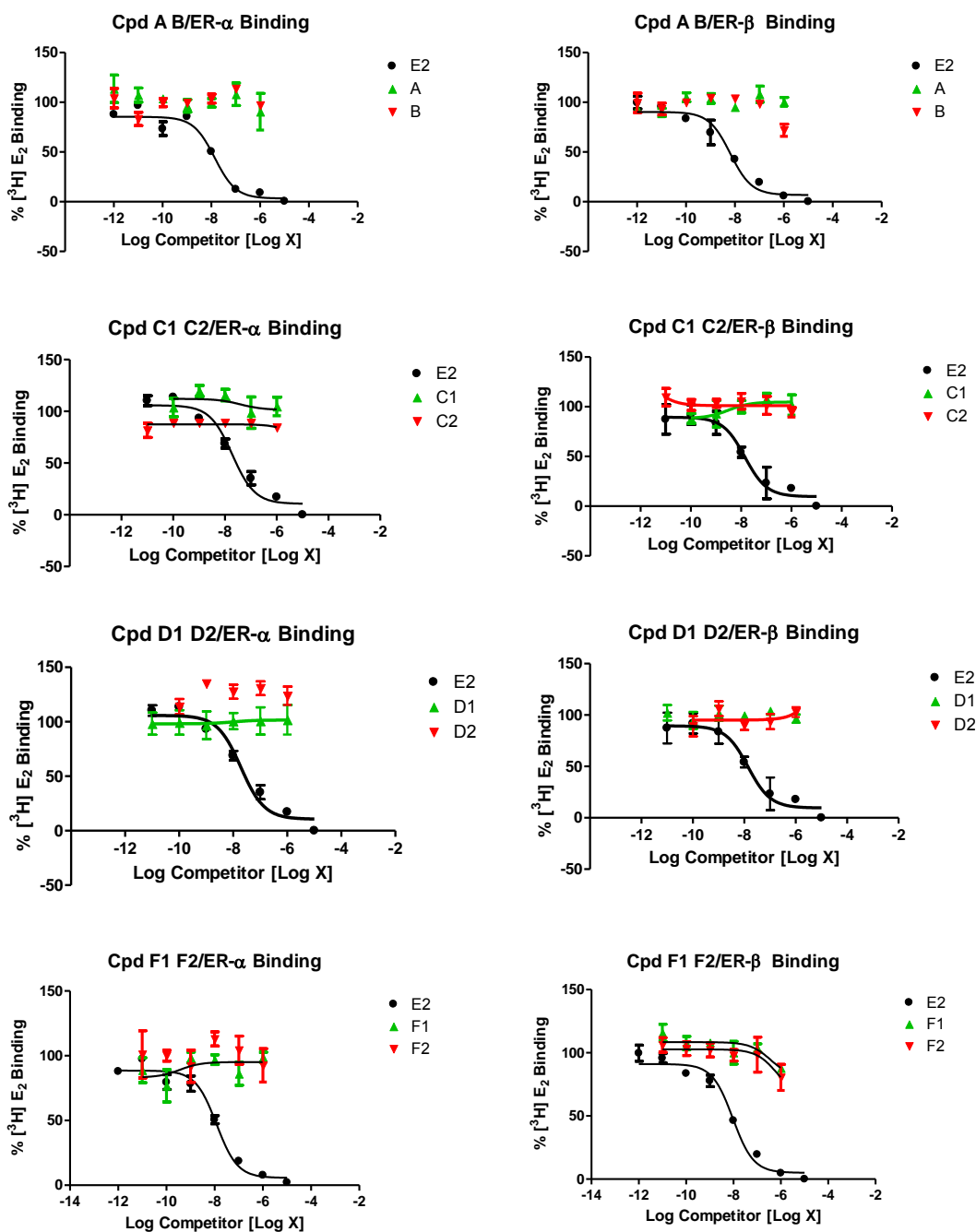
ER-α IC50 of E2 = -log7.7M   ER-β IC50 of E2 = -log7.9M

Figure 3.10 The binding affinity of flavan-3-ols compounds on ER-α and ER-β
Recombinant human full length ER-α or ER-β protein with 10^{-8}M radiolabeled [3H]E2 were co-incubated with 10^{-11} to 10^{-5}M of non-radiolabeled E_2, 10^{-11} to 10^{-6}M of compound C1, C2, D1, D2, F1 and F2 (7% v/v DMSO) overnight. Non specific binding was determined by 1000-fold molar excess of non-radiolabeled E2. Displacement curve was obtained by non-linear fit one site binding (n=3)

3.4   Discussion

3.4.1   Bone protective effects of synthetic flavan-3-ols

The compounds that could increase the osteoblastic cell proliferation in estrogen free environment might be useful to prevent bone loss in estrogen deficiency condition after menopausal (Ernst, Heath et al. 1989). Our results suggested that the synthetic flavan-3-ols as well as the catechins can stimulate the osteoblast proliferation **(Figure 3.2 & 3.3)**. Five synthetic compounds at physiological achievable range like 10^{-10} to 10^{-8}M could promote the growth of UMR-106 cells. Different structures of compounds exerted different proliferative effects on UMR-106 cells. Among the five synthetic compounds, only compound A and B are linked with functional groups in R4 position. Compound A has a carboxylic group in R4 position and compound B has a cyclic structure between R3 and R4 positions. The cyclic structure of compound B might be too bulky and reduces the proliferative activity toward bone cells. Compound C1 (2*R*, 3*R*) and D1 (2*R*, 3*S*) are diastereomers with different orientation in the R2 and R3 positions. The orientation might also affect the activation of the compounds toward the corresponding receptors and affect the proliferation rate. The hydroxyl group at R3 position in compound F1 is replaced by ketone group. This also suppressed the proliferation rate at 1μM which was not observed in the other synthetic compounds. Our results also suggested that the low concentration of catechins could stimulate the cell proliferation. However, most of the studies on tea catechins on bone cells were reported at concentration higher than or equal to 1μM (Ko, Lau et al. 2009; Lin, Chen et al. 2009; Wei, Tsai et al. 2011). Our result was consistent with *Ko, et al* (2009) that (-)-EGC did not stimulate the

proliferation UMR-106 at 1μM but we were not able to compare our lower catechins concentration with others report.

In fact, the first batch of synthetic compounds was dissolved in dimethyl sulfoxide (DMSO). DMSO is widely used in cell culture because of the relative low toxicity and strong dissolving power of many compounds (Santos, Figueira-Coelho et al. 2003). It is also used to form the cryogen preserved cell stock. Recent findings suggested that DMSO possess anti-inflammatory properties and acts as a free radical scavenger (Xing and Remick 2005). It is also reported as a differentiation inducer in preosteoblast cells. In murine preosteoblastic MC3T3-E1 cells, 1% (v/v) of DMSO is adequate for inducing nodules formation, differentiation as well as upregulating the gene candidates such as Runx2 and Osterix (Cheung, Ng et al. 2006). Where the final concentration of DMSO used in our study was 1% (v/v). As the present study of flavan-3-ols was mainly focused on bone metabolism involving osteoblast and osteoclast, therefore, ethanol instead of DMSO was used in the latter part of experiment. This can prevent the possible osteogenic effect caused by DMSO.

The second batch of synthetic stereoisomeric compounds C1, C2, D1, D2, F1 and F2 were dissolved in EtOH. Their effects were not as potent as in the previous experiment. This might due to the high solubility of DMSO in culture medium to facilitate the transport of synthetic compounds into the cells. This effect was mostly observed in compound F1 as the significant proliferative effect of F1 was not found in the experimental condition without DMSO. Without using the potential osteogenic agent in the culture, the ALP activities were measured in the second batch of compounds. ALP is commonly used to evaluate the differentiation of osteoblastic (Gray, Flynn et al. 1987). Our results suggested that only C1 could increase the ALP

activities on UMR106 cells. This indicated that these compounds were not active in promoting the ALP activities in mature osteoblastic cells. Another differentiation assay with 48 hours treatment was also conducted in UMR-106 cells by these compounds but the effects were not significant as well (data not shown).

3.4.2 Estrogen-like activities on cell level

The estrogenic effects of flavan-3-ols were determined by an ER-α positive human breast cancer MCF-7 cell line. MCF-7 has long been used for the mechanistic studies of estrogen-like activities (Rivas 2002). The cell viability in MCF-7 was found to be increased by phytoestrogens such as naringin (Chang, Lee et al. 2003) and genistein (Hsieh, Santell et al. 1998). It is not surprising that flavan-3-ols were able to increase the proliferation of MCF-7 cells because the structures of flavan-3-ols are similar to the phytoestrogens such as naringin.

All the synthetic compounds increased the cell number of MCF-7 (**Figure 3.4 & 3.5**). This implied that this class of compounds could exert estrogenic effects in human breast cancer cells. The estrogenic effect is stronger in compound A and B in term of the proliferative rate. This might due to the presence of functional group in the R4 position which can only be found in compound A and B. Compound C1 was stronger in stimulating MCF-7 cells than D1. This suggested that the orientation of the R2 and R3 at the same planar could exert a stronger proliferative effect. Compound F1 also promoted the proliferative effects of MCF-7 cells at 10^{-12} to 10^{-8}M even the R3 hydroxyl group is replaced by ketone group. Additional hydroxyl group on the R3' and R5' of the flavan-3-ols does not alter the proliferative effects of MCF-7 cells. The effective concentrations of flavan-3-ols were different in MCF-7 cells and UMR-106 cells. This might be due to the different activation pathways involved in

different cell types. For example, the expression level of ER-α in MCF-7 cells is higher than UMR-106 cells. The same concentration of compound might be able to activate the cells with more receptors but not the other one. In addition, the regulation of cell growth is always cell type specific which the same compound might act as an agonist in one type of cell but act as an antagonist in another one. Therefore, the actions of flavan-3-ols on MCF-7 and UMR-106 were not the same. Similar to the results from UMR-106 cell proliferation assay, the proliferative effects of these compounds were found to be reduced at 1μM. The stimulatory effects of flavan-3-ols and tea catechins found in MCF-7 cells suggesting that these compounds are estrogen-like in nature.

To further characterize the estrogen-like properties of flavan-3-ols, the estrogenic study was extended to bone model. Using UMR-106 cells alone might not be optimal for demonstrating the estrogenic properties as the ER-α expression is relative low in UMR-106 cells (Davis 1994). Therefore, a popular estrogen receptor antagonist, ICI 182780, was used to test for their estrogenic properties. ICI 182 780 is an ER antagonist that prevents the activation of ER mediated pathway through direct binding to them (Howell, Osborne et al. 2000). The stimulatory effects of flavan-3-ols on bone cells could be blocked by ER antagonist. This indicated that these actions were estrogen receptor dependent. Only the proliferative effect of compound F was not blocked by the ER antagonist significantly. This implied that the alternation of R3 position might alternate the estrogenic properties of the flavan-3-ols. Our results suggested that the stimulatory effects of these compounds in UMR 106 cells were ER dependent.

3.4.3 ER mediated actions of flavan-3-ols

The estrogen-like activities of flavan-3-ols were demonstrated on cell level by MCF-7 cells as well as the co-incubation of ER antagonist in UMR-106 cells. The possible estrogenic actions of these synthetic compounds were further characterized by transfecting the ERE luciferase reporter into the UMR-106 cells and measuring the luciferase activity. As mentioned, ERE is located at the promoter region of some ER related genes. ERE can be activated by ER binding in the classical ER activation (Maggi 2011). The activities of ERE transcriptional events by these compounds reflect some of the estrogenic properties in gene level.

Our results suggested that C1 and C2 behaved differently toward the ERE luciferace responses. C1 only selectively activated ER-α mediated ERE luciferase activity while C2 strongly activates both ER subtype mediated ERE luciferase. The orientation of the R2 and R3 planar might affect the ERE luciferase activities between C1 and C2. Another pairs of diastereoisomer, D1 and D2, behaved similarly in the ERE luciferase activities. The orientations did not select toward different ER subtypes mediated ERE luciferase responses. The diastereoisomer of F1 and F2 only weakly activated the ERE luciferase activities in UMR-106 cells. F2 activated both ERE transcriptional events while F1 only selectively activated the ER-β mediated ERE transcriptional event but not ER-α at high concentration. The conversion of 3-OH to 3=O reduced the activation of flavan-3-ols to the ERE luciferase reporter gene. This result was consistent with the ER antagonist assay as the cell proliferative effect of F1 cannot be blocked by the ICI 182780 significantly. The structure activity of stereospecific flavan-3-ols could be differentiated by the ER mediated ERE transcriptional luciferase activity.

3.4.4 Structure-estrogenic activity relationship

The radiolabeled [3H]17β-estradiol competitive binding assays demonstrated the binding affinities of these synthetic compounds to ER **(Table 3-1)**. The ER binding ability of flavan-3-ols might explain the classical activation of ER. In this competitive binding assay, the concentrations of the synthetic compounds were only up to 1μM because it is difficult to maintain the high molar concentration of compounds in the animal body although some of them might be able to displace the [3H]E2 at very high concentrations. Therefore, we are only interested in the concentration among the physiological achievable range.

Among these synthetic flavan-3-ols, only F1 and F2 were found to have a slight displacement at 1μM in ER-β. It was also found that they activate the ER-β ERE transcriptional event at that concentration. This suggested that the activation of the ER-β mediated ERE transcriptional event might due to direct binding of F1 and F2. Because other flavan-3-ols could not displace the [3H]E2 but still activating the ER mediated ERE transcriptional events. This implied that the mechanisms of activating ERs of F1 and F2 are different from the other flavan-3-ols.

Vaya and Tamir (2004) stated some properties that are important for ER binding in flavoniods. Some of them could also be found in our synthetic flavan-3-ols. They summarized the importance of different functional groups in common dietary flavonoids binding to ER-α from different authors. Firstly, the A and B aromatic ring are found to be essential for the estrogen-like activities (Vaya and Tamir 2004). Secondly, the 4'-OH or 7-OH presence in flavanoids is corresponding to the functional group 17β-OH of E2 (Le Bail, Varnat et al. 1998). Apart from these basic

requirements, they also suggested that the number of hydroxyl group could also affect the hydrophilicity and alter the binding affinity toward the receptors. Compound with more than four hydroxyl group would decrease the RBA to ER-α (Miksicek 1995; Tamir, Eizenberg et al. 2000). In addition, the presence of 5-OH could affect the hydrogen-donating ability to 7-OH which increase the RBA while the presence of 3-OH could reduce the estrogen-like activity of flavonoids (Le Bail, Laroche et al. 1998). Although our tested compounds fulfill some of the criteria listed above, their binding affinity to ERs was not significant.

Our results indicated that the estrogenic-like activities of these compounds demonstrated previously in this chapter were not likely activating the classical pathway. In fact, recent findings also suggested that not all phytoestrogens exert their estrogen-like activities by direct binding to ER. This property was also found in phytoestrogens like naringin and genistein. Both of them were found to improve bone properties in osteoporotic model by stimulating the growth of bone cells (Dixon and Ferreira 2002; Pang, Wang et al. 2010) without direct binding to ER-α (Branham, Dial et al. 2002). Recent findings only suggested that naringin (Guo, Wang et al. 2011) and genistein (Kuiper, Carlsson et al. 1997) selectively binding to ER-β with a higher affinity than ER-α. One of the possible way by which these compounds activate the ER-mediated ERE transcriptional events might involve the ligand-independent activation of ER, particularly in ER-α. There might be a cross talk between ER and MAPK and such cross talk might facilitate the ERE transcriptional events (Atanaskova, Keshamouni et al. 2002). Such mechanism was found in naringin, with the evidence of an increase in level of ER-α phosphorylated at serine 118 after the osteoblastic-like UMR-106 cells treated with naringin (Pang 2010).

3.4.5 Selection of flavan-3-ols candidate

Synthetic compound A and B are diastereoisomers racemic mixture. According to the guideline on "Development of New Stereoisomeric Drugs" from FDA (1992):<u>"There is no reason to consider developing mixtures of geometric isomers or diastereoisomers unless they fortuitously represent a reasonable fixed dose combination."</u> FDA does not recommend the use of racemic mixture in drug development because stereoisomers have identical physical and chemical properties might often be distinguished by biological systems with different pharmacokinetic properties, pharmacologic or even toxicological effects (Jozwiak 2012). Individual study of the entantiomer in a racemic mixture is needed for drug development. In addition, the use of stereochemically pure drugs are always preferred because it has a simply dose-response relationship and is able to reduce the total dose for minimizing the toxicity by the inactive isomer (Caldwell 1996).

One of the flavan-3-ol candidates will be selected for use in further study based on our previous results. Their effects are summarized on **table 3-2 & 3-3**. Compound A was found to be very potent in stimulating the growth of osteoblastic cells. However, due to the technical limitation, their diastereoisomer cannot be synthesized or isolated. Therefore, compound A is not the first choice for use in further study. Among the six stereospecific isomers, C1, C2, D1 and D2 were able to stimulate the growth of UMR-106 cells significantly and only compound C1 could increase the ALP activities of osteoblastic cells significantly. C1 is also found to be active in promoting the cell proliferation rate of UMR-106 cells at low concentration range. Therefore, C1 is having more advantage than the other compounds in the osteoblastic model.

In the ER activation, C1 selectively activated the ER-α mediated ERE transcriptional event but not ER-β. The activation of ERE transcriptional activities of C1 is found to be weaker than its enantiomers (C2) and diastereromers (D1 & D2). Compound C2, D1 and D2 activated both the ER-α and ER-β mediated ERE transcriptional events with at least one fold difference to the negative control group. The activity on ERE transcriptional event might not be the key factor that affects the osteoprotective effect of compound. Using naringin as an example, our previous study had demonstrated that naringin could increase the BMD of ovariectomized (OVX) mice but naringin could only weakly activate ER-α and ER-β mediated ERE luciferase activities in UMR 106 cells (Pang, Wang et al. 2010). This indicated the activation of ERE-dependent transcriptional activities of naringin at a particular time point might only relate to part of the bone protective effects and hence the weak activation of ERE transcriptional events in C1 might not affect its bone protective effects. In addition, the weak ERE transcriptional events in C1 might also reduce the side effects as strong ER activation might sometime related to the stimulation of breast cancer cells.

By integrating this information, C1 are selected as the candidate for further characterization on cell remodeling process by using pre-osteoblast MC3T3-E1 and pre-osteoclast RAW264.7 cells.

3.5   Summary

In this chapter, the bone protective effects of different flavan-3-ols compounds were demonstrated by the cell proliferation and cell differentiation rate in osteoblastic-like UMR-106 cells. Flavan-3-ols were found to exert estrogen-like activities which were demonstrated by their abilities to induce the growth of ER positive human breast cancer MCF-7 cells. The blocking effects of ER antagonist on the growth of UMR-106 cells also confirmed the estrogen-like activities of flavan-3-ols. These estrogenic properties were found to be related to the chemical structure and orientation of the flavan-3-ols which could be reflected by ER-mediated ERE luciferase activities but not direct ER binding. These results facilitated the selection of a flavan-3-ols candidate for further investigation of its effects on bone metabolism.

C1 or (-)-epiafzelechin was selected for further investigation as it could promote the cell proliferation and cell differentiation rate in UMR-106 cells. It could also activate the ER-α mediated ERE transcriptional response selectively.
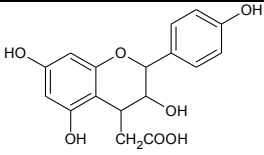
Compound	ER-α Binding	ER-β Binding
Compound A	X	X
Compound B	X	X
Compound C$_1$	X	X
Compound C$_2$	X	X
Compound D$_1$	X	X
Compound D$_2$	X	X
Compound F$_1$	X	X
Compound F$_2$	X	X
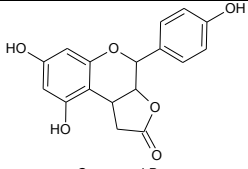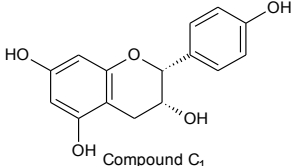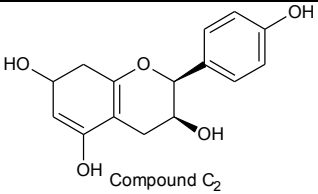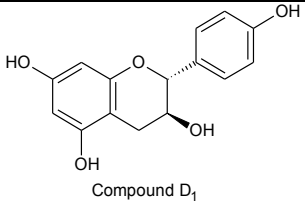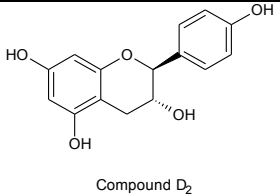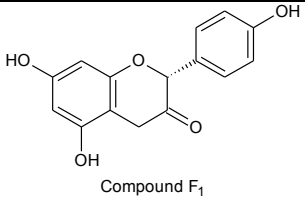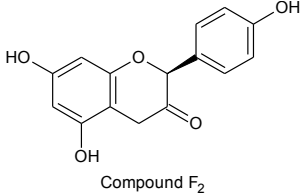
Table 3-1 Summary table of flavan-3-ols structures and their ER binding affinities

	Treatment	0	10^{-14}	10^{-12}	10^{-10}	10^{-8}	10^{-6}	Co-incubation of 10^{-8}M compound and 10^{-7}M ER blocker
					Concentration			
	E2		-	-	-	1.44***	-	-47%^^^
	A		1.07	1.12**	1.45***	1.52***	1.13*	-36%^^^
UMR-106	B	1.00	1.05	1.12*	1.15**	1.35***	1.30***	-30%^^^
Cell Proliferation	C1		1.36**	1.26*	1.24*	1.12	1.02	-27%^
	D1		1.20	1.36*	1.40**	1.56**	1.06	-39%^^
	F1		1.48**	1.39**	1.38**	1.37***	0.82***	-14%
	E2		-	-	-	1.19**	-	
	A		1.58***	1.46***	1.46***	1.41***	1.13*	
MCF-7	B	1.00	1.50*	1.49***	1.42***	1.44***	1.18*	
Cell Proliferation	C1		1.30***	1.28**	1.27**	1.37***	1.15**	
	D1		1.27**	1.23**	1.06	1.21**	0.95	
	F1		1.02	1.36***	1.25*	1.32*	0.91	

Table 3-2 Summary table for the results of flavan-3-ols
**P<0.01 & ***P<0.001 vs Ctrl; ^P<0.05, ^^P<0.01 & ^^^P<0.001 compared among same group with and without blocker, n=3

	Treatment	Concentration					
		0	10^{-14}	10^{-12}	10^{-10}	10^{-8}	10^{-6}
	E2		-	-	-	1.32***	-
	C1		1.31*	1.13**	1.12**	1.10*	1.14***
UMR-106	C2		1.19*	1.25**	1.08*	10.9*	1.17**
Cell Proliferation	D1	1.00	1.10*	1.08	1.03	1.08*	1.10
	D2		1.12*	1.03	0.97	0.96	0.97
	F1		1.06	1.07	1.04	0.94	0.96
	F2		1.14	1.07	1.04	0.99	1.05
	E2		-	-	-	1.11**	-
	C1		1.06	1.06*	1.02	1.04	1.00
UMR-106	C2		1.02	1.04	1.03	0.97	0.94
Cell Differentiation	D1	1.00	1.01	1.03	1.04	1.05	1.05
	D2		1.08	1.06	0.98	1.03	0.95
	F1		1.54	1.01	0.87	0.97	1.01
	F2		0.88	0.93	0.93	0.98	1.02
	E2		-	-	-	2.77***	-
	C1		1.59*	1.53	1.02	1.00	1.18
	C2		2.56***	2.93***	3.07***	2.50***	2.11***
ER-α mediated ERE luciferase activity	D1	1.00	1.17	2.21*	2.58**	2.37*	2.53**
	D2		1.11	2.25**	2.13***	2.29**	2.58**
	F1		1.53	1.46	1.51	1.60	1.42
	F2		1.76	1.40	1.51	1.58	1.40*
	E2		-	-	-	4.68***	-
	C1		1.44	1.19	0.92	0.94	0.87
	C2		3.00***	2.65***	3.08***	2.64***	2.21***
ER-β mediated ERE luciferase activity	D1	1.00	1.08	2.50***	2.55**	3.98***	2.99***
	D2		1.13	2.06***	2.10*	2.19**	2.79**
	F1		1.04	1.14	1.39	1.44	1.92***
	F2		1.23**	1.31*	1.24	1.22	1.64**

Table 3-3 Summary table for the results of stereospecific flavan-3-ols
* *P*<0.05, **P*<0.01 & ***P*<0.001 vs Ctrl, n=3

4   Characterization of Selected Flavan-3-ol on Osteoblasts and Osteoclasts

Functions

4.1   Introduction

Based on the results from the previous chapter, compound C1 was selected as the candidate for further study in the protective effects on bone. It was chosen because of its stereo-specificity and the ability to promote the growth and differentiation of UMR-106 cells. The chemical name of C1 is (-)-epiafzelechin or 3:5:7:4' tetrahyfroxy-flavan. It was earliest discovered in the ether-extracts of the heartwood of *Afzelia* species in 1955 and was named as epiafzelechin owing to the structure similarity to epicatechin (King 1955). (-)-Epiafzelechin was also found in plants such as *Cassia sieberiana*, *Typha capensis*, *Artocarpus dadah* and *Drynaria fortunei* (Wan and Chan 2004; Kafui Kpegba 2011). 94 mg of (-)-epiafzelechin could be extracted from 6kg of DF raw herbs with a series of chromatography procedures. Large amount of (-)-epiafzelechin could only be obtained from plant source in a large scale separation and purification processes. The limited supply of (-)-epiafzelechin do not favor the study of (-)-epiafzelechin in different biological system. In contrast, the chemical synthesis of (-)-epiafzelechin might be a good source to providing sufficient amount of high purity (-)-epiafzelechin for larger scale characterization in biological system.

Biological study suggested that (-)-epiafzelechin could inhibit the cyclooxygenase-1 (COX-1) enzyme activities to relief pain and inflammation where COX activity is used to evaluate the cancer chemopreventive properties of drug candidates (Su, Cuendet et al. 2002). (-)-epiafzelechin could also stimulate the proliferation on osteoblastic cells (Wan and Chan 2004) and protect the body by its antioxidative properties (Kpegba 2011). Because we are interested in the bone protective effects of

(-)-epiafzelechin and hence we extended the study to the effects of (-)-epiafzelechin on the bone remodeling process.

Bone remodeling is a continuous process involving bone formation and bone resorption. They are regulated by osteoblasts (Ob) and osteoclasts (Oc). The greater bone formation rate than bone resorption rate resulted in bone gain while the greater bone resorption rate than bone formation rate resulted in bone loss. The previous part of our study employed a mature osteoblastic UMR-106 cells which could only reflect the effects of flavan-3-ols in a highly differentiated Ob model. In the present study, the precursor cells involved in osteoblastogenesis and osteoclastogenesis were used to elucidate the actions of (-)-epiafzelechin on the bone remodeling process.

Murine pre-osteoblastic MC3T3-E1 cell line (Kartsogiannis and Ng 2004) was used to characterize the differentiation effects of (-)-epiafzelechin on osteoblastogenesis. MC3T3-E1 subclone 14 used in this study exhibits high level of Ob differentiation and mineralization in the presence of ascorbic acid and inorganic phosphate (Wang, Christensen et al. 1999). The bone formation markers such as ALP activity, collagen level and calcium deposition were measured to indicate the degree of Ob differentiation. ALP activity is a common bone formation marker in Ob. It is also used to evaluate the effects of treatment on bone formation in animal study. Collagen is found abundantly in the organic matrix of bone. The high collagen level expressed in extracellular matrix (ECM) indicates the differentiation rate of Ob. Calcium is found abundantly in the inorganic matrix to build up the hydroxylapatite (HAP) structure. The calcium deposition reflects the degree of mineralization upon Ob differentiation. Apart from the bone formation markers, gene expression such as osteoblast-related transcription factor Cbfa1/Runx2, and osteocalcin (OCN)

expressed in MC3T3-E1 were also used to characterize the degree of Ob differentiation (Wang, Christensen et al. 1999). Runx2 is a transcriptional factor that regulates Ob differentiation (Karsenty 2000). It is also found to be positively related to the expression of OCN, or bone gamma-carboxyglutamic acid-containing protein and collagen 1a1 protein (Ducy, Zhang et al. 1997).

Murine leukemia monocyte RAW264.7 cells (Vincent 2009) was used to characterize the effects of (-)-epiafzelechin on osteoclastogenesis. RAW264.7 is a common *in vitro* model representing the Oc. There are two main stages of RAW264.7, precursor cells and mature cells. The effects of (-)-epiafzelechin were characterized in both precursor cells and mature cells of RAW264.7. The toxicity effects of (-)-epiafzelechin on pre-Oc was determined by the cell viability of the RAW264.7 precursor cells while the effects of (-)-epiafzelechin on differentiating mature Oc was determined by the RAW264.7 mature cells.

RAW264.7 cells expressed high level of transmembrane protein – receptor activator of NF-κB (RANK) (Cuetara, Crotti et al. 2006). It can be differentiated into mature Oc by the induction of RANK ligand (RANKL) (Khosla 2001; Boyce and Xing 2008). The degree of differentiation of RAW264.7 cells was determined by the tartrate resistant acid phosphtase (TRAP) enzyme activity upon RANKL induction.

RAW264.7 mature cells express high TRAP enzyme activity (Cuetara, Crotti et al. 2006) that could hydrolyze the phosphate esters and anhydrides in acidic condition. Total immunoreactive TRAP is increased in growing children and post-menopausal women, suggesting that TRAP is important in bone resorption (Oddie, Schenk et al. 2000). *In vitro* study also demonstrated the use of anti-TRAP antibodies could reduce the bone resorption activities (Moonga, Moss et al. 1990).

Hunter and Goldberg (1994) suggested that BSP could stabilize the HAP by nucleating HAP into steady state. While TRAP was suggested to digest phosphoproteins such as BSP found in the matrix (Andersson and Ek-Rylander 1995). Taken these into account, the digestion of BSP by TRAP could destabilize the HAP and lead to bone resorption (Hunter and Goldberg 1994). In addition, other mechanistic study also suggested that BSP is the substrate for TRAP. Upon binding, TRAP dephosphorylates the serine residue of osteopontin and facilitates migration of Oc across the bone surface for new resorption site (Ek-Rylander, Flores et al. 1994). These evidences suggested that the TRAP is an important protein during bone resorption. Hence, the expression of TRAP in mature Oc upon RANKL induction was used to determine the effects of (-)-epiafzelechin in bone resorption.

By the observations of Ob and Oc, the bone protective effects of (-)-epiafzelechin could be elucidated in this study.

4.2　Methodology

4.2.1　Culture of murine pre-osteoblastic and leukemia osteoclastic cell lines

MC3T3-E1 subclone 14 pre-osteoblastic cells and RAW 264.7 leukemia cells were cultured in modified eagle medium alpha (MEMα) (Gibco, USA) and Dulbecco's Modified Eagle's Medium (DMEM, ATCC), respectively, with the supplementary of 10% fetal bovine serum (FBS), 100 U/ml penicillin and 100μg/ml streptomycin (Invitrogen, Carlsbad, CA). The culture environment was controlled at 37°C, 95% humidity and 5% of CO_2. Cells were sub-cultured every 3-4 days for routine culture. During treatment, Ob differentiation medium (MEMα with 10% FBS, 100 U/ml penicillin, 100μg/ml streptomycin, 25μg/ml of ascorbic acid and 10mM of β-glycerophoshpate) was used to differentiate MC3T3-E1 cells, while Oc differentiation medium (MEMα with 10% FBS, 100 U/ml penicillin and 100μg/ml streptomycin with 100ng/ml RANKL) was used to differentiate RAW 264.7 cells.

4.2.2　ALP activities of MC3T3-E1 cells

MC3T3-E1 cells were cultured in 24 well plates with a cell density of 1.2×10^{4} cells per well. After two days of culture, the medium was replaced by differentiation medium with 10^{-8}M E2, vehicle and different concentrations of compound C1. The medium was changed for every 3 or 4 days. After 7 days, the cell lysate was collected by passive lysis buffer (Promega). The ALP activity was determined by Wako lab assay ALP (Wako, Japan) and the protein content was determined by Bradford protein assay (Bio-rad). The optical density of 405nm and 595nm was recorded by spectrophotometric plate reader (Bio-Rad model 550) for ALP and Bradford, respectively.

4.2.3 Mineralization of MC3T3-E1 cells

MC3T3-E1 cells were cultured in 12 well plate with a cell density of 2×10^4 cells per well. After two days of culture, the medium was replaced by differentiation medium with 10^{-8}M E2, vehicle and different concentrations of compound C1. The medium was changed for every 3-4 days. After 21 days, the cells were washed with PBS and fixed in 50% ethanol. Cells were then stained with 1% Alizarin Red S for five minutes. The stained cells image was captured for visual comparison. The stained cultures were further dissolved in 0.5M HCl and 5% SDS and shake for 30 minutes. The optical density of the dissolved culture was detected by spectrophotometric plate reader at 415nm and was referred to the degree of mineralization (Bio-Rad model 550, Japan).

4.2.4 Extracellular matrix (ECM) Collagen of MC3T3-E1 cells

MC3T3-E1 cells were cultured in 12 well plate with a cell density of 2×10^4 cells per well. After two days of culture, the medium was replaced by differentiation medium with 10^{-8}M E2, vehicle and different concentrations of compound C1. Acid-pepsin soluble collagen was extracted from cell layers by 0.5M of acetic acid and 0.1mg/ml pepsin at 4^oC overnight. After incubation, the lysed was centrifuged for 1 hour at 14,000g. The supernatant was used to conduct collagen assay according to the soluble collagen assay (Sircol, UK) manual. In brief, the supernatant was mixed with the Sircol Dye reagent and placed in a shaker for 30 minutes. It is than placed in a microcentrifuge and spin for 12,000 r.p.m for 10 minutes. The dye was removed and the pellet was washed by the acid-salt wash and underwent centrifugation again. The pellet was dissolved in alkaline solution for determining the optical density at 540nm by spectrophotometric plate reader (Bio-Rad model 550, Japan).

4.2.5 Gene expression of MC3T3-E1 cells

MC3T3-E1 cells were cultured in 12 well plate with a cell density of 2 x 10^4 cells per well. After two days of culture, the medium was replaced by differentiation medium with 10^{-8}M E2, vehicle and different concentrations of compound C1. The cells were washed with ice-cold PBS. 1ml of Trizol (Invitogen) was added and total RNA was extracted according to the manufacturer's manual with chloroform and isopropanol. Total RNA concentration was measured by the 260/280nm ratio. 2µg of total RNA was used to perform reverse transcription (RT) polymerase chain reaction (PCR) to construct the complementary cDNA by cDNA synthesis kit (Applied biosystems). The cDNA was then diluted for real time PCR analysis by using 7900HT (Applied biosystems) and EvaGreen real time PCR supermix (Bio-rad). The standard curve was constructed by using the vehicle cDNA template in different concentration. The concentrations of unknown samples were calculated by fitting the ct value to the standard curve by the SDS software (Applied biosystems).

Gene	Forward	Reverse	Tm
Runx2	gTCAgCAAAgCTTCTTTTgg	TTgTTgCTgTTgCTgTTgTT	57^oC
OCN	CgCTCTgTCTCTCTgACCTC	TCACAAgCAgggTTAAgCTC	57^oC
Col-1	AATggTgCTCCTggTATTgC	ggCACCAgTgTCTCCTTTgT	58^oC
β-actin	AAgAgCTATgAgCTgCCTgA	TggCATAgAggTCTTTACgg	56^oC

Table 4-1 Forward and Reverse Primers for gene candidates in MC3T3-E1 cells

4.2.6   Cell proliferation of RAW264.7 cells

RAW 264.7 cells were cultured in 96 well plate with a cell density of 10^4 cells per well. After one day, 10^{-8}M E2, vehicle and different concentrations of compound C1 were added to the medium and cultured for another 4 days. After treatment, the cells viability was determined by MTS assay (3-(4,5-dimethylthiazol-2-yl)-5- (3-carboxymethoxyphenyl)-2-(4-sulfophenyl)- 2H-tetrazolium). (Promega) After 2 hours, the optical densities at 490nm were recorded by spectrophotometric plate reader (Bio-Rad model 550, Japan).

4.2.7   TRAP staining of RAW264.7 cells

RAW 264.7 cells were cultured in 12 well plate with a cell density of 10^5 cells per well. After one day, the medium was replaced by differentiation medium with 10^{-8}M E2, vehicle and different concentration of compound C1. The medium was changed for every two to three days. After 5 days of culture, cells were collected for cytochemical staining. Cells were fixed and stained for TRAP by using acid phosphatase staining kit (Sigma). TRAP-positive multinucleated cells showing more than three nuclei were countered as mature osteoclasts.

4.2.8 TRAP activity measurement of RAW264.7 cells

RAW 264.7 cells were cultured in 12 well plate with a cell density of 10^5 per cells well. After one day, the medium was replaced by differentiation medium with 10^{-8}M E2, vehicle and different concentrations of compound C1. The medium was changed for every two to three days. After 5 days of culture, the TRAP activities of RAW264.7-derived osteoclasts were measured by the acid phosphatase assay kit (BioVision, USA). In brief, the cells were lysed and incubated with reaction buffer containing paranitrophenylphosphate (pNPP) for 1 hour. The optical densities at 405nm were recorded by using spectrophotometric plate reader. ODs were compared to a standard curve calibrate with paranitrophenol (pNP). Protein contents were quantified by Bradford protein assay (Biorad). Results were expressed as micro-moles of pNP/mg protein.

4.2.9 Statistical Analysis

Results were reported as mean ± standard error mean (SEM). Significant differences between different groups of means were evaluated by student t-test in confidence level at 95% ($P<0.05$).

4.3 Results

4.3.1 Effect of compound C1 on ALP activities of MC3T3-E1 cells

Upon 7 days treatment, the ALP activities of pre-osteoblast MC3T3-E1 cells were increased by the treatment of E2 and C1 **(Figure 4.1)**. E2 increased the ALP activity by 24% ($P<0.01$ vs. Ctrl) and C1 increased the ALP activity by 14% ($P<0.05$ vs. Ctrl), 29% ($P<0.05$ vs. Ctrl) and 22% ($P<0.01$ vs. Ctrl) at 10^{-10}, 10^{-8} and 10^{-6}M respectively. The effect of C1 was not significant at the lower concentrations. The ALP activity was not significantly increased in MCM3T3-E1 cells for 3 days treatment of C1 and E2 (data not shown). The mRNA expression of ALP was also found to be low in MC3T3-E1 cells for 3 days C1 and E2 treatments (data not shown).

4.3.2 Effect of compound C1 on ECM collagen content of MC3T3-E1 cells

Upon 7 days treatment, ECM collagen level was significantly suppressed in response to E2 ($P<0.01$) but significantly increased in response to 10^{-10} to 10^{-6}M of compound C1 **(Figure 4.2)**. A dose dependent effect on ECM collagen level was observed for C1 and reached a peak at 10^{-7} (Increased by 41%, $P<0.001$ vs. Ctrl).
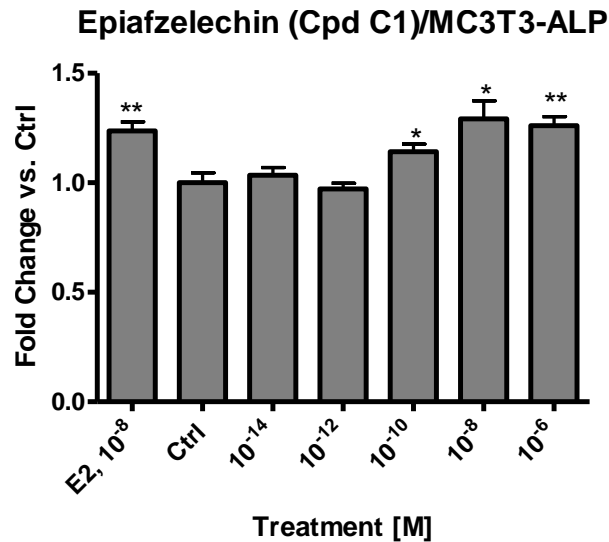
Figure 4.1Effect of compound C1 on the ALP activity in MC3T3-E1 cells
ALP assay was performed after cells were treated with 10^{-8}M of E_2, 10^{-14} to 10^{-6}M of compound C1 and its vehicle (1% EtOH v/v) for **7** days. The bars represent mean ± SEM value with n=3. *$P<0.05$ and **$P<0.01$ versus control.
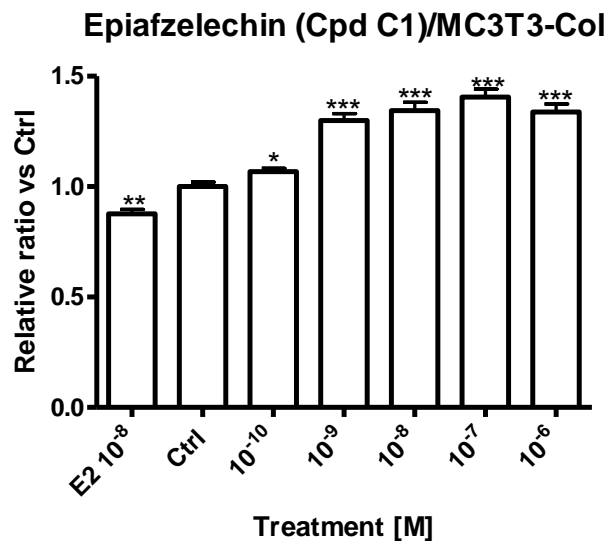
Figure 4.2Effect of compound C1 on ECM collagen content in MC3T3-E1 cells
Collagen assay was performed after cells were treated with 10^{-8}M of E_2, 10^{-10} to 10^{-6}M of compound C1 and its vehicle (1% EtOH v/v) for **7** days. The bars represent mean ± SEM value with n=3. *$P<0.05$, **$P<0.01$ and ***$P<0.001$ versus control.

4.3.3　Effect of compound C1 on Mineralization of MC3T3-E1 cells

The mineralization of pre-osteoblast was increased by 13% ($P<0.01$ vs. Ctrl) in response to treatment with E2 **(Figure 4.3)**. Compound C1 did not increase the level of mineralization of MC3T3-E1 cells. In contrast, inhibitory effects on mineralization were found in MC3T3-E1 cells in response to treatment with high concentrations of C1 at 10^{-7} and 10^{-6}M.

Epiafzelechin (Cpd C1)/MC3T3-ARS

Figure 4.3 Effect of compound C1 on Mineralization of MC3T3-E1 cells
Alizard Red S staining was performed after cells were treated with 10^{-8}M of E_2, 10^{-10} to 10^{-6}M of compound C1 and its vehicle (1% EtOH v/v) for **21** days. The stained plated were dissolved in 5% SDS and 0.5M HCl for colorimetric determination. The bars represent mean ± SEM value with n=3. *$P<0.05$, **$P<0.01$ and ***$P<0.001$ versus control.

E2

Ct

C1 10^{-10}

C1 10^{-9}

C1 10^{-8}

C1 10^{-7}

C1 10^{-6}

Figure 4.4 Effect of compound C1 on Alizard Red S staining of MC3T3-E1 cells
Alizard Red S staining was performed after cells were treated with 10^{-8}M of E_2, 10^{-10} to 10^{-6}M of compound C1 and its vehicle (1% EtOH v/v) for 21 days.

4.3.4 Effect of compound C1 on osteoblast-specific gene expression in MC3T3-E1 cells

Runx2 mRNA expression

Treatment with E2 at 10^{-8}M for 3 days significantly increased the Runx2 mRNA expression ($P<0.001$ vs. Ctrl) in MC3T3-E1 cells (**Figure 4.5A**). Similarly, C1 could significantly increased Runx2 mRNA expression by 1.3 fold ($P<0.01$ vs. Ctrl), 0.8 fold ($P<0.05$ vs. Ctrl) and 0.8 fold ($P<0.01$ vs. Ctrl) at 10^{-8}, 10^{-7} and 10^{-6}M, respectively. This effect was not significant in the lower concentrations range of C1.

Collagen 1α1 mRNA expression

Treatment with E2 at 10^{-8}M for 3 days did not increase the collagen1α1 gene expression in MC3T3-E1 cells (Figure 4.5B). Collagen1α1 gene expression was upregulated by C1 at 10^{-8}M in MC3T3-E1 cells by 0.8 fold ($P<0.05$ vs. Ctrl) but not the other concentrations.

Osteocalcin mRNA expression

Treatment with E2 at 10^{-8}M for 3 days significantly increased the osteocalcin mRNA expression by 40% ($P<0.01$ vs. Ctrl) in MC3T3-E1 cells (Figure 4.5C). C1 increased osteocalcin gene expression in MC3T3-E1 cells by 444% ($P<0.01$ vs.ctrl) and 38% ($P<0.01$ vs.ctrl) at concentration 10^{-8} and 10^{-6}M, respectively.

A

B

Epiafzelechin (Cpd C1)/MC3T3-Runx2-gene

Epiafzelechin (Cpd C1)/MC3T3-Col1-gene

C

Epiafzelechin (Cpd C1)/MC3T3-Osc-gene
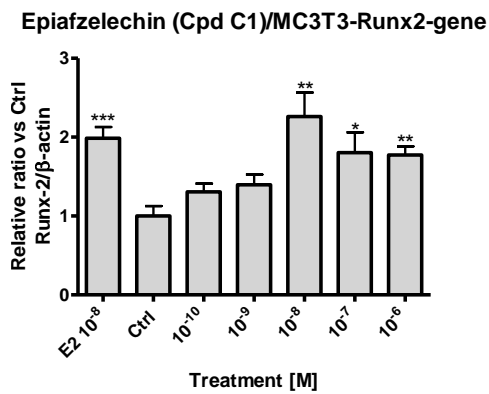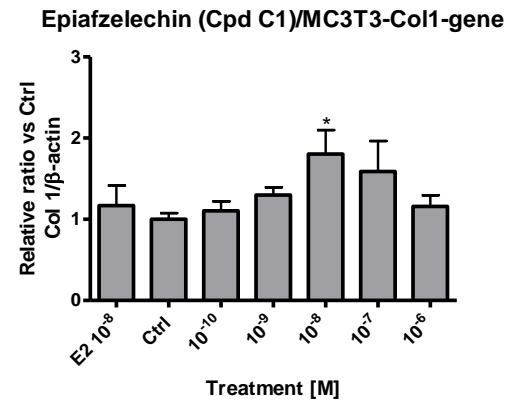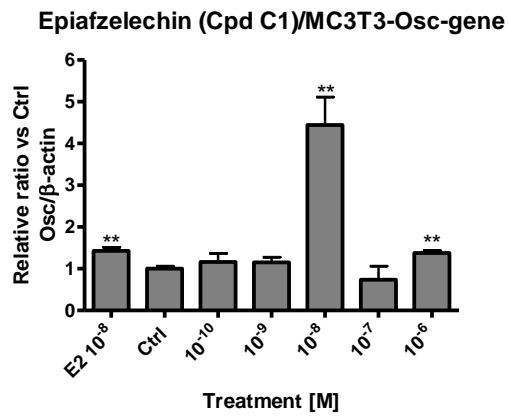
Figure 4.5 Effect of compound C1 on osteoblast-specific gene expression in MC3T3-E1 cells

The gene expression level of (A) Runx2, (B) Col 1, and (C) Osc were determined after cells were treated with 10^{-8}M of E_2, 10^{-10} to 10^{-6}M of compound C1 and its vehicle (1% EtOH v/v) for **3** days. 2μg RNA was collected by Trizol® reagent and underwent rt-PCR to yield cDNA template for Q-PCR. The bars represent mean ± SEM value with n=3. *$P<0.05$, **$P<0.01$ and ***$P<0.001$ versus control.

4.3.5 Effect of compound C1 on the cell viability of RAW 264.7 cells

E2 treatment at 10^{-8}M did not alter the growth of osteoclast precursor cells RAW264.7 (**Figure 4.6**). In contrast, treatment of RAW 164.7 cells with C1 (10^{-10} to 10^{-6}M) for 4 days significantly reduced the growth of osteoclasts precursor cells by 47% to 61% ($P<0.05$).

Epiafzelechin (Cpd C1)/RAW-MTS
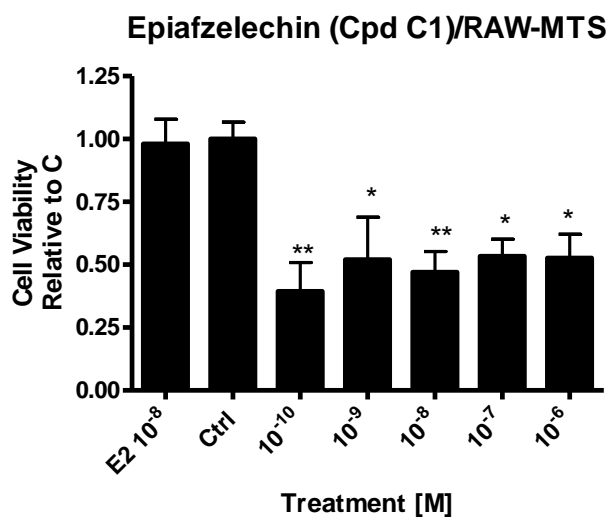
Figure 4.6 Effect of compound C1 on the cell viability of RAW 264.7 cells
MTS assay was performed after cells were treated with 10^{-8}M of E_2, 10^{-14} to 10^{-6}M of compound A, B, C1, D1, F1 and its vehicle (1% EtOH v/v) for four days. The bars represent mean ± SEM value with n=3. *$P<0.05$ and **$P<0.01$versus control.

4.3.6 Effect of compound C1 on the morphology and number of multinucleated cells formed in RANKL induced RAW 264.7 cells

Both E2 and C1 treatment prevented the formation of multinucleated cells in RAW264.7 cells upon RANKL induction. The cells with more than three nucleuses were counted as multinucleated mature osteoclasts. The multinucleated cell counting was decreased by 37% ($P<0.001$ vs. Ctrl) in RANKL-induced RAW264.7 cells with E2 treatment at 10^{-8}M **(Figure 4.7)**. The inhibitory effect was also observed in cells treated with 10^{-10} to 10^{-6}M of C1. The number of multinucleated cells formed was decreased by 14% to 30% in RANKL-induced RAW 264.7 cells upon treatment with C1 ($P<0.05$ vs. control). The maximum inhibitory effect was observed in cells treated with high concentration of C1 (10^{-6}M).

4.3.7 Effect of compound C1 on the TRAP activities in RANKL induced RAW 264.7 cells

E2 inhibited TRAP activity in RANKL-induced RAW264.7 cells by 12% ($P<0.05$ vs. Ctrl). This effect was also observed in cells treated with 10^{-10} to 10^{-6}M of C1. TRAP activities in RANKL-induced RAW 264.7 cells were found to be decreased by 13% to 26% in the presence of C1 **(Figure 4.9).**
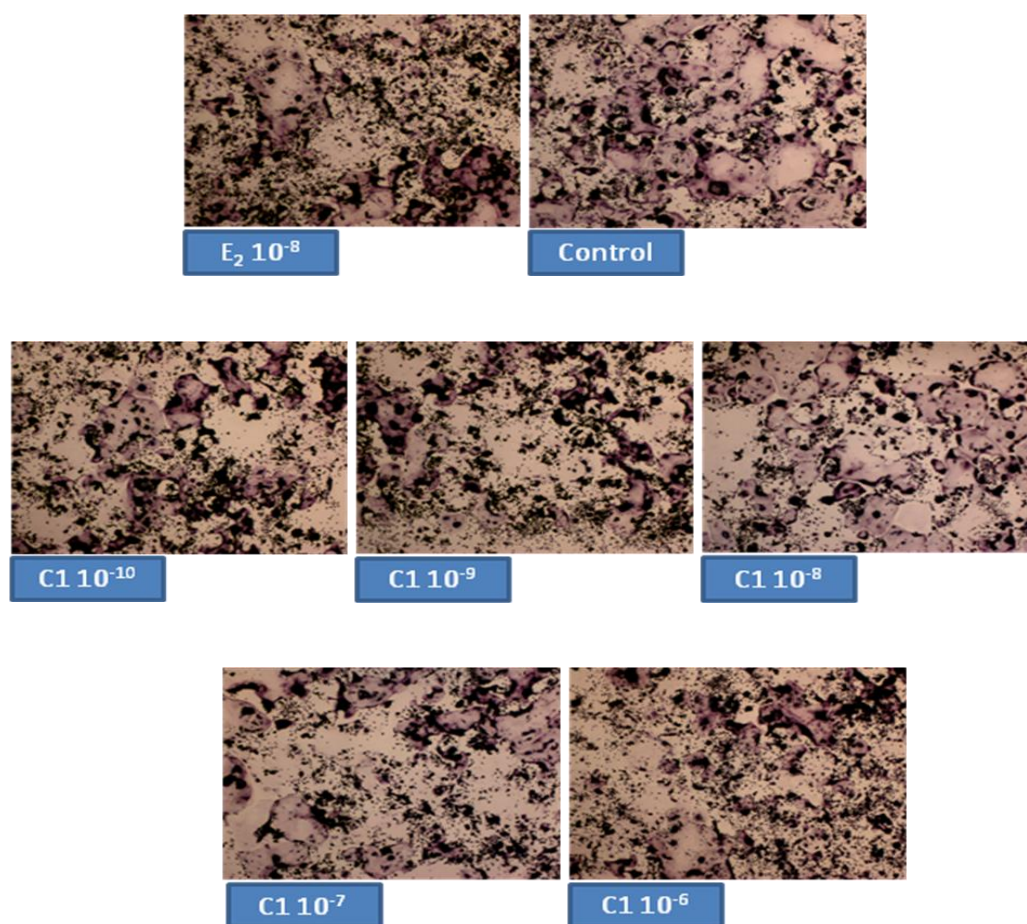
Magnification: 200x

Figure 4.7 The morphology of RANKL induced maturation of RAW 264.7 cells after TRAP staining
TRAP staining was performed after cells were treated with 10^{-8}M of E_2, 10^{-10} to 10^{-6} M of compound C1 and its vehicle (1% EtOH v/v) for five days.

Epiafzelechin (Cpd C1)/RAW-No.Oc
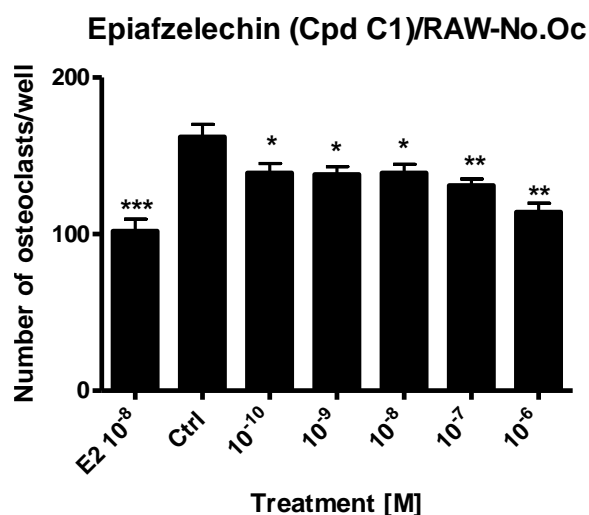
Figure 4.8 Effect of compound C1 on the number of TRAP stained multinucleated cells formed in RANKL-induced RAW 264.7 cells
TRAP staining was performed after cells were treated with 10^{-8}M of E_2, 10^{-10} to 10^{-6}M of compound C1 and its vehicle (1% EtOH v/v) for five days. The bars represent mean ± SEM value with n=3. *$P<0.05$ and **$P<0.01$versus control.

Epiafzelechin (Cpd C1)/RAW-TRAP
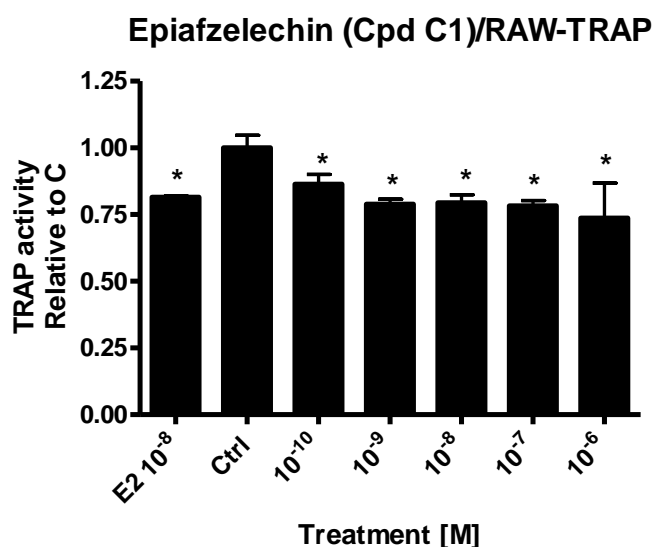
Figure 4.9 Effects of compound C1 on the TRAP activities in RANKL-induced RAW264.7 cells
TRAP activity was determined after cells were treated with 10^{-8}M of E_2, 10^{-10} to 10^{-6}M of compound C1 and its vehicle (1% EtOH v/v) for five days. The bars represent mean ± SEM value with n=3. *$P<0.05$ versus control.

4.4   Discussion:

4.4.1   Bone Formation Marker – ALP

ALP activity is measured in bone related studies to represent the differentiation of *in vitro* osteoblastic cells and the bone formation of *in vivo* animals (Kushida 1995). A significant increased in ALP activities were observed in 7 days but not 3 days treatment of E2 and C1 in MC3T3-E1 cells. An adequate treatment time is necessary for E2 and C1 to induce the ALP expression in pre-osteoblastic MC3T3-E1 cells. In fact, a low ALP mRNA expression was also found in the gene expression analysis on day three of treatment. A longer time is required for the cells to express the ALP by the ascorbic acid and inorganic phosphate presence in the differentiation medium (Wang, Christensen et al. 1999).

The promotional effects on ALP activity in MC3T3-E1 cells was at a higher concentration range of C1 tested range (e.g. 0.1nM to 1µM). The concentration range used in this assay was based on the previous results using UMR 106 cells in the previous chapter that cover 10^9 fold with 100 folds interval. To narrow down the range, the active range (0.1nM to 1µM) of C1 in promoting the ALP activities were selected for further characterization in the bone remodeling process. The active range of C1 in mature osteoblastic-like UMR-106 cells and pre-osteoblast MC3T3-E1 cells were different. This might due to different cell type response differently to C1. On the other hand, the incubation time of C1 was longer in MC3T3-E1 cells than UMR-106 cells. The C1 might be metabolized by the cells in longer incubation time and reduce the C1 availability. Hence, a higher concentration was needed for a significant effect.

4.4.2   Bone Organic Deposition by MC3T3-E1

Osteoblasts are involved in the deposition of organic matrix on the bone formation surface. The deposition begins in the early phase of the maturation of pre-osteoblast (Quarles, Yohay et al. 1992). Treatment of C1 increased the collagen content in maturing Ob cells that helps the formation of ECM layer. The collagen assay used in this study is a dye-based method which cannot differentiate the types of collagens. It measured the total collagen rather than a specific type 1 collagen majorly found in bone formation. This method was acceptable because only single Ob cell line was cultured in the *in vitro* study (Manzano, Lozano et al. 2011) and the interference of other collagen found in other tissue was minimized. To further confirm the collagen formed was bone related, the bone related collagen type 1 alpha1 mRNA was also measured. The result was consistence with the collagen level in ECM layer. In both assay, the treatment of E2 did not increased the collagen level as well as the mRNA of collagen 1a1 in MC3T3-E1 cells. C1 is found to increase the ECM collagen level at all concentrations significantly but the collagen type 1 alpha1 mRNA was only significantly increased at 10^{-8}M. This discrepancy might be due to the use of different treatment time in these two assays.

Other than collagen, osteocalcin is another NCP found abundant in bone. It is secreted by Ob in serum and believed to regulate the bone metabolism by the recruitment of osteoclasts and osteoblasts (Chenu, Colucci et al. 1994). Osteocalcin is uniquely expressed by Ob but not the other cell types (Ducy 1995). The high binding affinity between osteocalcin and hydroxyapatite also suggesting osteocalcin is important for forming the crystal lattices structure of hydroxyapatite (Hoang, Sicheri et al. 2003). The upregulated osteocalcin mRNA expression also reflected the

increased differentiation rate of Ob by the treatment of E2 and C1. In fact, the secretory osteocalcin could also be detected by oseocalcin ELIZA kit. However, due to the low stability of osteocalcin, only the mRNA level for coding osteocalcin was measured in the current study.

4.4.3 Bone Mineralization by MC3T3-E1

After the deposition of organic matrix on the bone formation surface, the pre-osteoblast begins to mineralize by forming the crystal lattices structure with hydroxyapatite (Hoang, Sicheri et al. 2003). This is the later phase of bone formation in pre-osteoblastic cells. Hydroxyapatite is the dominate molecule found in bone, it is mainly composed of calcium and phosphate. The measurement of calcification in pre-osteoblast indicates the degree of mineralization (Choi, Lee et al. 1996). The stained region of calcified region of Ob was increased in MC3T3-E1 cells in response to treatment with E2 but not C1. Higher concentration of C1 treatment was found to decrease the mineralization of pre-osteoblast, which might delay the maturation of pre-osteoblasts to osteoblasts.

4.4.4 Regulation of MC3T3-E1

Cbfa1/Runx2 is an osteoblast-specific transcription factors (OSFs). It is a key regulator for Ob differentiation as well as bone formation (Zuo, Huang et al. 2012). The expression of Cbfa1/Runx2 is found in the whole process of osteoblastogenesis including the osteoprogenitor, pre-osteoblast, mature Ob and osteocyte cells (Westendorf, Kahler et al. 2004). It encodes the factors binding to osteoblast-specific element 2 (OSE2) and activates the gene in promoter region (Merriman, Vanwijnen et al. 1995). OSE2 or Cbfa1/Runx2 binding sites was found in osteocalcin, collagen

1a1, bone sialoprotein and osteopontin genes in osteoblasts where all these genes candidate are recognized as Ob differentiation markers (Ducy, Zhang et al. 1997).

The mRNA expression Cbfa1/Runx2 as well as the downstream gene candidate osteocalcin and collagen 1a1 were measured in this study. Interestingly, the activation of Runx2 gene did not upregulate all the responsive genes that contains OSE2 promoter. Both E2 and C1 were active in promoting Runx2 gene expression in MC3T3-E1 cells. However, E2 was only able to upregulate osteocalcin gene but not collagen 1a1 gene in MC3T3-E1 cells, while C1 was able to upregulate both of the gene candidates at 10nM. In contrast, the calcification of bone by pre-Ob was found in the treatment with E2 but not C1 although both treatments could activate Runx2 gene. Thus, the induction of Runx2 gene by C1 in MC3T3-E1 cells did not resulted in the increase in calcification of bone by pre-Ob. This might be explained by the fact that Runx2 activity could be controlled by post-translation modification. Others had reported that serine phosphorylation could alter the activity of Runx2 which in turn affect the downstream activation of other gene candidates (Franceschi, Ge et al. 2009). In fact, the regulation of Ob functions is far more complex (Zuo, Huang et al. 2012). Transcription factors other than Cbfa1/Runx2 might also be involved in the Ob regulation and affected the regulation of specific genes transcription.

4.4.5   Osteoclast precursor cells growth

The measurement of cell viability of RAW264.7 cells indicated C1 is a potential growth inhibitor of monocytes or the precursor cell of Oc. The decline in Oc precursor cells number might reduce the formation of Oc upon RANKL induction and reduce the rate of bone resorption. Interestingly, *Su and et al.* suggested that C1 was an anti-inflammatory agent (Su, Cuendet et al. 2002). This is in agreement with

our result shown that C1 was able to reduce the cell viability of monocytes, which is an important cell type involved in the inflammation process.

4.4.6 Bone resorption marker – TRAP

TRAP staining has indicated that the RANKL induced multinucleated Oc cells number was significantly decreased by C1 and E2 treatments. Because the former cell viability test suggested that C1 could decrease the cell number of RAW264.7 cells. The decreased in multinucleated Oc might due to less precursor cells upon the treatment by C1. Unlike C1, E2 did not reduce the cell viability of precursor cells. Thus, the reduction of TRAP+ multinucleated cells by E2 might due to its direct inhibiting actions on osteoclastogenesis. However, the reduction of TRAP+ multinucleated cells by C1 was not known as it might due to the toxicity effect to the precursor cells. In order to determine if C1 exerts direct inhibiting actions on Oc maturation, the TRAP activities in RANKL-induced Oc were detected. This assay provides a more specific measurement of the TRAP activity in mature osteoclastic cells. The protein assay included was used to normalize the cell content to eliminate the potential reduction of cells number due to the toxicity effects of C1. Our results suggested that both C1 and E2 were able to reduce the TRAP activities of mature osteoclastic cells, suggesting that C1 was not only reducing TRAP activities by decreasing the cell number of precursor cells but also prevent the RANKL-induced maturation of precursor cells.

4.4.7 The overall effects of C1 on Osteoblastogenesis and Osteoclastogenesis

In this study, C1 is hypothesized as a phytoestrogen to exert bone protective effects through regulating the bone remodeling process. C1 is found to increase osteoblastogenesis of pre-osteoblastic MC3T3-E1 cells by increasing ALP activity, ECM collagen content and various gene candidates such as Runx2, osteocalcin and collagen 1a1 **(Table 4-2 & Figure 4.10)**. It is also found to reduce the cell viability and prevent the maturation of Oc precursor cells **(Table 4-3 & Figure 4.10)**. Some of these effects are found to be comparable to E2.

The effects of C1 on bone metabolism are somehow similar to E2 but not exactly the same. The differential regulations of different biochemical markers or gene candidates by C1 and E2 implied that their behaviors on bone metabolism are somehow different. This might due to the different activation pattern to the corresponding receptors. At least, from the findings in chapter 3, the activation of our suggested corresponding receptors – ERs were not the same for E2 and C1. E2, as an agonist of ER, could bind to ER and activate both ER subtypes mediated ERE luciferase activity significantly. However, C1 could only selectively activate ER-α mediated ERE luciferase activity without any direct binding to ERs. The regulation of bone remodeling process is more complex and might involve other signaling pathways.

4.5   Summary

Taking the earlier and later phase of osteoblastogenesis of pre-osteblast into account, the effects of E2 and C1 share some similarity in the regulation of Runx2 and osteocalcin gene expressions. These suggested that C1 is likely to exert estrogenic-like activity on bone. The effects of E2 and C1 on collagen synthesis and calcification are different. The effects of E2 appeared to act on the latter stage of osteoblastogenesis while those of C1 appeared to act on the earlier stage of osteoblastogenesis **(Table 4-2 & Figure 4.10)**. In the osteoclastogenesis, treatment of C1 reduced the population of monocytes but not E2. Both C1 and E2 reduced the maturation of precursor cells of osteoclasts **(Table 4-3 & Figure 4.11)**. These results demonstrated E2 and C1 could enhance bone formation and inhibit bone resorption. The abilities of C1 to promote bone formation and prevent bone resorption concluded it as a potential candidate for managing osteoporosis. Hence, a further *in vivo* study will be important for elucidating the activities of C1 on bone and mineral metabolism in animal body.

Treatment 10^{-8}M	Gene expression			ALP	ECM Collagen	Mineralization
	Cbfa1/Runx2		Collagen 1a1			
E2	99%***	43%**	X	24%**	X	13%**
C1	126%**	344%**	81%**	29%*	41%***	X

Table 4-2 Summary table for the effects of E2 and C1 at 10^{-8}M on the osteoblastogenesis of MC3T3-E1 cells
* $P<0.05$, **$P<0.01$ & ***$P<0.001$ vs Ctrl
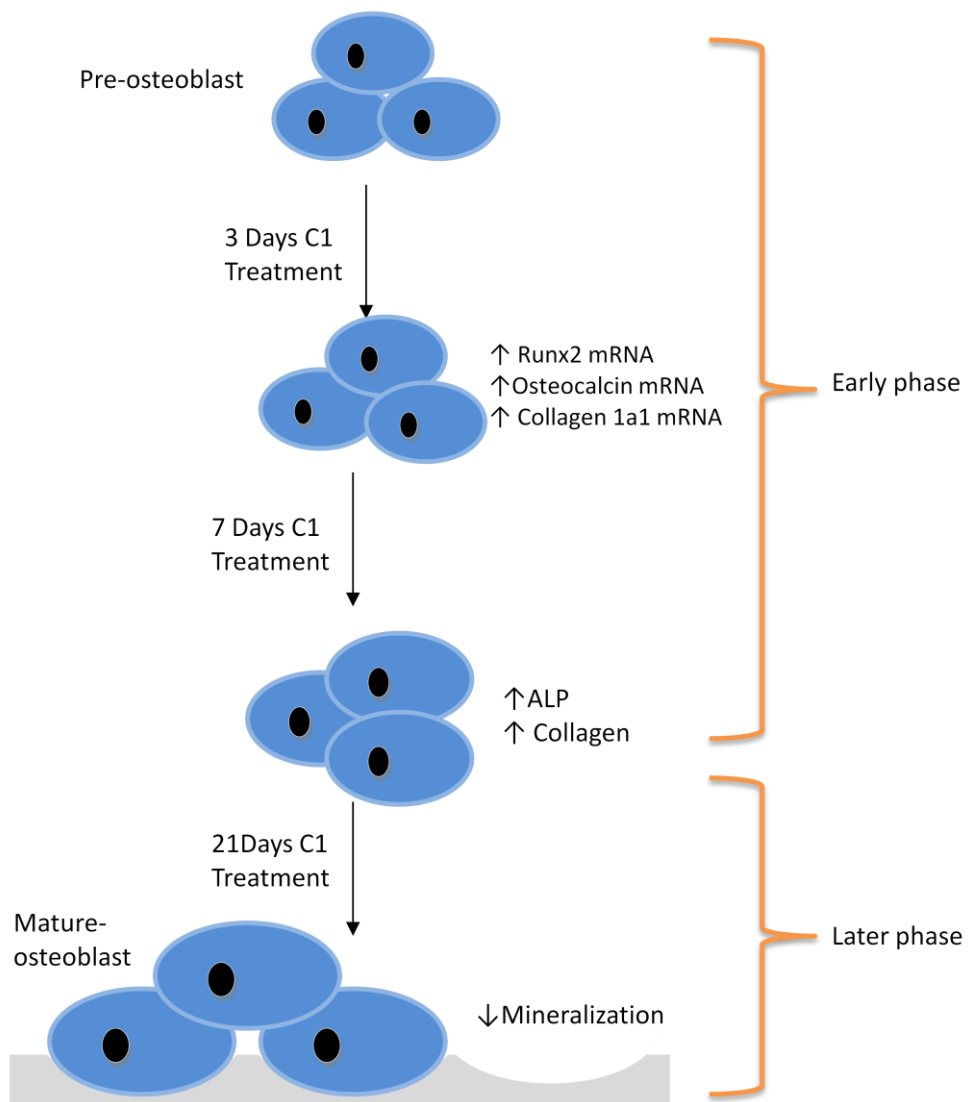
Figure 4.10 Graphical Illustrations of the effects of C1 on Osteoblastogenesis

Treatment 10^{-8}M	Precursor Cell viability	TRAP multinucleated cells	TRAP activity
E2	X	-37%***	-18%*
C1	-53%**	-14%**	-21%*

Table 4-3 Summary table on the effects of E2 and C1 at 10^{-8}M on the osteoclastogenesis of RAW 264.7 cells
* *P<0.05, **P<0.01 & ***P<0.001 vs Ctrl*
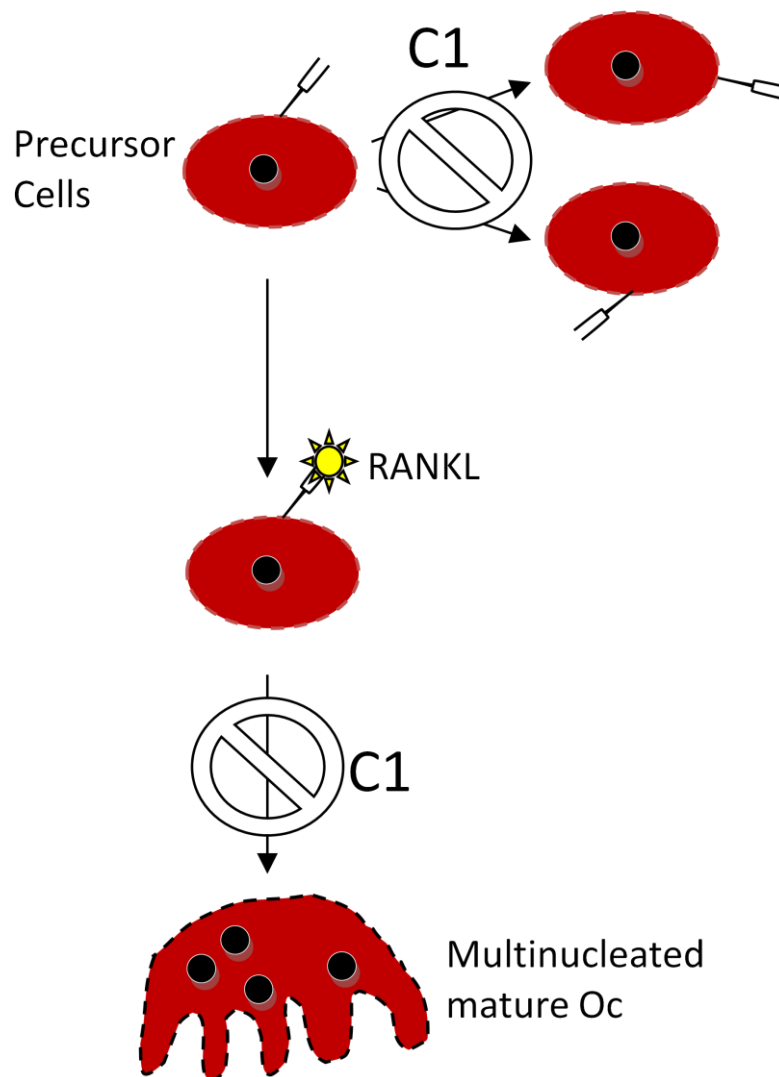
Figure 4.11 Graphical Illustrations of the Effects of C1 on Osteoclastogenesis

5 Method Development for the Detection of (-)-Epiafzelechin

5.1   Introduction:

The activities of C1 were demonstrated through *in vitro* osteoblastic and osteoclastic models in the previous chapter. Because of the potential beneficial effects of C1 on bone, therefore, we are interested in further characterize its bone protective effects in osteoporotic animal model. Study of bone protective agents in animal takes a long duration because bone remodeling is a slow process. The treatment time for the animal studies usually take at least two months (Mok, Chen et al. 2010). To ensure the effective dosage can be reached in the animal body, it is important to detect the plasma C1 concentration after administration. The plasma drug concentrations can be used to construct a pharmacokinetic profile for C1 to determine the dosage used in animal study. Well characterized chemicals are often detected by standard detection method such as functional assays or commercial available ELISA kits. However, there is not a standard detection method of (-)-epiafzelchin. Therefore, the detection methods for C1 in biological matrix are worthy to develop. Detection methods for compound with similar structure to C1 can be used as reference. Catechin, which is also classified as flavan-3-ols with one more hydroxyl group on the B ring of R5' than C1, has long been studied by analytical methods using high performance liquid chromatography (HPLC) (Chen, Lee et al. 1997; Fu 2008; Wang 2010; Zhang, Wang et al. 2012).

HPLC is favorable in many biological studies such as detecting the metabolite or desired compound in biological samples with a suitable inline detector. The separation of HPLC is based on different affinity between the adsorbent surface inside the column and the analytes in mobile phase. Optimization is always needed for a high efficient separation and sensitive detection (Lobrutto 2007). A structure

similar compound catechin has been detected and quantified by different detectors such as UV (Fu 2008), fluorescence (Ho, Lee et al. 1995), coulometric electrochemical array (Chen, Lee et al. 1997; Chu, Wang et al. 2004; Silberberg, Morand et al. 2005) and mass spectrometer (MS) (Wang 2010; Chang 2011; Zhang, Wang et al. 2012) in biological matrix. The detection of catechin from plasma using HPLC-UV and HPLC-F are not popular owning to their limited sensitivities. In contrast, HPLC coupled with coloumetric electrochemical array is found to be a popular method to detect catechin in animal plasma (Chen, Lee et al. 1997; Chu, Wang et al. 2004; Silberberg, Morand et al. 2005). Coulometric electrochemical array detection is commonly used to detect polyphenolic compounds with a lower detection limit than UV and fluorescence detectors. This detection method is based on the voltametric behavior of the compound with high selectivity (Acworth 2011). It is commonly found in natural compound laboratories. Apart from coulometric electrochemical array detection, LC/MS-MS also provided a high sensitivity and selectivity method to detect catechin (Wang 2010; Chang 2011; Zhang, Wang et al. 2012). It is a highly specific detection method as it measures the m/z ratio of ionized and fragmentized compound.

In this study, HPLC-UV and LC-MS/MS method were developed to detect pure C1. The low inventory cost makes HPLC-UV readily available in many laboratories. Also, it provides a simple operation mode which is suitable for initialization a new method development process. However, the sensitivity of HPLC-UV is limited and it is highly affected by the contaminants found in biological matrix (Svobaite, Solassol et al. 2008). Therefore, a more advanced LC-MS/MS C1 detection method was also developed to fulfill the needs of application.

The detection of analyte in blood is challenging because blood itself is a complex biological matrix. It composes of different enzymes, hormones, cells, and contaminants that cause interference to the detector. Blood sample has to be extracted before detection. The extraction process depends on the affinities of analyte between two phases. Catechin is able to extract from plasma by using liquid/liquid extraction (LLE) with ethyl acetate (EA) (Chen 1997; Fu 2008; Wang 2010; Zhang, Wang et al. 2012). Extraction process helps to eliminate the interference from plasma as well as to recover the analyte. The recovery rate of an extraction process is the portion of analyte in extracted sample over the unextracted sample. It is not necessarily to be 100% recovery for the extraction method. Indeed, the interference in the extracted sample plays a more important role on the detection. In HPLC-UV detection, interference might absorb the same wavelength as the analyte and shift the detection base line. While in LC-MS/MS detection, the matrix effect could enhance or suppress the ionization of the analyte and alternate the detection response (Matuszewski, Constanzer et al. 2003).

The detection method should also include an internal standard (IS) for normalizing the injection error and matrix interferences (Miller 2005). An ideal IS should have the same structure to the analyte with isotopic label. They could be ionized and fragmentized into a similar product with a fixed m/z ratio difference. However, it is not always feasible to make an isotopic labeled compound. Hence, other well characterized structure similar compounds might also be used as a reference. (+)-catechin has been extensively reported in different analytical article was chosen as the potential IS candidate for quantifying C1.

5.2   Methodology

5.2.1   Standard solution preparation

C1 stock solution at 10^{-2}M used in HPLC-UV was prepared by dissolving 2.74mg of C1 in 1000μl of EA and stored at -20°C. C1 working solution at 10^{-6}, 10^{-5}, 10^{-4} and 10^{-3} were prepared by serial dilution using EA. Another C1 stock solution at 1000ppm used in LC-MS/MS was prepared by dissolving 1mg of C1 in 1000μl of MeOH and stored at -20°C. C1 working solution at 5 and 25ppb were prepared by serial dilution using MeOH.

5.2.2   HPLC-UV method

Agilent 1100 HPLC machine equipped with auto sampler and UV detector were used to detect C1. Agilent Pre-SIL (5μm, 4.6x250mm) normal phase column was used in the stationary phase while 65% Hexane: 25% Ethyl acetate (EA): 10% Methanol (MeOH) were used in the mobile phase. The flow rate of mobile phase was configured at 1ml/min in isocratic elution. 20μl of sample dissolved in EA was injected to the HPLC for analysis. The detection was set at 276 nm to monitor the absorbance change. Each separation and detection run last for 45 minutes.

5.2.3   MS and tandem MS total ion scan

Waters SQ detector quadrupole MS and Micromass Ultimate Quattro triple quarterpole MS were used in the ion scan of C1. C1 dissolved in ACN with 0.5% v/v formic acid was injected to the ionizer at 10μl/min by Harvard syringe pump. MS was operated in positive electrospray ionization (+ESI) with the supply of 50L/h cone gas, 400L/h desolvation gas, 80°C source temperature, 150°C desolvation temperature, 30V cone voltage and 3kV of capillary voltage. For MS/MS operation,

the parent ions at m/z 275 were selected and underwent fragmentation to yield daughter ions. The collision energy was configured at 0, 5, 15 or 20 eV collision voltages with C.I.D. argon gas pressured at 5.5 x 10^{-5} Torr.

5.2.4 LC-MS/MS method

Waters Acquity H class ultra performance liquid chromatography coupled with Micromass Ultimate Quattro triple quadrupole mass spectrometer was used to detect the analyte. Waters Acquity UPLC BEH C18 (1.7μm, 2.1x50mm) column was used in the stationary phase while water (0.1% v/v formic acid) and ACN (0.1% v/v formic acid) were used in the mobile phase. The flow rate was kept at 0.4ml/min. During separate, a gradient protocol was used as follow – initiation: 0-1min 100% water; elution gradient: 1-11min 0→70% ACN; and regeneration: 11-16min 100% water. The sample was dissolved in MeOH and kept in the auto sampler at 4°C. 2μl of sample was injected for analysis. MS was operated in +ESI mode with the supply of 150L/h cone gas, 550L/h desolvation gas, 150°C source temperature, 350°C desolvation temperature, 30V cone voltage and 3kV of capillary voltage. The collision energy was configured at -18eV collision voltage with C.I.D. argon gas pressure at 5.5 x 10^{-5} Torr. The ions were monitored by multiple reaction monitor (MRM) mode for (-)-epiafzelechin (m/z 274→139) and (+)-catechin (m/z 293→139).

5.2.5   Experimental animals

Young male SD-rats (200-220g) and female C57BL/6J (20-25g) mice were obtained from the Chinese University of Hong Kong and the University of Hong Kong, respectively. They were housed at $22^{o}C$ with 12-h light and dark cycle and free access to water and diet. All experimental procedures were approved by the Animal Ethics Committee of the Hong Kong Polytechnic University.

5.2.6   Plasma collection

Young male SD-Rat mice and female C57BL/6J mice were anaesthetized with 100mg/kg ketamine and 10mg/kg xylazine via i.p. injection. The animals will be fallen into deep sleep and lose conscious. They were then sacrificed by cardiac stick exsanguinations during blood sample collection. The blood samples were mixed with EDTA and centrifuged for 15 minutes at 3,500 x g to yield plasma. The plasma was collected and kept at $-20^{o}C$ for further use.

5.2.7   Plasma extraction

<u>HPLC-UV</u> C1 spiked plasma was prepared by mixing 25μl of C1 at10^{-2}M into 500μl of rat blank plasma. 500μl of blank plasma or spiked plasma were extracted by EA or ether. 1000 μl of solvent was added to the plasma and vortex for 30s. The mixture was centrifuged at 3500 x g for five minutes. The supernatant was transferred to another tube. The solvent extraction procedure was repeated for three times. The collected supernatant was dried in stream of dry air and re-dissolved in 500μl of EA for HPLC-UV analysis

<u>LC-MS/MS</u> C1 spiked plasma was prepared by mixing 2μl of C1 at 1000ppb into 50μl of mouse blank plasma. 50μl of mice blank plasma or spiked plasma were extracted by EA. 100 μl of solvent was added to the plasma and vortex for 30s. The mixture was centrifuged at 3500 x g for five minutes. The supernatant were transferred to another tube. The solvent extraction procedure was repeated for three times. The collected supernatant was dried in stream of dry air and re-dissolved in 50μl of MeOH for LC-MS/MS analysis

5.3 Result:

5.3.1 UV absorption spectrum of pure C1

Two absorption peaks at 245 nm and 276nm was found in the UV absorption scan of pure C1 (**Figure 5.1**). These absorption peaks could be used to monitor the presence of C1 in the mobile phase for quantification. UV absorption at 276nm gave a higher response than 245nm which was chosen as the detection wavelength. Because the plasma contain lots of proteins and small molecules that have a high absorption function in the shorter wavelength region (Motrescu 2006). Using the longer absorption wavelength region of C1 could minimize the overlapping absorption region between plasma interference and C1 absorption.

5.3.2 HPLC-UV detection of pure C1

Pure C1 was successfully separated in HPLC with normal phase column and 65% Hexane: 25% EA: 10% MeOH solvent (**Figure 5.2**). Several peaks were found in the first five minutes of elution. C1 was eluted at around 13 minutes after injection. The injection concentration was decreased from 10^{-4} to 10^{-6}M (**Figure 5.3**) to determine the quantification limit of C1. For injecting 20 μl of 10^{-6}M (0.274ppm) C1, the signal to noise (S/N) ratio of the basal UV absorption and C1 is 3 which is defined as the lower limit of detection (LOD). The basal UV absorption level was around 0.3 mAU in this detection method.
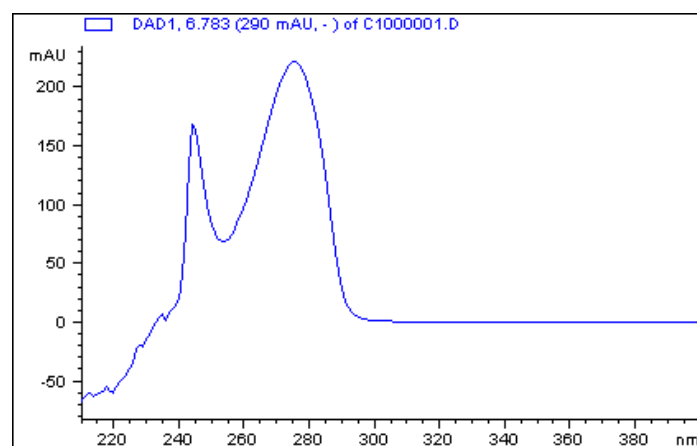
5.1 UV absorption spectrum of C1

C1 at 10^{-3}M were detected by HPLC-UV using 65% Hexane: 25% EA: 10% MeOH isocratic elution at flow rate of 1 ml/min and last for 45 minutes. The UV absorption was scanned as a full spectrum and yielded the absorption spectrum of C1.
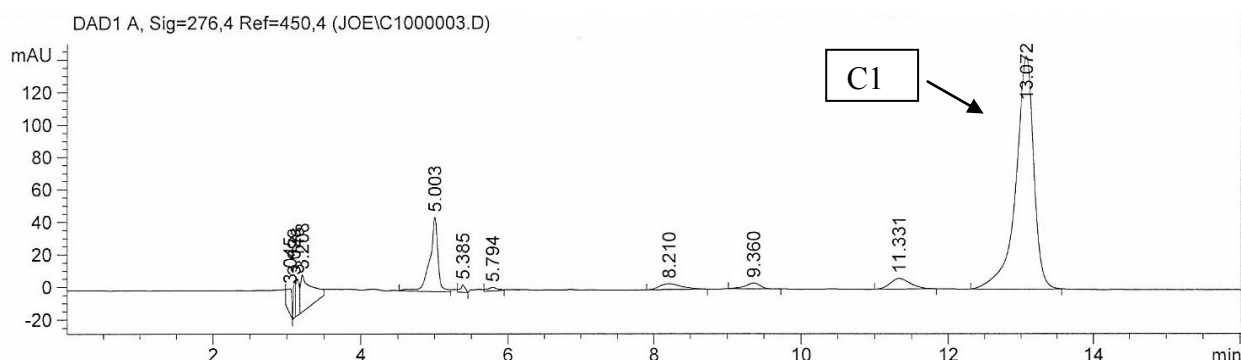
Figure 5.2 Chromatogram of HPLC-UV detection of pure C1

20µl of EA dissolved pure C1 at 10^{-4}M was detected by HPLC-UV using 65% Hexane: 25% EA: 10% MeOH isocratic elution at flow rate of 1 ml/min. The detection wavelength was configured at 274nm.
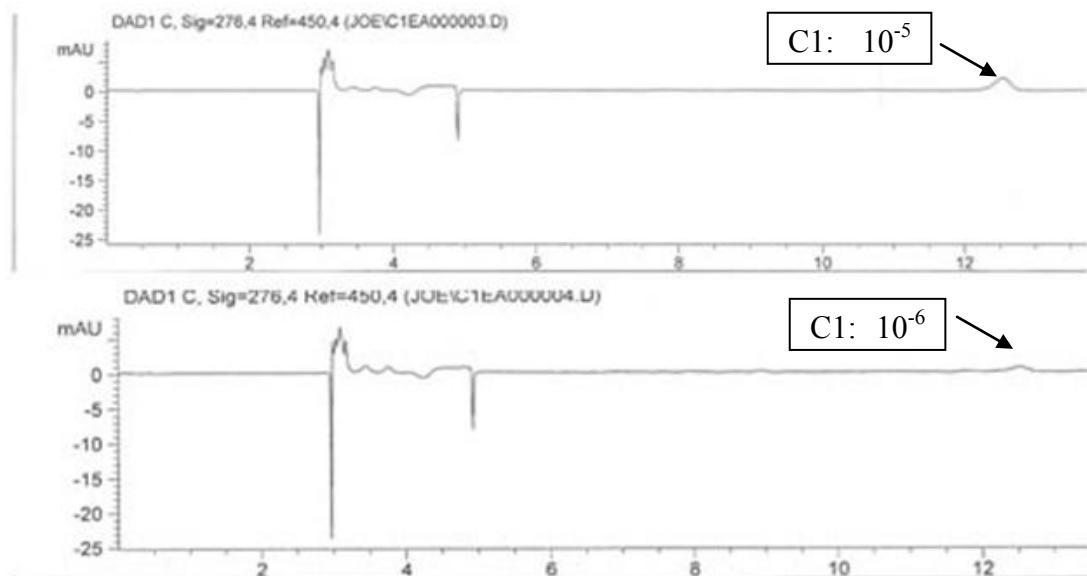
Figure 5.3 HPLC-UV Chromatogram of C1 detection

20μl of EA dissolved pure C1 at 10^{-6} to 10^{-5}M were detected by HPLC-UV. The mobile phase was 65% Hexane: 25% EA: 10% MeOH isocratic elution at flow rate of 1 ml/min. The detection wavelength was configured at 274nm.
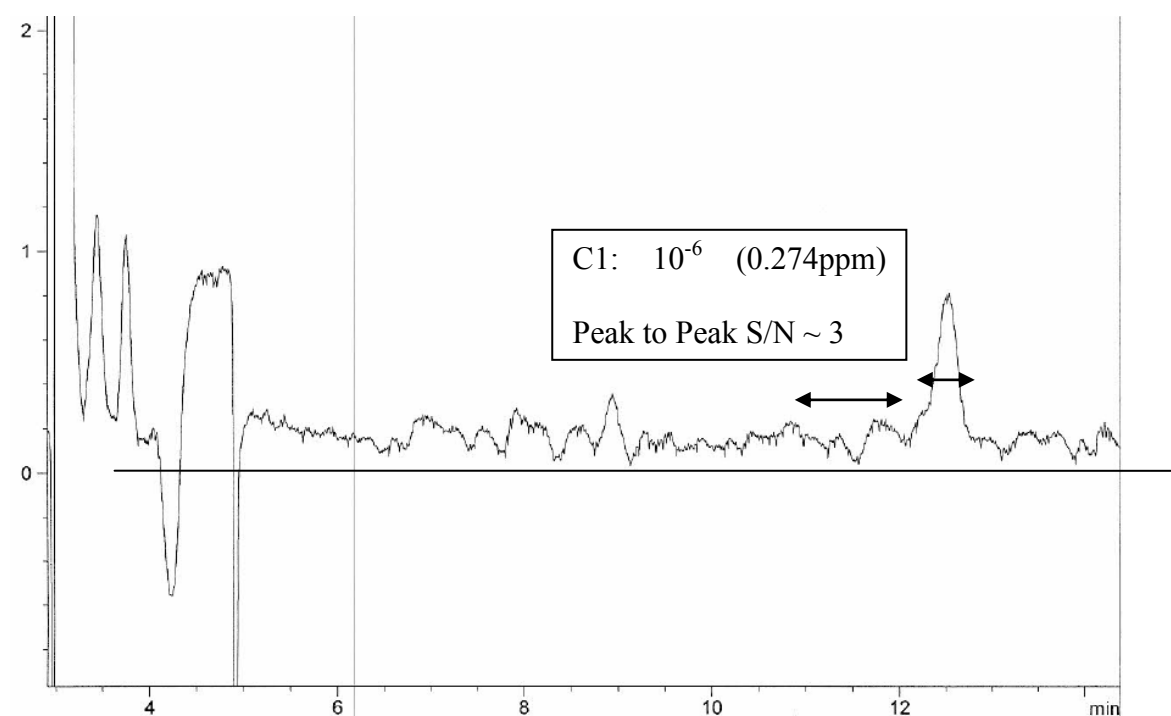
Figure 5.4 Chromatogram of HPLC-UV detection of C1 at 10^{-6} M

20μl of EA dissolved pure C1 at 10^{-6} was detected by HPLC-UV using 65% Hexane: 25% EA: 10% MeOH isocratic elution at flow rate of 1 ml/min. The detection wavelength was set as 274nm. This chromatogram was used to calculate the signal to noise ratio.

5.3.3　HPLC-UV detection of solvent extracted rats plasma

5.3.3a Extraction of blank plasma

The blank plasma extraction by EA and ether were detected by HPLC-UV method. The EA extracted plasma contains certain amount of molecule having an absorbance in 276nm. Several peaks were found at 2.5 to 14.0 minutes after injection. The maximum peak height was 37 mAU (**Figure 5.5A**). Similar to EA extraction, ether extracted plasma contains interference having an absorbance in 276nm (**Figure 5.6A**). In contrast, ether extraction gave a distinguishable peak at around 3.1 minutes with an intensity of 280 mAU. After 7.5 minutes of injection, a relative stable UV basal absorption chromatogram was observed and most of the peaks were diminished.

5.3.3b Extraction of C1 spiked plasma

C1 added blank plasma was extracted by EA and ether and underwent HPLC-UV detection. Both EA and ether were able to extract C1 from the plasma. The extracted plasma did not affect the elution time of C1 in both preparations. The peak area of C1 extracted by EA and ether were 5553.21 (**Figure 5.5B**) and 4860.84 (**Figure 5.6B**), respectively. By the same extraction protocol using different solvent, EA was able to extract more C1 than ether.

A
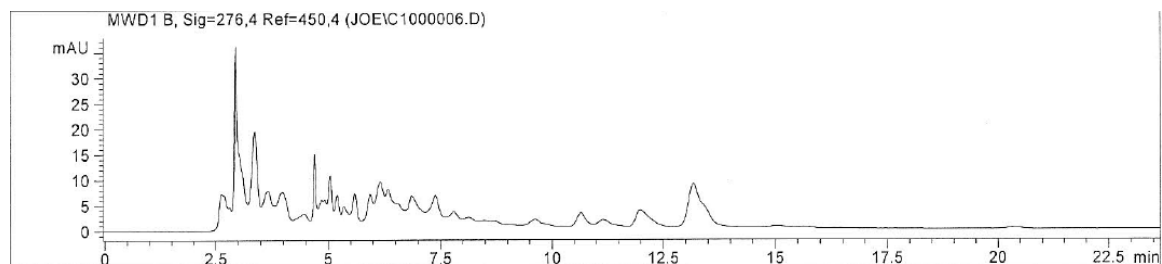
B
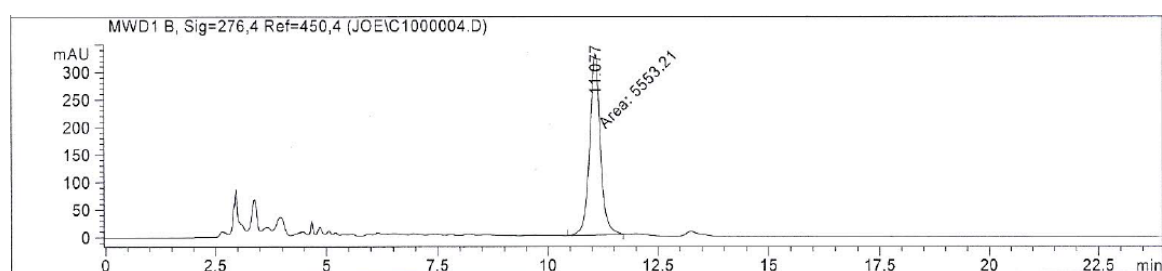
Figure 5.5 Chromatogram of HPLC-UV detection of EA extracted rat plasma
(A) Blank plasma extract; and (B) Plasma spiked with 54.8µg of C1 and underwent extraction. 100µl of blank plasma or spiked plasma was extracted by 200 µl of EA for three times. Solvent were dried and dissolved in 30µl of EA for HPLC analysis. 25µl of EA dissolved plasma extract was detected by HPLC-UV. The mobile phase was 65% Hexane: 25% EA: 10% MeOH isocratic elution at flow rate of 1 ml/min and last for 45 minutes. The detection wavelength was configured at 274nm.

A
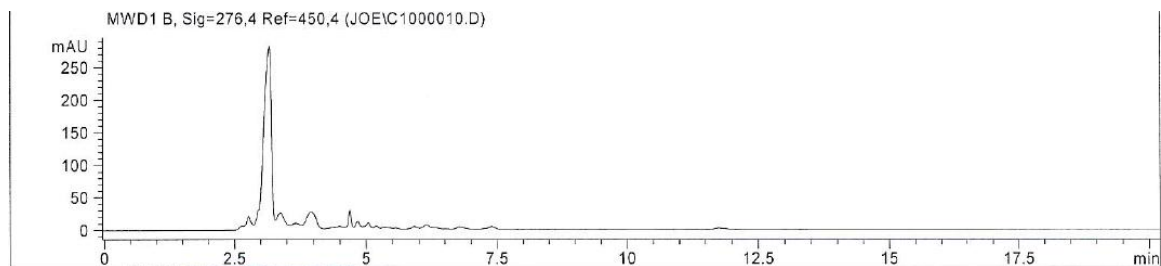
B
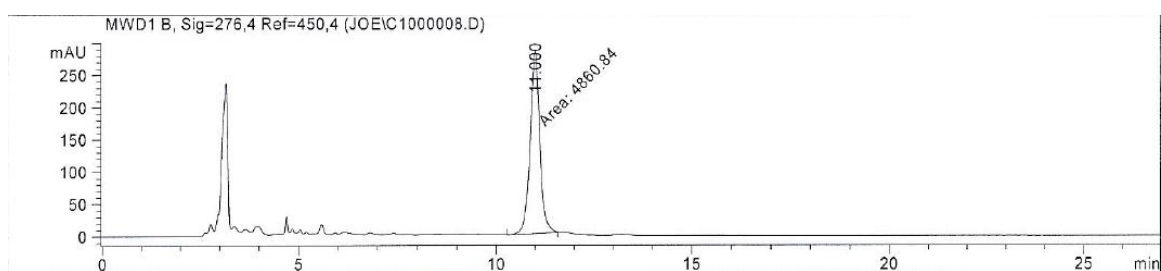
Figure 5.6 Chromatogram of HPLC-UV detection of ether extracted rat plasma
(A) Blank plasma extract; and (B) Plasma spiked with 54.8µg of C1 and underwent extraction. 100µl of blank plasma or spiked plasma was extracted by 200µl of ether for three times. Solvent were dried and re-dissolved in 100µl of ether for HPLC analysis. 25µl of ether was injected detected by HPLC-UV. The mobile phase was 65% Hexane: 25% EA: 10% MeOH isocratic elution at flow rate of 1 ml/min and last for 45 minutes. The detection wavelength was configured at 274nm.

5.3.4 MS and tandem MS Ion scanning of pure C1

Pure C1 was ionized and detected by mass spectrometry by +ESI and -ESI mode. The [M+H] and [M-H] ions were not found in both scanning mode (data not shown). Formic acid was then added to enhance the protonation of C1. The [M+H] ion of C1 was found in m/z 274.81 on the TIC **(Figure 5.7)** upon +ESI MS detection. The parent ion of C1 was selected and underwent collision-induced dissociation (C.I.D.) to yield daughter ions. The collision energy was increased from 0 to 20 eV to find out the most abundant fragment ions of C1 in different eV. The fragment ions with m/z 106.9, 139.0, 140.0, 191.1 and 275.3 were found **(Figure 5.8)**. It was found that the fragment ion m/z 139.0 was having a highest intensity at collision energy 18eV. The structure of the m/z 139.0 ion fragment was proposed and shown in **figure 5.8** (Chang 2011). The detection of C1 by MS in this study was operated in MRM mode based on these optimized parameters.

5.3.5 LC-MS/MS detection of pure C1

Pure C1 was successfully separated in LC with C18 column and gradient elution – initiation: 0-1min 100% water; elution gradient: 1-11min 0→70% ACN; and regeneration: 11-16min 100% water. C1 was eluted at around 4.5 minutes after injection. The injection concentrations at 9.1×10^{-8}M (25ppb) and 1.82×10^{-8}M (5ppb) **(Figure 5.9)** were used to determine the quantification limit of C1. For injecting 2 μl of 9.1×10^{-8} M of C1, the S/N ratio is 20. The LOD of C1 detection in this method was found at 1.82×10^{-8}M (5ppb) with the S/N ratio equal to 3.
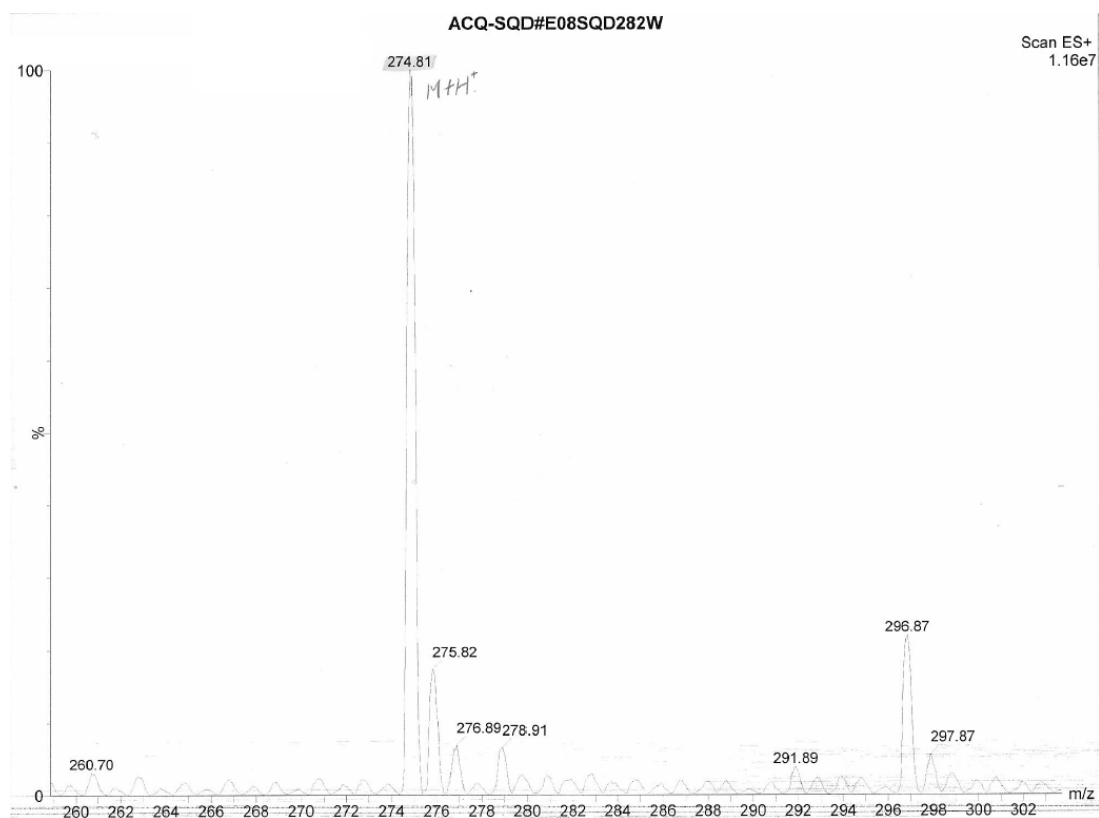
Figure 5.7 MS Total Ion Chromatogram of Pure C1

Pure C1 dissolved in ACN with 0.5% v/v formic acid was injected to the ionizer at a flow rate 10μl/min by Harvard syringe pump. MS was operated in positive electrospray ionization (+ESI) with the supply of 50L/h cone gas, 400L/h desolvation gas, 80°C source temperature, 150°C desolvation temperature, 30V cone voltage and 3kV of capillary voltage.
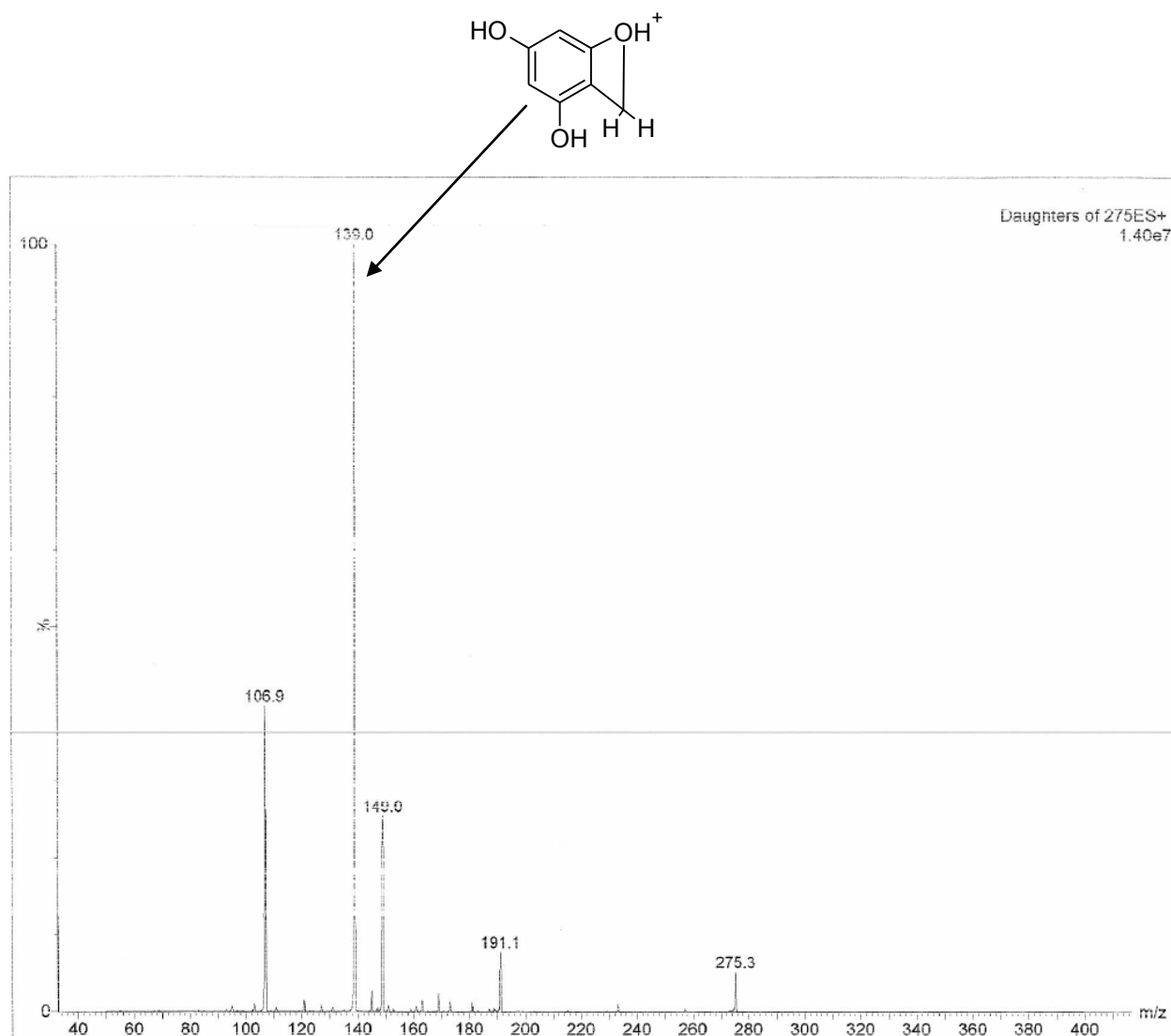
Figure 5.8 MS Daughter Ion Chromatogram of Pure C1

Pure C1 dissolved in ACN with 0.5% v/v formic acid was injected to the ionizer at a flow rate 10μl/min by Harvard syringe pump. MS was operated in positive electrospray ionization (+ESI) with the supply of 50L/h cone gas, 400L/h desolvation gas, 80°C source temperature, 150°C desolvation temperature, 30V cone voltage and 3kV of capillary voltage. For MS/MS operation, the parent ions at m/z 275 were selected and underwent fragmentation to yield daughter ions. The collision energy was configured at 15 eV collision voltages with C.I.D. argon gas pressured at 5.5 x 10^{-5} Torr.

A
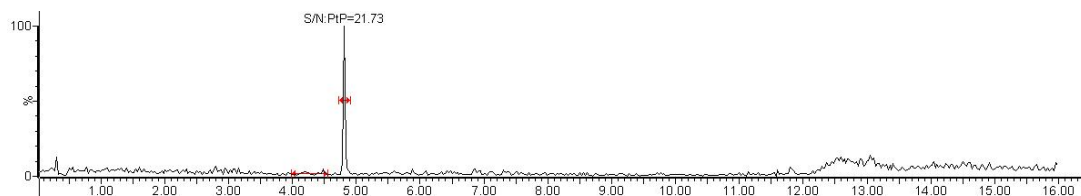
B
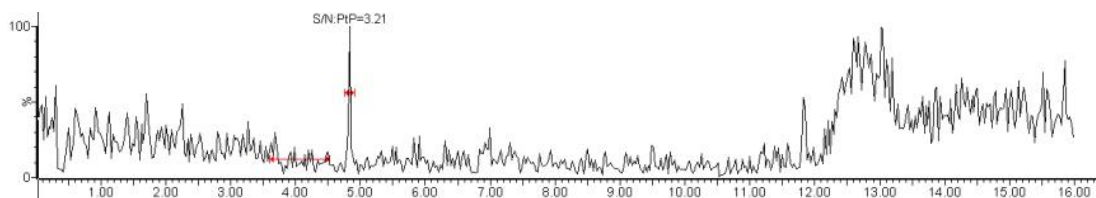
Figure 5.9 LC-MS/MS TIC of Pure C1

2µl of MeOH dissolved pure C1 at (A) 25ppb (9.1×10^{-8}M) and (B) 5ppb (1.82×10^{-8}M) were detected by LC-MS/MS using gradient elution – initiation: 0-1min 100% water; elution gradient: 1-11min 0$\rightarrow$70% ACN; and regeneration: 11-16min 100% water. MS detection of C1 was operated in +ESI mode with the supply of 150L/h cone gas, 550L/h desolvation gas, 150^{o}C source temperature, 350^{o}C desolvation temperature, 30V cone voltage and 3kV of capillary voltage. The collision energy was configured at -18eV collision voltage with C.I.D. argon gas pressure at 5.5×10^{-5} Torr. The ions were monitored by MRM mode for C1 (m/z 274$\rightarrow$139)

5.3.6 LC-MS/MS detection of solvent extracted mice plasma

The blank plasma extracted by EA was detected by LC-MS/MS method. The EA extracted plasma contains certain molecule that gave signal in the early elution with a maximum intensity at 3.95×10^3 and the intensity decreased by time. C1 was not found in the blank mice plasma **(Figure 5.10A)**. EA was able to extract C1 in plasma and the extracted C1 was successfully detected by LC-MS/MS method. There was not a sharp peak in the extracted plasma overlapped with C1. Also, the extracted plasma did not affect the elution time of C1 **(Figure 5.10B)**.

5.3.7 LC-MS/MS detection of IS (+)-catechin

Internal standard (IS), (+)-catechin, was detected by the same LC-MS/MS method for C1 by using another MRM channel (m/z 293→139) in the MS/MS detection. A peak was found in 4.14 minutes after the injection of (+)-catechin **(Figure 5.11)**.

5.3.8 Simultaneous detection of C1 and (+)-catechin by LC-MS/MS

C1 and (+)-catechin was simultaneous detected by a single LC-MS/MS method with two MRM channels. Two distinguishable peaks were found at 3.32 minutes (C1) and 4.11 minutes (IS) without overlapping.

A
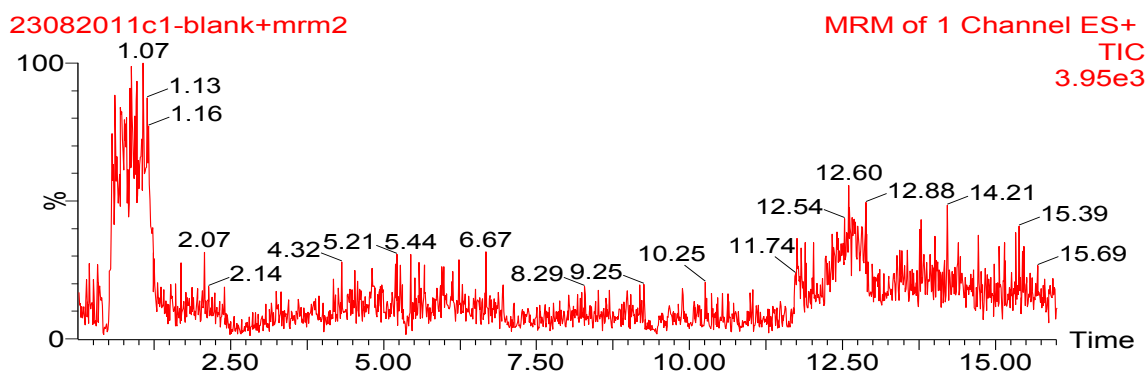
B
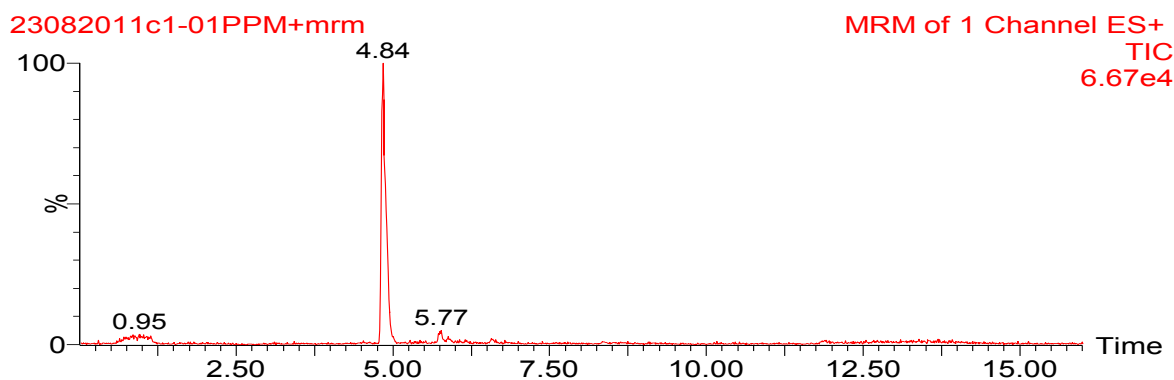
Figure 5.10 LC-MS/MS TIC of Pure C1

(A) Blank mice plasma extract; and (B) Mice plasma spiked with 5ng of C1 and underwent extraction. 50µl of blank plasma or spiked plasma was extracted by 100 µl of EA for three times. Solvent were dried and dissolved in 100µl of MeOH for LC-MS/MS analysis. 2µl of reconstitute was analyzed by LC-MS/MS using gradient elution – initiation: 0-1min 100% water; elution gradient: 1-11min 0→70% ACN; and regeneration: 11-16min 100% water. MS detection of C1 was operated in +ESI mode with the supply of 150L/h cone gas, 550L/h desolvation gas, 150°C source temperature, 350°C desolvation temperature, 30V cone voltage and 3kV of capillary voltage. The collision energy was configured at -18eV collision voltage with C.I.D. argon gas pressure at 5.5×10^{-5} Torr. The ions were monitored by MRM mode for C1 (m/z 274→139)
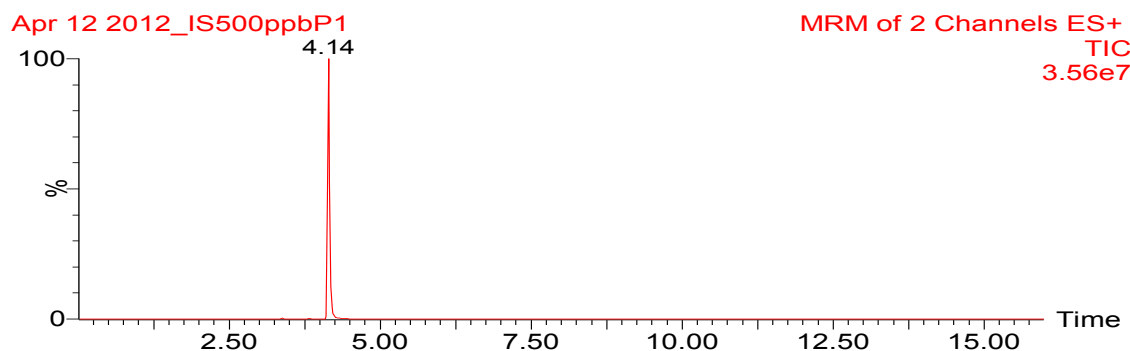
Figure 5.11 LC-MS/MS TIC of IS (+)-catechin

5ng of (+)-catechin was dissolved in 50µl of mice plasma extracted reconstitute in MeOH. 2µl of the sample was detected by LC-MS/MS using gradient elution – initiation: 0-1min 100% water; elution gradient: 1-11min 0→70% ACN; and regeneration: 11-16min 100% water. MS detection of IS was operated in +ESI mode with the supply of 150L/h cone gas, 550L/h desolvation gas, 150°C source temperature, 350°C desolvation temperature, 30V cone voltage and 3kV of capillary voltage. The collision energy was configured at -18eV collision voltage with C.I.D. argon gas pressure at 5.5 x 10^{-5} Torr. The ions were monitored by MRM mode for (+)-catechin (m/z 293→139)
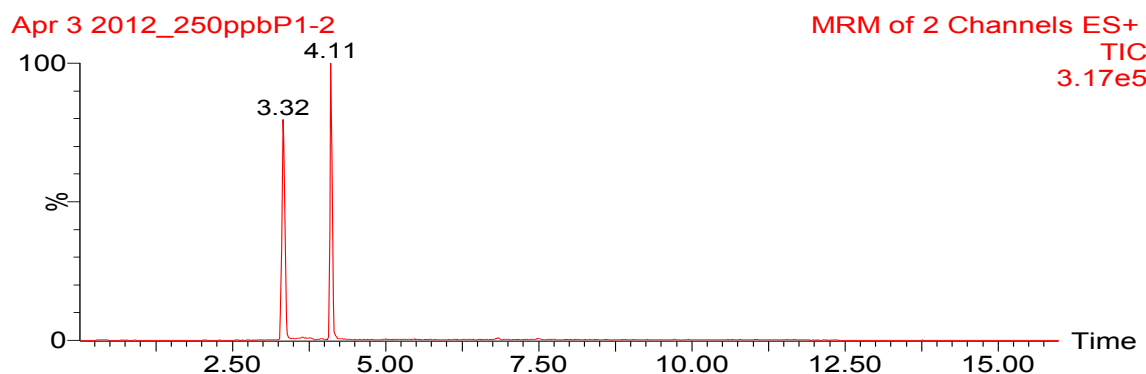
Figure 5.12 TIC of simultaneous detection of IS (+)-catechin and C1 by LC-MS/MS

2.5ng of C1 and 5ng of (+)-catechin were dissolved in 50µl of mice plasma extracted reconstitute in MeOH. 2µl of the sample was detected by LC-MS/MS using gradient elution – initiation: 0-1min 100% water; elution gradient: 1-11min 0→70% ACN; and regeneration: 11-16min 100% water. MS detection of C1 and IS was operated in +ESI mode with the supply of 150L/h cone gas, 550L/h desolvation gas, 150°C source temperature, 350°C desolvation temperature, 30V cone voltage and 3kV of capillary voltage. The collision energy was configured at -18eV collision voltage with C.I.D. argon gas pressure at 5.5 x 10^{-5} Torr. The ions were monitored by MRM mode for C1 (m/z 274→139) and (+)-catechin (m/z 293→139)

5.4 Discussion:

5.4.1 HPLC-UV detection of C1

Pure C1 was successfully separated by using a normal phase HPLC with the solvents of hexane, EA and MeOH. Normal phase (NP) and reverse phase (RP) HPLC are commonly used in separating bioanalytes. NP HPLC uses hydrophilic stationary phase and non-polar solvent while RP HPLC uses hydrophobic stationary phase and more polar solvent. C1 is predicted to have a long retention time in NP HPLC as C1 is water soluble. Plasma sample contains different molecules that are having a high absorbance in the UV region (Motrescu 2006). These interference molecules are eluted in early part of the elution (Lee, Wang et al. 1995; Lee, Prabhu et al. 2000). A longer elution time might be able to provide more time for the column to wash away those UV absorbing contaminant found in plasma to reduce the interference signals.

In fact, the use of HPLC-UV to detect catechin in biological matrix is uncommon. This is mainly due to the limited sensitivity of UV detection in biological matrix (Ho, Lee et al. 1995). Our results also suggested that the detection of C1 by HPLC-UV is not suitable for use in the proposed pharmacokinetic (PK) study. In the previous chapter, we have demonstrated that the active range of C1 in cell culture model was around 10^{-8} to 10^{-6}M which could not be detected by the current HPLC-UV method.

5.4.2 Plasma extraction of C1 detected by HPLC-UV

HPLC-UV was used to determine if the LLE method could be used to extract C1. EA and ether were used to extract C1 from spiked rat plasma. Both of them are immiscible to plasma and are able to precipitate the proteins. In addition, they have low vapor pressure which is favorable in the drying process of extraction. Our results suggested that these solvents are able to extract C1 from the plasma. As the HPLC-UV detection method for C1 was not validated, therefore, the recovery rate could not be calculated. A direct comparison of the HPLC chromatogram of EA and ether extracted C1 indicated that EA could extract more C1 than ether in the same extraction procedure.

LLE is a non-specific extraction method. Analyte as well as other polar and non-polar contaminants in plasma are also extracted (Chu, Wang et al. 2004). Especially for a low specificity detection method like HPLC-UV, the blank plasma extraction often gives a noisy background on the chromatogram (**Figure 5.5A and 5.6A**). The overlapped peak between the analyte and the background reduced the sensitivity of the detection method. In fact, the extraction can be improved by using a more specific solid phase extraction (SPE) to eliminate the interference. SPE cannot get rid of all contamination from plasma, but the column wash of SPE could reduce the amount of contaminants (Umegaki, Sugisawa et al. 2001; Chu, Wang et al. 2004). Apart from switching the extraction method, introducing a more specific detection method could also be helpful to control the interference problem encountered.

5.4.3 LC-MS/MS detection of C1

Due to the limit sensitivity and specificity of C1 detection in HPLC-UV, other detection method was explored. From the literature research of catechin detection, LC-MS/MS is popularly used to detect catechin (Wang 2010; Chang 2011; Zhang, Wang et al. 2012) for PK studies. The parent and daughter ion of C1 was scanned to determine the m/z ratio monitored in the multiple reaction monitoring (MRM). The most abundant daughter ion was found at m/z139 and the structure was proposed in **figure 5.8** (Chang 2011). A RP LC method was used to separate C1 in MS/MS detection. Mild solvents such as ACN and water were used in the mobile phase of RP LC to reduce the solvent damage to the MS machine. C1 was found to be eluted at 4.6 minutes by this method with a detection limit at about 10^{-8}M. The overall run time of LC-MS/MS and HPLC-UV detection of C1 was found to be 16 and 45 minutes, respectively. In addition, the detection limit of C1 in LC-MS/MS was found to be 100 fold less than HPLC-UV. With these advantages, LC-MS/MS is more favorable to use in PK study for detecting C1.

5.4.4 Plasma extraction of C1 detected by LC-MS/MS

Rodents such as rat and mouse are often used in PK study. In HPLC-UV detection of C1, rat plasma was used because the plasma had to be concentrated before undergoing detection. However, the large body size of rat required large amount of synthetic C1 for the study. In order to reduce the amount of C1 used, smaller animal such as mouse is preferred. The volume of plasma from a single mouse was found to be adequate for C1 detection by LC-MS/MS without further concentrating.

EA extracted mice plasma was detected by LC-MS/MS and the blank plasma did not contain interference on the elution time of C1. There was fewer interference peaks found in LC-MS/MS when compared with HPLC-UV detection. The noise control in LC-MS/MS is better than HPLC-UV because of the use of specific ion detector. Other research groups had reported that the use of coulometric electrochemical array as a detector for catechin in animal plasma with a comparable detection limit to the LC-MS/MS (Chen, Lee et al. 1997; Chu, Wang et al. 2004; Silberberg, Morand et al. 2005). Coulometric method is likely to detect C1 in a more economy way but it takes 36 minutes for a complete analyze where the overall run time is also a concern (Chu, Wang et al. 2004). In addition, the coulometric electrochemical array is only commonly found in natural products laboratory which is not available in our laboratory. In conclusion, the lower detection limits, shorter time for analyze, and better noise control make LC-MS/MS a better way to detect C1 in the animal plasma.

5.4.5 Simultaneous detection of C1 and (+)-catechin

Internal standard (IS) such as deoxyhegenamine (Ho, Lee et al. 1995), vanillin (Wang 2010), scopoletin (Zhang, Wang et al. 2012) had been used to quantify catechins in different studies. Like other analytical method, internal standard was needed for the quantification of C1. The potential use of catechin as an internal standard for C1 was evaluated. Without changing the LC method, catechin was eluted at 4.14 minutes (**Figure 5.11**). A simultaneous detection of C1 and (+)-catechin showing these two structures eluted at different time without overlapping. In addition, (+)-catechin was able to extract by EA. Therefore, (+)-catechin could be a good IS for use to quantify C1. The method developed for C1 shall be validated with the (+)-catechin for use in further PK study.

5.5 Summary

HPLC-UV and LC-MS/MS detection methods were successfully developed to detect C1 in plasma by using EA. LC-MS/MS offered a lower detection limit, down to 10^{-8}M, which could be used in the PK study. The LC-MS/MS detection method could simultaneously detect and differentiate C1 and (+)-catechin. This allows the use of (+)-catechin as an internal standard (IS) in this bioanalytical method. This detection method will be validated to determine if this method is suitable for use in quantifying C1 in animal plasma.

6   **LC-MS/MS Determination of (-)-Epiafzelechin for Pharmacokinetic Study**

6.1 Introduction:

The ability of (-)-epiafzelechin to promote osteoblastogenesis and inhibit osteoclastogenesis were found in tissue culture models. An osteoporotic ovariectomized (Ovx) C57BL/6J mice model can be used to further characterize the bone protective effects of (-)-epiafzelechin in animal model. However, there is not any information on the bioavailability of (-)-epiafzelechin in animal study. Hence, a pharmacokinetic (PK) study is useful to describe the absorption, distribution, metabolism and elimination (ADME) behavior of (-)-epiafzelechin in animal body. The plasma drug concentration- time curve is commonly used to determine the drug PK parameters in compartmental modeling. PK parameters such at the maximum drug concentration (Cmax) and elimination half-life ($T_{1/2}$) can be used to determine the dosage in different administration route and the drug administration interval. PK also describes the drug behavior in animal body that can provide more information on the drug design and formulation for optimizing the use of drug (Hedaya 2012).

The administration route to be used in animal study was determined in this PK study. An intravenous (i.v.) injection is always preferred in the PK study because the drug can get into the blood without any barrier. However, this administration route is not suitable for use in long term study and hence it is not the first priority for constructing the PK profile in the present study. Oral administration is suitable for long term study but the limited supply of (-)-epiafzelechin cannot sustain the long term osteoporotic animal study last for two months. In contrast, intraperitoneal (i.p.) injection is a better choice for the long term injection of limit supplied compound. Therefore, i.p. injection is chosen for the drug administration route in this PK study.

In the previous chapter, a bioanalytical method was developed to detect (-)-epiafzelechin in animal plasma. This analytical method has to be validated to ensure the quality and reliability of results. The method validation in this study was referred to the "Validation of Analytical Procedures: Text and Methodology" from ICH and "Guidance for Industry: Bioanalytical Method Validation" from FDA. In the validation process, an internal standard (IS) was included for quality control. (+)-catechin, a flavan-3-ols with a similar structure to (-)-epiafzelechin, has long been studied in different analytical method was used as the IS in this study (Pan, Liu et al. 1991; Ho, Lee et al. 1995; Carando, Teissedre et al. 1998; Zhang, Wang et al. 2012).

A method validation consists of different components including selectivity, accuracy, precision, limits of detection (LOD)/limits of quantification (LOQ), calibration curve, recovery and stability. The selectivity can be work out by analyzing different individual biological matrix with and without the spiked compound at LOQ. It is important to determine the detection limit before preceding other components of method validation. In fact, most of the parameters in the method validation can be work out by constructing a standard curve with at least 5 concentration points covers from the LOQ to 80 or 120% of the test concentrations. Three concentration points (Low, Mid and High) can be added to the curve for determining the within-run precision. The relationship between the responses from the detector and the amount of analyte is used to construct a standard curve to determine the linearity. With the standard curve, the accuracy can be determined by comparing the actual value between the three concentration points and the standard curve. This procedure can be repeated in different days to determine the intermediate precision or reproducibility. The recovery rate is found by comparing two samples; (1) spiking known amount of

compound into the plasma and undergo extraction; and (2) adding known amount of extract plasma reconstitution. The stability of compound are determined by storing the compound in different condition and compared with the original stock.

The calibration curve is important for determining the concentration of compound in plasma. A suitable linear regression model describes the concentration-response relationship of the standard curve. Simple linear regression model such as least squares linear regression is always preferred but it might not be able to describe the linear relationship accurately. Hence a more complex regression equation is sometime needed. A weighting least squares linear regression (WLSLR) is useful in the bioanalytical field in different pharmacokinetic studies (Almeida, Castel-Branco et al. 2002; Fu 2008; Li Xiao-Hong 2010). The weighing factors of WLSLR are lower in higher concentrations. This prevents the high influence of the large deviations present at high concentration in the linear regression line (Almeida, Castel-Branco et al. 2002). Different models have its own limitation and therefore, a justification is needed for choosing an appropriate linear regression model in this study.

6.2 *Material and method:*

6.2.1 LC-MS/MS method

Waters Acquity H class Ultra performance liquid chromatography coupled with Micromass Ultimate Quattro triple quadrupole mass spectrometer was used to detect the analyte. Waters Acquity UPLC BEH C18 (1.7μm, 2.1x50mm) column was used in the stationary phase while water and acetonitrile (ACN) with 0.1% formic acid were used in the mobile phase. The flow rate was kept at 0.4ml/min. A gradient elution was used to separate the analyte as follow – initiation: 0-1min 100% water; elution gradient: 1-11min 0→70% ACN; and regeneration: 11-16min 100% water. The sample was dissolved in methanol (MeOH) and kept in the auto sampler under $4^{o}C$. 2μl of sample was injected for analysis. MS was operated in positive electrospray ionization (+ESI) with the supply of 150L/h cone gas, 550L/h desolvation gas, $150^{o}C$ source temperature, $350^{o}C$ desolvation temperature, 30V cone voltage and 3kV of capillary voltage. The collision energy was configured at -18eV collision voltage with C.I.D. argon gas pressure at 5.5×10^{-5} Torr. The ions were monitored by multiple reaction monitor (MRM) mode for (-)-epiafzelechin (m/z 274→139) and (+)-catechin (m/z 293→139).

6.2.2 Experimental animals

Young female C57/BL6J mice (20-25g) were obtained from the University of Hong Kong. They were housed at $22^{o}C$ with 12-h light and dark cycle and free access to water and diet. All experimental procedures were approved by the Animal Ethics Committee of the Hong Kong Polytechnic University. Mice were starved for 12 hours before drug administration.

6.2.3 Drug administration

Intraperitoneal (i.p.) injection was used in the drug administration route. (-)-Epiafzelechin was weighted and dissolved in ethanol at 50 mg/ml solution and filtered by 0.22μm membrane filter. The working solution was freshly prepared by diluting with PBS to 2.5 mg/ml (5% EtOH v/v). The mice were injected with 10mg/kg of C1. After 5, 10, 15, 30, 60, 120, 240 and 360 minutes of drug administration, the mice were sacrificed and the blood samples were collected.

6.2.4 Plasma collection

Young female C57BL/6J mice were anaesthetized with 100mg/kg ketamine and 10mg/kg xylazine via i.p. injection. The animals were fallen into deep sleep and lose consciousness. They were then sacrificed by cardiac stick exsanguinations during blood sample collection. The blood samples were mixed with EDTA and centrifuged for 15 minutes at 3,500 x g to yield plasma. The plasma was kept at -20°C for further analysis.

6.2.5 Plasma Extraction

50 μl of plasma were extracted by EA. 100 μl of solvent was added to the plasma and vortex for 30s. The mixture was allowed to stand for 3 minutes and immediately centrifuged at 3,500 x g for 5 minutes. The supernatant was collected into a new tube and the pellet was extracted again for two times to yield 300μl supernatant. The supernatant was dried by stream of dry air and re-dissolved in 50μl of methanol for LC-MS/MS analysis.

6.2.6 Standard solution preparation

(-)-Epiafzelechin and (+)-catechin stock solution at 1000ppm were prepared by dissolving 1mg of C1 or IS in 1000μl MeOH and stored at -20°C. C1 working solution at 12.5, 50, 250 and 1000ppb were prepared by serial dilution using MeOH. IS working solution at 500ppb was prepared by serial dilution.

6.2.7 Method Validation

The method for determining the concentration of C1 was validation according to the guidance from US FDA and ICH.

6.2.7.1 Calibration curve: A bulk plasma extraction was performed according to the plasma extraction procedure. The air dried residue was reconstituted by 500ppb IS working solution to yield plasma blank IS solution. 50μl of 0, 12.5, 25, 50, 100, 500 and 1000ppb C1 solution were dried in 1.5ml centrifuge tubes with a stream of dried air. The centrifuge tubes containing dried C1 were reconstituted by 50μl plasma blank IS solution and underwent LC-MS/MS analysis. The results were analyzed by linear regression (1) least squares method without passing through the origin; (2) least squares method passing through the origin; and (3) $1/y^2$ weighted least squares liner regression.

6.2.7.2 Accuracy and precision: Bulk plasma extract with 500ppb IS was used to prepare C1 solution at 12.5, 50, 250 and 1000ppb for LC-MS/MS analysis for five times at the same day of constructing the calibration curve. The amount of C1 in the samples was calculated from the standard curve and compared to the standard amount to determine the accuracy. The CV of the five determinations was calculated for the intra-batch precision. This experiment was conducted in another day for inter-day precision determination.

6.2.7.3 Recovery: Bulk plasma extract with 500ppb IS was used to prepare C1 solution at 12.5, 50, 250 and 1000ppb. Another sets of blank plasma spiked with 12.5, 50, 250 and 1000ppb of C1 were extracted according to the plasma extraction procedure and reconstituted by MeOH with 500ppb IS. The extracted C1 and non-extracted C1 in plasma were analysed by LC-MS/MS for calculating the recovery rate.

6.2.8 Statistical analysis

The least squares linear regression was constructed by GraphPad Prism4 and the weighted least squares linear regression was constructed by SPSS v7.0. The pharmacokinetic parameters were calculated by Summit PK solutions v2.0.3.

6.3 *Results:*

6.3.1 Calibration curve of C1

The calibration curve covered the range from 12.5ppb (LLOQ) to 1000ppb.

6.3.1a Regression line without passing through the origin

The liner regression of the calibration curve without passing through the origin of C1 is shown in **figure 6.1A**. The linearity and equation of C1 between 12.5 and 1000ppb were $r^2=0.994$ and y = 0.007x + 0.105, respectively. A significant non-zero ($P<0.0001$) was observed in the curve.

6.3.1b Regression line passing through the origin

The liner regression of the calibration curve passing through the origin of C1 is shown in **figure 6.1B**. The linearity and equation of C1 between 12.5 and 1000ppb were $r^2=0.992$ and y = 0.007x, respectively.

6.3.1c Weighted least squares linear regression

The linearity and equation of the weighted least squares liner regression for the calibration curve of C1 between 12.5 and 1000 ppb were $r^2=0.978$ and y = 0.008x + 0.002, respectively.

A. C1 Calibration Curve

$y = 0.007x + 0.105$
$R^2 = 0.9942$

B. C1 Calibration Curve, through origin

$y = 0.0072x$
$R^2 = 0.9929$
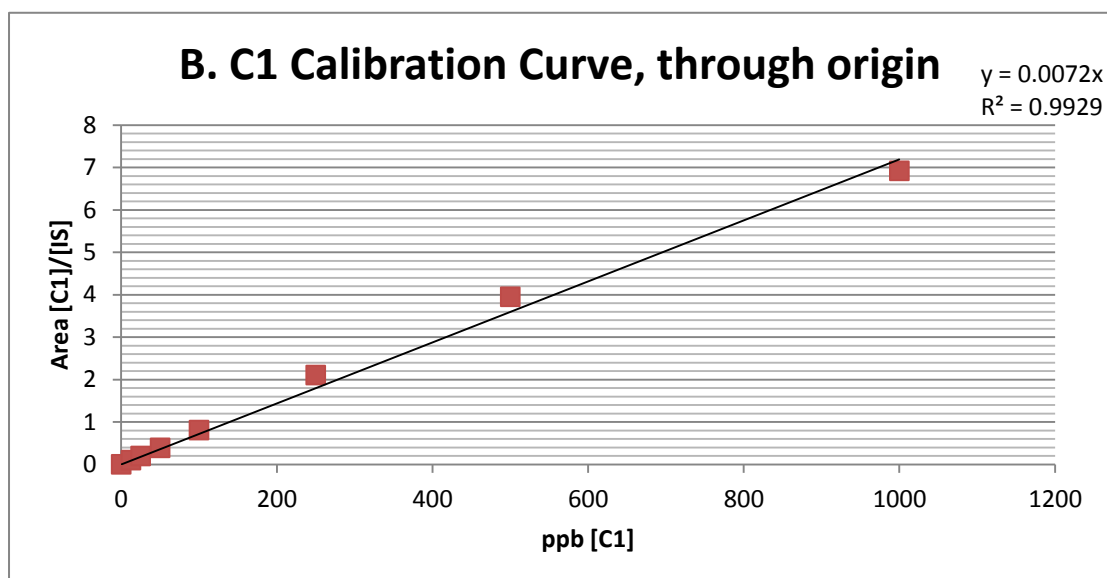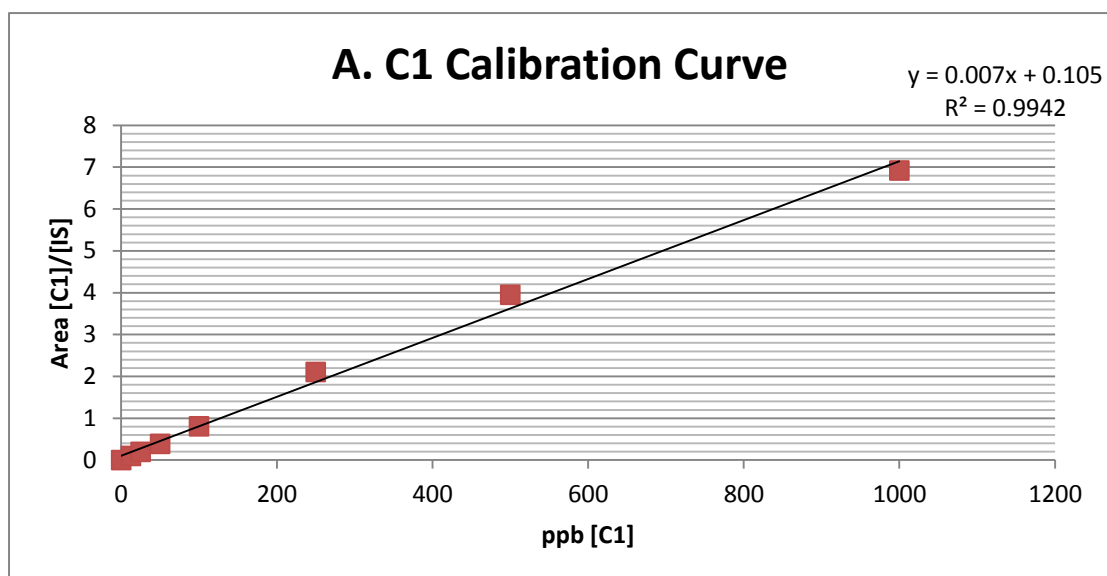
Figure 6.1 Calibration curve of C1

2μl 0, 12.5, 25, 50, 100, 500 and 1000ppb of C1 with 500ppb IS plasma extract were analyzed by LC-MS/MS method to construct the standard curve of C1. The response was calculated by the area of C1 over the area of IS. Area [C1]/[IS] versus concentration of C1 was plot. A simple linear regression line was obtained by least squares method with (A) regression line without passing through the origin; and (B) regression line passing through the origin. (n=3)

6.3.2 Accuracy

6.3.2a Accuracy determined by linear regression passing though the origin

The accuracies measured in 12.5, 50, 250 and 1000ppb of C1 were -4.4, 89.6, 96.6 and 100.6%, respectively (**Table 6-1A**). This equation is not suitable for use in determining the low level of analyte.

6.3.2b Accuracy determined by linear regression without passing though the origin

The accuracies measured in 12.5, 50, 250 and 1000ppb of C1 were 112.4, 108.3, 113.4 and 96.1%, respectively (**Table 6-1B**). All value fulfilled the suggestion from FDA which the deviation is within 15% to the actual value.

6.3.2c Accuracy determined by weighted linear regression

The accuracies in 12.5, 50, 250 and 1000ppb of C1 were 99.2, 96.9, 102.0 and 86.4%, respectively **(Table 6-1C)**. All value fulfilled the suggestion from FDA which the deviation is within 15% to the actual value.

A

Actual [C1] (ppb or ng/ml)	Found [C1] (ppb) Mean ± SD	Accuracy (%)
12.5	-0.54 ± 1.73	-4.4
50	44.75 ± 3.62	89.6
250	241.41 ± 14.79	96.6
1000	1006.37 ± 17.20	100.6

B

Actual [C1] (ppb or ng/ml)	Found [C1] (ppb) Mean ± SD	Accuracy (%)
12.5	14.05 ± 1.69	112.4
50	54.14 ± 4.23	108.3
250	287.00 ± 17.25	113.4
1000	960.58 ± 16.72	96.1

C

Actual [C1] (ppb or ng/ml)	Found [C1] (ppb) Mean ± SD	Accuracy (%)
12.5	12.40 ± 1.52	99.2
50	48.47 ± 3.80	96.9
250	254.93 ± 15.53	102.0
1000	864.27 ± 17.20	86.4

Table 6-1 Accuracy of C1 determination

2μl 12.5, 50, and 1000ppb of C1 with 500ppb IS plasma extract were analyzed by LC-MS/MS. The response was calculated by the area of C1 over the area of IS. The concentration was found by using a (1) least squares method linear equation without passing through the origin $y = 0.007x + c$; (2) least squares method linear equation passing through the origin $y = 0.007x$; and (3) weighted least squares linear equation $y = 0.008x + 0.002$ from the calibration curve. The mean and standard deviation (SD) value were calculated. Accuracy % = Found [C1] / Actual [C1] x 100%. (n=5)

6.3.3 Precision

The coefficients of variation (CV) of intra run precision at 12.5, 50, 250 and 1000ppb of C1 were 11.99, 7.81, 4.52 and 7.50, respectively (**Table 6-2**). The CV of inter run precision at 12.5, 50, 250 and 1000ppb of C1 were 11.16, 8.08, 7.54 and 6.78, respectively. All value fulfilled the suggestion from FDA which all the CV values do not excess 15%.

6.3.4 Recovery

The extraction recovery of C1 at 25, 250 and 1000ppb were 62.3% ± 3.40, 106% ± 2.37 and 77% ± 2.87, respectively (**Table 6-3**).

Concentration of C1 (ppb or ng/ml)	Intra-run RSD (%CV) (n=5)	Inter-run RSD (%CV) (n=10)
12.5	11.99	11.16
50	7.81	8.08
250	4.52	7.54
1000	7.50	6.78

Table 6-2 Intre-run and inter-run precision of C1 determination
2μl 12.5, 50, and 1000ppb of C1 with 500ppb IS plasma extract were analyzed by LC-MS/MS in two different days, Day1 and Day2. The response was calculated by the area of C1 over the area of IS. %CV = SD /Mean x 100%.

	Concentration (ppb)	Extraction Recovery (%)
	25	62.3 ± 3.40
C1	250	106 ± 2.37
	1000	77 ± 2.87

Table 6-3 Recovery of C1 from plasma by EA extraction
2μl 25, 250, and 1000ppb of C1 with 500ppb IS plasma extract were analyzed by LC-MS/MS. The response was calculated by the area of C1 over the area of IS. Extraction recovery was calculated by the response from EA extracted analyte over the response from unextracted analyte. (n=5)

6.3.5   Plasma drug concentration time curve for i.p. injection

Administration of 10mg/kg of C1 to the mice by i.p. increased the plasma C1 concentration to a peak at 15 minutes (Tmax) with a concentration of 5.8µg/ml (Cmax). The rapid absorption was mainly due to the high water soluble property of C1. The concentration of C1 slowly increased from 5 to 15 minutes because most of the administrated C1 was absorbed from the peritoneal region and the absorption rate become lower than distribution rate. The plasma C1 concentration dropped dramatically from 15 to 30 minutes was mainly due to the high distribution rate of C1 throughout the body. The plasma C1 concentration decreased at a slower rate from 30 to 60 minutes as most of the C1 had been distributed to different organs. The body C1 concentration had reached an equilibrium state. At 60 minutes the plasma C1 concentration decreased at a very slow rate. The further decreased in C1 concentration was mainly due to the metabolism and elimination. At 360 minutes, the plasma C1 concentration fell below to the LOQ region which could not be quantified but it was still at the LOD region (**Figure 6.2**).

6.3.6   Pharmacokinetic parameters

The time for reaching the maximum plasma C1 concentration was 15 minutes with a concentration of 5.8µg/ml. The alpha and beta phase half-life of C1 were 12.4 and 146.3 minutes, respectively. The area under the curve from time zero to 360 minutes was 154967.8ng-min/ml and from time zero to infinity was 156784.9ng-min/ml. The clearance of C1 was 63.8ml/min/kg (**Table 6-4**).

A
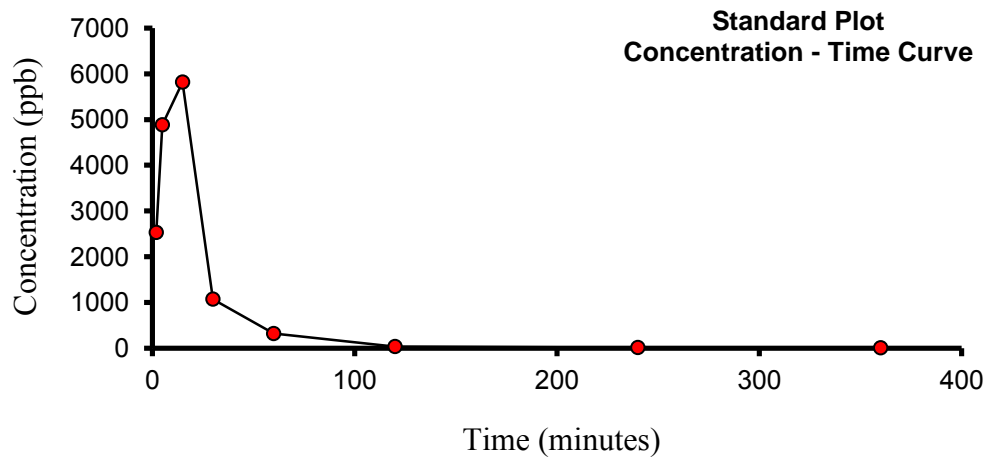
B
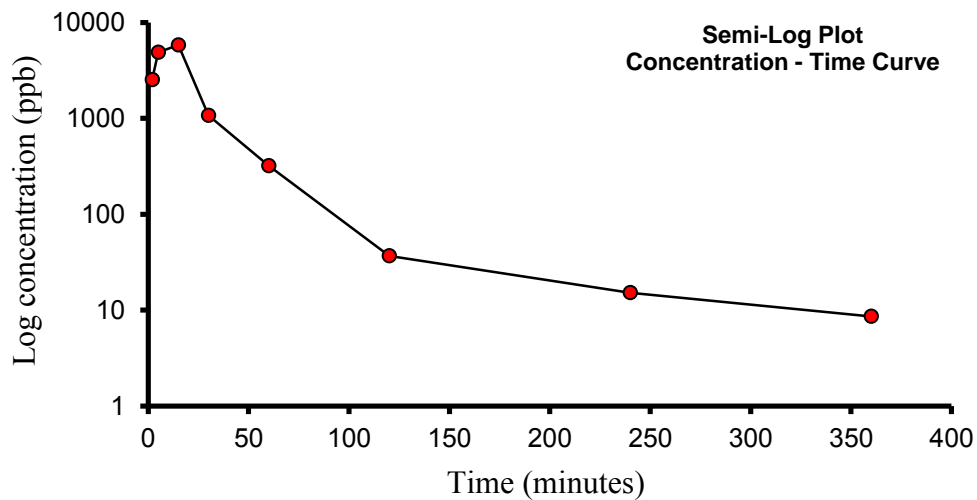
Figure 6.2 Plasma C1 concentration time curve after a single bolus i.p. injection of 10mg/kg

(A) Normal plot and (B) Semi-log plot of C1 concentration – time curve; Young female C57BL/6J mice were injected with 10mg/kg C1. After 2, 5, 15, 30, 60, 120, 240 and 360 minutes, mice were sacrificed by cardiac stick exsanguinations during blood collection. The blood were treated with EDTA and centrifuged to yield plasma. C1 was extracted from the plasma by EA and underwent LC-MS/MS analysis. The response was converted to concentration by a calibration curve. The C1 concentrations in plasma were plot against different time point. n=5

Tmax	15 minutes
Cmax	5816.6ng/ml
AUC (0-t)	154967.8ng-min/ml
AUC (0-∞)	156784.9ng-min/ml
$T_{1/2,\,\alpha}$	12.4min
$T_{1/2,\,\beta}$	146.3min
CL (area/kg)	63.8 ml/min/kg

Table 6-4 Pharmacokinetic parameters from single bolus i.p. injection of 10mg/kg

These parameters obtained either from the direct observation from the plasma C1 concentration time curve or by Pharmacokinetic software – Summit® PK solution.

6.4   Discussion:

6.4.1   Calibration curve

The calibration curve is important for the accurate determination of the unknown analyte in an analytical method. The linearity is a key parameter to tell if the relationship between the analyte response and concentration follow a linear function in a given range. A good linearity is always important for a good calibration curve. However, a good linearity only demonstrates that the well prepared samples have been analyzed in a well designed analytical method. A good linearity itself does not mean an accurate determination of unknown analyte unless a suitable regression line is employed.

Two linear regression lines (**Figure 6.1A & B**) are constructed from the same set of data. They are constructed based on two assumptions, with or without passing through the origin. Both curves are having a good linearity with different linear equation. The data obtained from the linear equation without passing through the origin were found to have a lower accuracy in low concentration range. This is due to the deviation at the higher concentration out weight the regression line and influence the accuracy in the lower end range (Szabo, Browne et al. 1994). This calibration curve failed to estimate the C1 at the lower concentration range and gave a negative value of C1 at LLOQ. However, this calibration curve was able to determine an unknown C1 concentration accurately at the high concentration range. In contrast, the linear regression line passing through the origin provided a positive value at the LLOQ which gave a better accuracy on the lower range. The accuracies of different concentrations were found to be within 15% from the actual value. Apart from the simple linear regressions, WLSLR was also used to construct the linear regression of

the calibration curve. This method gives the most accurate C1 determination in 12.5, 50, and 250ppb but the accuracy was reduced at 1000ppb. The accuracies of different concentrations are also within 15% from the actual value.

Both linear regression line passing though the origin and WLSLR in this study fulfilled the guidance of bioanalytical method validation from FDA and both of them could be used in the determining the C1 plasma concentration. According to the FDA suggestion, a simple method is always preferred. Hence the linear equation passing though the origin was used in the remaining part of the study. In addition, a more accurate determination of the unknown analyte can be done by using a low range and high range calibration curve. This can reduce the order of magnitude of the calibration curve and reduce the influence by the higher variance at high concentration.

6.4.2   Administration routes

The aim of this pharmacokinetic study was to determine an optimum dose and administrate route of C1 for osteoporotic animal study. The usual practice for PK profile is referred to i.v. injection as all the drug will be administrated into the body. In this study, a small scale single bolus i.v. administration was conducted in mice for obtaining the preliminary results. For the i.v. administration dose of 0.1mg/kg and 1mg/kg, the plasma C1 concentration dropped dramatically to an undetectable level which indicating that those C1 has been distributed to different organ quickly without maintaining at the effective dose (10nM) found in the *in vitro* study (Data not shown). Hence, a higher dose was required. Since C1 is water soluble and it has no doubt that i.v. injection must be a valid administration route. It is also possible that a highly water soluble C1 could enter the circulatory system through the

intraperitoneal region of the animal. Therefore, an i.p. injection of 1mg/kg and 10mg/kg were also made. Similar to the i.v. injection, the 1mg/kg injection could not maintain the blood C1 concentration to the effective dose. The 10mg/kg injection was found be able to maintain the blood C1 concentration at the effective range and hence it had been chosen for used in the latter part of the PK experiment.

Indeed, the oral administration is always preferred as it is having the least stress for the animals during the experimental period when compared to i.v. or i.p. injections. Also, the oral administration offers the longest infusion time for C1 absorption which might give a more steady C1 plasma concentration. This prevents a sudden elevate of C1 in the plasma concentration to a very high level that might potentially cause toxicity effects. However, the absorption efficiency of oral administration is very low when compared to i.v. and i.p. injections which requires large amount of C1 for the study. A low bioavailability is predicted as the absorption efficiency for catchin in oral administration is limited, too (Chu, Wang et al. 2006). Therefore, the limit supply of C1 did not favor the oral administration of C1 to the animal in this study. However, it is still worthy to explore the potential use of oral administration in the PK study as well as the long term *in vivo* study.

6.4.3 Pharmacokinetic study

The plasma C1 concentration curve is fitted into a compartmental PK model. A maximum plasma concentration is found to be 1.97×10^{-5}M at 15 minutes after i.p. injection. The rapid distribution of C1 to different part of the body decreased the C1 concentration to 3.91×10^{-6}M at 30 minutes which is near to the effective range of C1 found in cell culture model. Between 30 to 60 minutes, equilibrium is reached in the body. The further decrease in C1 plasma concentration is mainly due to the

elimination and metabolism. The use of compartmental modeling in this study could calculate the elimination half-life. It is useful to estimate the plasma drug concentration for a particular time point after administration. The elimination half-life of C1 is found to be 146.3 minutes. Using the $T_{1/2,\,\beta}$ and the last point above the LOQ found in the curve, the plasma C1 concentration is estimated to fall below 10^{-8}M at around 600 minutes. This suggested that the single i.p. bolus can provide 10 hours of effective dose of C1 to the animal.

C1 was found to have a fast elimination half-life. This indicated that C1 could be distributed to the organs and tissues in a very short time. The short latency time makes C1 more readily to reach the target tissue and exert its effects. But, a short elimination half-life also gives rise to another problem. A higher administration dose or more frequent administration is needed for maintaining the C1 at effective concentration. This concern can be found in the PK profile **(Figure 6.2)** of administrating C1 by i.p. injection at 10mg/kg. The Cmax was found to be 20μM. The high concentration of C1 in plasma might cause undesirable to the animal body. Although this concentration did not last for too long, it is still important to perform a toxicity test on C1. Indeed, the integrations of PK, efficacy and toxicity study could be used to determine the most suitable administration route, dosage and dosing intervals of C1 with maximized effects but minimized side effects.

The drug concentration in different organ might sometime be determined because plasma drug concentration is too general for describing the drug in animal body. The drug concentration in organs such as liver, kidney and intestine responsible for absorption, metabolism and elimination are sometime measured to describe the drug behavior in the body. To tackle these problem, a more advance physiologically based

pharmacokinetic modeling (PDPK) could be used. PDPK is a multi-compartmental modeling that dissects the body into different tissue or organ compartments. This modeling integrates the *in vivo* and *in vitro* data to build up the whole model. PDPK could also be used to perform a toxicity test (McNally, Cotton et al. 2011). These PK studies would be useful upon the effects of (-)-epiafzelechin are further characterized in the animal.

6.4.4 Dosage and dosing interval for efficacy study

The plasma drug concentration curve by single i.p. injection of C1 provides the information of how long does C1 effective dose can be maintained in the circulatory system. This is useful for predicting the dosage to be used in the osteoporotic animal study. A 10mg/kg i.p. injection is found to be able to maintain plasma C1 concentration at 10^{-8}M. This dosage is likely to be used in the efficacy study. In fact, the UMR-106, MC3T3-E1 and RAW264.7 cell models suggested that the effective dose of C1 can sometime be lower than 10nM, which indicating the actions of C1 might last longer than 10 hours. It is not possible for injecting C1 twice a day as the i.p. injection might build up too much stress to the animals and even caused death. A daily i.p. injection of C1 for six days in a week last for two months will be good enough for the long term osteoporotic animal efficacy study.

6.5   Summary:

The LC/MS-MS method was successfully validated for use in determining the plasma concentration of (-)-epiafzelechin in mouse model. Simple least squares linear regression was used to construct the calibration curve of (-)-epiafzelechin. The current detection method for (-)-epiafzelechin was successfully validated in according to the guidance from ICH and FDA. (-)-Epiafzelechin could be found in the animal body by i.v. and i.p administration routes which can be used in other animal studies. A daily i.p. injection was chosen for used in the osteoporotic animal study because of the limited supply of (-)-epiafzelechin. (-)-Epiafzelechin could be maintained above the effective concentration 10^{-8}M for 10 hours by a single bolus of 10mg/kg C1 i.p. injection.

7   Discussion and Conclusion

7.1 Discussion:

7.1.1 Studying flavan-3-ols from DF

The use of Chinese medicine for managing osteoporosis was gaining more attention in recent year. More *in vitro* and *in vivo* studies suggested that different herbal extracts exert osteoprotective effects. DF was studied extensively in different research groups because of it efficacy (Sun, Lin et al. 2002; Sun, Dong et al. 2003; Chen LL 2011). In the meanwhile, naringin was found to be the representing active ingredients in DF (Zhang, Dai et al. 2009; Pang, Wang et al. 2010; Ang, Yang et al. 2011; Chen, Lei et al. 2011). Other than naringin, more active ingredients were isolated from DF and these compounds were identified as flavan-3-ols (Chang, Lee et al. 2003; Wang, Wang et al. 2008). These compounds share the backbone of flavan-3-ol with different functional group attached on the backbone. Their bone protective effects were analyzed by different biological assays. However, it lacks some comprehensive biological study to demonstrate their effects.

There are two main themes in the current study of the osteoprotective flavan-3-ols in DF. Firstly, we investigated the estrogen-like bone protective effects of flavan-3-ols by using *in vitro* bone remodeling models. Secondly, we determined the bioavailability of flavan-3-ols using *in vivo* pharmacokinetic study. The current study of active compounds in DF broadens our understanding on flavan-3-ols and strengthens the evidence that flavan-3-ols are the active ingredients in DF. By incorporating our previous findings in DF (Pang 2010) and naringin (Pang, Wang et al. 2010), we are able to better elucidate the pharmacological actions of DF in bone.

The use of single compound in this study minimizes the interactions between the compounds found in DF. At least, from the pharmacokinetic point of view, the absorption will not be affected by the other compounds existed in the mixture. This could reduce the dosage use in the treatment and maximize the therapeutic effect. On the other hand, the flavan-3-ols used in study were chemically synthesized. The bioavailability might also be increased by a suitable chemical structure modification on the compounds for making them as a pro-drug. These strategies could be helpful for developing the active compound for therapeutic use in managing bone disorder.

7.1.2 Activities of flavan-3-ols on bone cells

Flavan-3-ols exerted proliferative effects on bone cells. These effects were not affected by the functional group or the stereochemistry of flavan-3-ols. In contrast, flavan-3-ols were not active in promoting the ALP activities of mature osteoblastic cells **(Table 7-2)**. In the bone formation model, treatment of (-)-epiafzelechin for three days upregulated Cbfa1/Runx2, osteocalcin and collagen 1a1 genes on MC3T3-E1 cells. It also increased the ALP activity, collagen content in 7 days culture but decreased the calcification in 21 days culture. (-)-epiafzelechin mainly acted on the pre-osteoblasts in early phase osteoblastogenesis. In the bone resorption model, (-)-epiafzelechin decreased the number of osteoclast precursor cells viability. It also reduced the TRAP multinucleated cells as well as the TRAP activities of RAW cells in the presence of RANKL **(Table7-3)**. (-)-Epiafzelechin was found to be able to prevent the maturation of osteoclastic precursor cells. This information supported that flavan-3-ols, particularly (-)-epiafzelechin, were the active ingredients in DF. The most abundantly found flavan-3-ols – (-)-epiafzelechin was found to modulating the bone remodeling process.

7.1.3 Flavan-3-ols activate ER and Runx2

In chapter 3, the estrogen-like activities of different structures and isomeric forms of flavan-3-ols were demonstrated by the proliferating effects on estrogen sensitive cells, the abolishing effects by ER antagonist and the activating effects on ER mediated ERE luciferase gene. In chapter 4, we discovered that C1 and E2 are able to activate the Cbfa1/Runx2 related gene during osteoblastogenesis.

This information raises a question if there is any signal transduction between ER and Cbfa1/Runx2 as both E2 and C1 are able to upregulate the Runx2 gene expression. *Thomas and et al.* (2003) suggested that the ligand bound ER-α could heterodimerize with transcription factor Runx2 and act on the Runx response elements (RRE) for activating the downstream gene candidates. In addition, *Khalid, Baniwal et al.* also found that there is physical interaction between ER-α and Runx2 during immunoprecipitation (Khalid, Baniwal et al. 2008). This might explain the effect of ligand binding action of estrogen to ER-α and activates Runx2. However, the ligand independent estrogenic effects of C1 could not be explained as flavan-3-ols do not directly bind to ER at physiologically concentration. Therefore, we are looking for another pathway that regulates Runx2. Indeed, Cbfa1/Runx2 was also found to be regulated by the MAPK (Xiao, Jiang et al. 2000), while MAPK is involved in the ligand independent ER-α activation pathway. With this information, we proposed that the activation of RRE might due to a similar mechanism. First of all, the ER-α is phosphorylated by the MAPK upon the induction of flavan-3-ols. The conformational changed pER-α bind to Runx2 and forming a pER-α/Runx2 complex. This complex is then binds to the RRE and activates the corresponding downstream

gene candidates. However, this hypothesis has to be further proven by a series of biological study between the signal transduction of ER-α and Runx2.

7.1.4   The importance of stereospecificity

The stereospecificity of compound was one of the concerns throughout this study because it could affect both the analytical and biological evaluations. In the pharmaceutical industry, more drugs were being switched from racemic mixture to stereospecific compounds (Patel 2004) because more recent findings suggested that the different isoforms of compound in racemic mixture might not have the same biological activities and even have undesirable effect. (Kasprzyk-Hordern 2010). The different biological activities of the enanitomers hinder the use of racemic mixture in the drug industrial. Propranolol, a beta blocker drug for treating hypertension, is a typical example of the importance of stereospecific. The S(-)propranolol is found to be 100 times more active than R(+)-propranolol as a beta blocker (Kasprzyk-Hordern 2010). Other agent such as ketamine has also demonstrated the differentiation effects on different isomers. S(+)-Ketamine is anaesthetic and analgesic while R(-)-ketamine produces side effects such as hallucination and agitation. S(+)ketamine is also found to be more potent in mice than R(-)-ketamine (Kanellopoulos, Lenz et al. 1998). Hence, the potential therapeutic agents in stereospecific forms are studied one by one to minimize the potential undesirable effects cause by the individual isomer (Wermuth 2008). In chapter 3, we had demonstrated the effects of epiafzelechin isomers on bone and estrogen-like activities. Although there was not a big different between the isomers in the bone cell model but the stereochemistry did affects the analysis in chapter 5 and chapter 6.

Racemic mixture is not easy to separate. In LC, it requires a specific chiral column to separate two compounds in a racemic form. In chapter 5, we developed a bioanalytical method for detecting C1 but it could not differentiate all the isomers in the racemic mixture. We successfully separated C1 and D1 (epimer) from a mixture but not C1 and C2 (enantiomer) in our described method (data not shown). Unable to differentiate enantiomer might cause a problem during the PK study. Enantiomers which having the same physicochemical properties but differ in biological properties (Kasprzyk-Hordern 2010) might have different pharmacokinetic behavior. This might due to their different affinities toward the receptors affinities or different behavior toward the enzymetic reactions (Caldwell 1996). In such case, one of the isomers might easily absorb into the body but not the other. As the bioanalytical method could not distinguish the isomer, this could underestimate the absorption rate for the drug compound and draw a wrong conclusion. This problem might be solved by developing a chrial specific detection method to illustrate the behavior in different drug isomers (Pham-Huy, Radenen et al. 1995). Indeed, a better solution is to use the stereospecific isomer in a study. From our result, different stereochemistry of flavan-3-ols did not affect much of the biological activity, at least in bone cells. But, there is not any information regarding the effects of flavan-3-ols on other tissues and organs. It is unsure that the stereoisomers might have any undesired effects on other organs. At least, the activations of ERE transcriptional events were not the same in different stereoisomers. Their structure difference might also affect the behavior in ADME process with a different PK profile. Therefore, stereospecificity is regarded as an important issue in studying the biological effects of different therapeutic agents.

7.1.5 Active ingredients in DF

Naringin was reported as the major active ingredients in DF (Chang, Lee et al. 2003). The bone protective effects were studied extensively in different *in vitro* and *in vivo* models (Wong and Rabie 2006; Hirata 2009; Pang, Wang et al. 2010; Chen LL 2011). In addition, the pharmacokinetics of naringin and its metabolite was also studied by using different bioanalytical methods (Hsiu, Huang et al. 2002; Li 2010). Although naringin is described as the major active ingredients in DF, it may not be the most abundant flavanoid compounds in DF. In fact, 94mg of (-)-epiafzelechin or C1 and 15.9mg of naringin were extracted from 6kg raw dried DF according to the method described by *Chang et al.* (2003). This indicated the amount of C1 in DF is larger than naringin. In chapter 4, the bone protective effects of C1 are demonstrated by osteoblasts and osteoclasts *in vitro* models. Our results suggested that C1 is likely to be another active ingredients found abundantly in DF which is worthy to further discover its effects on *in vivo* model. In addition, our previous study using DF total flavanoids extracts exert a better bone protective effect than using naringin alone in osteoporotoic mice model (Wong 2013). Taken these into account, the bone protective effects of DF might due to the multiple actions of different active ingredients in DF including naringin, C1 and other flavan-3-ols.

7.1.6 Bioanalytical method for studying DF

The aim of chapter 5 was to develop a bioanalytical method of C1 for use to determine the plasma C1 concentration. This method was used in chapter 6 to construct a PK profile of C1. The PK profile of C1 was used to determine the dose and dosage interval for further *in vivo* efficacy study. In fact, this detection method

can be extended to detect C1 in other samples such as urine or tissues for a more detailed PK study.

Indeed, the plasma C1 concentration can also be measured after the administration of DF total flavanoid extract as C1 is naturally existed in DF. The elevation of plasma C1 concentration to the pharmacological range after administration of DF further strengthened that C1 is the active ingredient in DF. Unlike pure C1 administration, DF contains other compounds that might also affect the ADME process of C1 and alter its bioavailability in the body. Apart from studying the plasma C1 concentration in animal fed with DF. It will also be useful to include the well characterized active ingredients, naringin in the further PK study of DF. *Li and et al.* (2010) developed a simultaneous detection method for naringin and naringenin in rat plasma. After oral fed the rats with DF, the amount of naringin and naringenin in rat plasma can be quantify. In a similar way, a simultaneous detection of C1, naringin and naringenin may be done by the modifying the current LC/MS-MS. The simultaneous detection of C1, naringin and naringenin in body after administration of DF could resolve the pharmacokinetic behavior of DF as our present results suggested that C1 is another an important active ingredient in DF. This might be useful to explain our previous result that DF total flavanoids extract exerts a better bone protective effect than using naringin alone in osteoprotoic OVX mice model (Wong 2013).

7.1.7 *In vitro* efficacy and pharmacokinetic studies

The *in vitro* efficacy studies of (-)-epiafzelechin demonstrated the potential bone protective effects while the pharmacokinetic study suggested that the effective concentration of (-)-epiafzelechin could be maintained in the animal body. These results suggested that (-)-epiafzelechin is likely to exert bone protective effects in animal body. However, there are still many factors that could affect the efficacy in the complex animal body such as the distributions and metabolisms of compound. The PK experiment results suggested that (-)-epiafzelchin could be distributed throughout the animal body in a very short time. However, this was based on the plasma drug-concentration curve and the assumption of one compartmental modeling. The distributions of (-)-epiafzelechin might be different from organ to organ. This might affect the actual efficacy of the active compound. The metabolism of compound might also convert the active compound into inactive form and minimize the actions. Therefore, an *in vivo* efficacy is needed for further characterizing the active compound.

7.1.8 *In vivo* model for pharmacokinetic and osteoporotic studies

In chapter 6, the pharmacokinetic of C1 was conducted by using C57BL/6J mice. The selection of animals was based on the use of osteoporotic models because our primary aim is to study the osteoprotective effects of flavan-3-ols with *in vitro* and *in vivo* models. The use of the same strain and genetic background of animals in different *in vivo* studies could minimize the biological variation.

In fact, different animal models have been used for studying osteoporosis. Rodents are commonly used in osteoporosis studies because of their fast generation and short life span (Turner 2001). However, rodents do not experience a natural menopause and therefore, an ovariectomy (Ovx) operation is required for simulating menopausal in animals (Kalu 1991). The use of rats is more popular than mice in osteoporotic study in the earlier time because of the non-invasive measurement of BMD such as DXA requires a larger animal size (>50g) for reaching the accuracy limit (Grier, Turner et al. 1996). The BMD measurement is improved nowadays by using a higher resolution microcomputed tomography (micro-CT). This allows the use of smaller animals in the bone studies (Martin-Badosa, Amblard et al. 2003). As mentioned, the supply of flavan-3-ols is limited from natural source as well as the current synthetic technology. The smaller animal size minimized the use of compound which is more favorable in our current study. Among the osteoporotic mice model, C57BL/6J is found to be a useful model for studying age-related osteoporosis (Ferguson, Ayers et al. 2003). This model was successfully used in our group to demonstrate the osteoprotective effects of DF and naringin previously (Yin 2007; Pang, Wang et al. 2010).

7.1.9   Further Study

The current study of DF flavan-3-ols includes an *in vitro* efficacy studies on different cell lines as well as an *in vivo* pharmacokinetic study. A long term study using an osteoporotic OVX mice model will be conducted. In addition, the toxicity study as well as a more comprehensive pharmacokinetic study will also be important for studying the biological effects of flavan-3-ols.

On the other hand, the *in vitro* efficacy study can be extended to the earlier stage of osteoblastogenesis. The osteoblastogenesis starts from the differentiation of pluripotent mesenchymal stem (MSC) cells. Under the regulation of Wnt signaling, the MSC cells will be differentiated into osteoprogenitors, pre-osteoblasts, mature osteoblasts and finally osteocytes (Westendorf, Kahler et al. 2004). In the current study of flavan-3-ols, we have demonstrated that flavan-3-ols could stimulate the pre-osteoblasts and mature osteoblasts with two established cell lines, MC3T3-E1 and UMR-106, respectively. The use of cells involved in earlier osteoblastogenesis, MSC cells, might help to elucidate the effects of flavan-3-ols on the earlier phase of bone cells development. Chen *et al.* (2005) has reported that green tea catechin could enhance osteogenesis in MSC cells. They found that the ALP activity, Runx2 and Ocn gene expression were upregulated by catechin (Chen, Ho et al. 2005) where these results are similar to our study of (-)-epiafzelecin in pre-osteoblastic cells. Hence, the use of MSC might lead us to further explore the effects of flavan-3-ols on a much earlier phase of osteoblastogenesis. For osteoclastogenesis, the analysis on cell cycle as well as DNA fragmentation can be used to characterize the apoptotic effects of flavan-3-ols on RAW 264.7 cells.

7.2 Conclusion:

In conclusion, this study indicated flavan-3-ols are phytoestrogens which could stimulate the proliferation of bone cells through ER. A structure activity relationship of flavan-3-ols was observed in ERE transcriptional activities but not in ER binding. These differences did not affect their proliferative effect on bone cells. (-)-epiafzelechin or C1 was found to be one of the bone protective flavan-3-ols in DF. It modulated the bone remodeling process by promoting osteoblastogenesis and inhibiting osteoclastogenesis in cell culture models within the physiologically achievable concentration between 10nM to 1μM.

On the other hand, the bioanalytical method was successfully developed for the detection of C1 in plasma by using LC-MS/MS. This method was used to construct a PK profile for C1 by a single bolus i.p. injection at 10mg/kg. This PK profile was used to determine the dose and dosing interval for use in the long term osteoporotic study by using OVX mice. It is hope that the current study could provide more information for the investigation of active ingredients in DF as well as to elucidate the potential use of flavan-3-ols as a bone protective agent.

Cpd:	A	B	C1	D1	F1
Cell Proliferation (UMR-106)	↑	↑	↑	↑	↑
Cell Pro (MCF-7)	↑	↑	↑	↑	↑
ER dependency Cell Proliferation (UMR-106)	↓	↓	↓	↓	-

Table 7-1 Summary table for the result of flavan-3-ols dissolved in DMSO
↑ : increase; ↓ decrease & - no effect

Compounds		C1	C2	D1	D2	F1	F2
Cell Pro. UMR106	24Hr	↑	↑	↑	↑	X	X
	48Hr	↑	↑	↑	↑	X	↑
Cell Diff. UMR106	24Hr	↑	X	X	X	X	X
ER-α mediated ERE transcription		↑	↑	↑	↑	X	↑
ER-β mediated ERE transcription		X	↑	↑	↑	↑	↑
ER-α Binding		X	X	X	X	X	X
ER- β Binding		X	X	X	X	X	X

Table 7-2 Summary table for the result of stereospecific flavan-3-ols
↑ : increase; ↓ decrease & - no effect

Treatment	Preosteoclastic MC3T3-E1 Cells						Preosteoclastic RAW 264.7 Cells		
	Gene expression			ALP	ECM Collagen	Mineralization	Precursor Cell viability	TRAP multinucleated cells	TRAP activity
	Cbfa1/Runx2	Osteocalcin	Collagen 1a1						
E2	↑	↑	-	↑	-	↑	-	↓	↓
C1	↑	↑	↑	↑	↑	↓	↓	↓	↓

Table 7-3 Summary table for the results of C1 on pre-osteoblast and pre-osteoclast cells
↑ : increase; ↓ decrease & - no effect

(A)

(B)

(C)

(D)
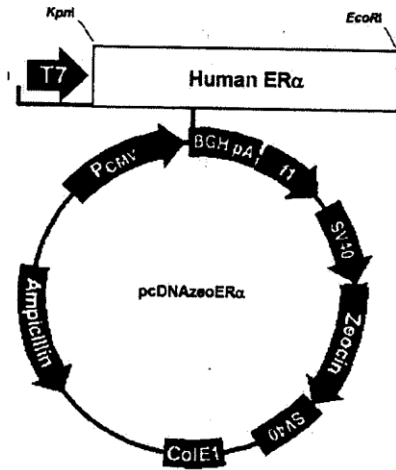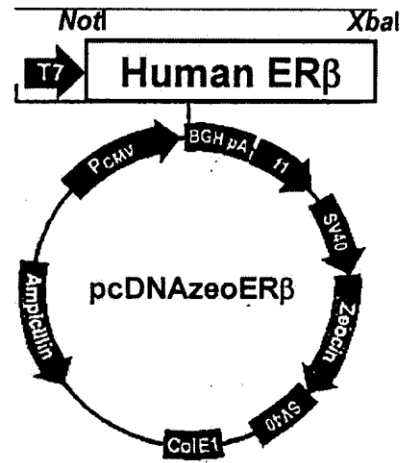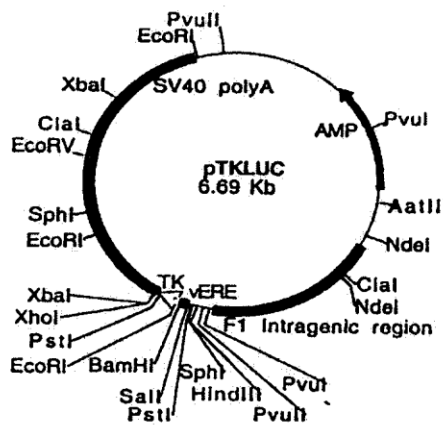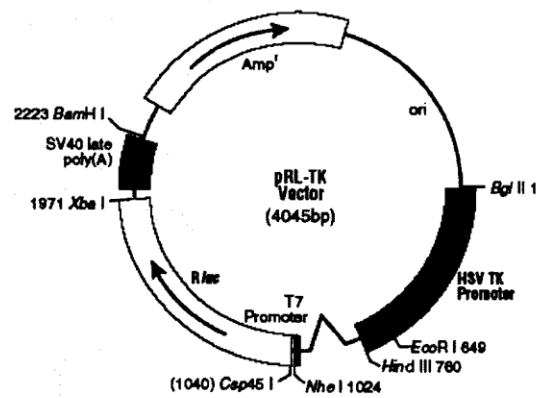
(A)hERα, (B)hERβ, (C)TK-linked luciferase plasmind, and (D)ERE-linked luciferase plasmid used in ER mediated ERE transcriptional assay

Reference

(1992). Development of New Stereoisomeric Drugs. U. S. F. a. D. Administration. US.

(2001). Guidance for Industry Bioanalytical Method Validation. U. S. D. o. H. a. H. Services. US.

(2005). Validation of analytical procedures: Text and Methodology, International Conference on Harmonisation of Technical Requirements for Registration of Pharmaceuticals for Human Use.

Acworth, I. U., P.; Waraska, J.; Gamache, P. (2011). Application of HPLC with Photodiode Array and Coulometric Electrochemical Array Detection to the Study of Natural Products, Botanicals, and Mammalian Tissues: From Targeted Analyses to Metabolomics. USA, Thermo Fisher Scientific.

Al-Dhaheri, M. H. and Rowan, B. G. (2007). "Protein kinase A exhibits selective modulation of estradiol-dependent transcription in breast cancer cells that is associated with decreased ligand binding, altered estrogen receptor alpha promoter interaction, and changes in receptor phosphorylation." Mol Endocrinol **21**(2): 439-456.

Almeida, A. M., Castel-Branco, M. M., et al. (2002). "Linear regression for calibration lines revisited: weighting schemes for bioanalytical methods." J Chromatogr B Analyt Technol Biomed Life Sci **774**(2): 215-222.

Andersson, G. and Ek-Rylander, B. (1995). "The tartrate-resistant purple acid phosphatase of bone osteoclasts--a protein phosphatase with multivalent substrate specificity and regulation." Acta Orthop Scand Suppl **266**: 189-194.

Ang, E. S., Yang, X., et al. (2011). "Naringin abrogates osteoclastogenesis and bone resorption via the inhibition of RANKL-induced NF-kappaB and ERK activation." FEBS Lett **585**(17): 2755-2762.

Aron, P. M. and Kennedy, J. A. (2008). "Flavan-3-ols: nature, occurrence and biological activity." Mol Nutr Food Res **52**(1): 79-104.

Aronica, S. M. and Katzenellenbogen, B. S. (1993). "Stimulation of estrogen receptor-mediated transcription and alteration in the phosphorylation state of the rat uterine estrogen receptor by estrogen, cyclic adenosine monophosphate, and insulin-like growth factor-I." Mol Endocrinol **7**(6): 743-752.

Atanaskova, N., Keshamouni, V. G., et al. (2002). "MAP kinase/estrogen receptor cross-talk enhances estrogen-mediated signaling and tumor growth but does not confer tamoxifen resistance." Oncogene **21**(25): 4000-4008.

Avioli, L. V. (1999). "SERM Drugs for the Prevention of Osteoporosis." Trends Endocrinol Metab **10**(8): 317-319.

Bayliss, P. J. E. A. P. B. M. K. (2000). "ADME/PK as part of a rational approach to drug discovery." Drug Discovery Today **5**(9): 436-444.

Bensky, D. C., S.; S. Erich (2004). Chinese Herbal Medicine, Materia Medica. USA, Eastland Press, Inc.

Berg, C. N., K.; Kirkpatrick, P. (2003). "Fresh from the pipeline Teriparaide." Nat Rev Drug Discov **2**: 257-258.

Bischoff, K. B. (1987). Physiologically Based Pharmacokinetic Modeling. Pharmacokinetic in risk assment - Drinking water and health. US, National Academy Press. **8**.

Bonate, P. L. (2006). The art of modeling. <u>Pharmacokinetic-pharmacodynamic modeling and simulation</u>, Springer.

Boonen, S., Body, J. J., et al. (2005). "Evidence-based guidelines for the treatment of postmenopausal osteoporosis: a consensus document of the Belgian Bone Club." <u>Osteoporos Int</u> **16**(3): 239-254.

Boyce, B. F. and Xing, L. (2008). "Functions of RANKL/RANK/OPG in bone modeling and remodeling." <u>Arch Biochem Biophys</u> **473**(2): 139-146.

Branham, W. S., Dial, S. L., et al. (2002). "Phytoestrogens and mycoestrogens bind to the rat uterine estrogen receptor." <u>J Nutr</u> **132**(4): 658-664.

Brzozowski, A. M., Pike, A. C., et al. (1997). "Molecular basis of agonism and antagonism in the oestrogen receptor." <u>Nature</u> **389**(6652): 753-758.

Bucay, N., Sarosi, I., et al. (1998). "osteoprotegerin-deficient mice develop early onset osteoporosis and arterial calcification." <u>Genes Dev</u> **12**(9): 1260-1268.

Burge, R., Dawson-Hughes, B., et al. (2007). "Incidence and economic burden of osteoporosis-related fractures in the United States, 2005-2025." <u>Journal of Bone and Mineral Research</u> **22**(3): 465-475.

Caldwell, J. (1996). "Importance of stereospecific bioanalytical monitoring in drug development." <u>J Chromatogr A</u> **719**(1): 3-13.

Calvo, M. S., Eyre, D. R., et al. (1996). "Molecular basis and clinical application of biological markers of bone turnover." <u>Endocr Rev</u> **17**(4): 333-368.

Carando, S., Teissedre, P. L., et al. (1998). "Comparison of (+)-catechin determination in human plasma by high-performance liquid chromatography with two types of detection: fluorescence and ultraviolet." <u>J Chromatogr B Biomed Sci Appl</u> **707**(1-2): 195-201.

Chan, M. C. L. K. C. W. W. Y. P. M. S. W. T. H. (2012). "Chemical synthesis and biological study of 4β-carboxymethyl-epiafzelechin acid, an osteoprotective compound from the rhizomes of Drynaria fortunei." Med Chem Commun **3**: 801-806.

Chang, C. L. W., R. T. (2011). "Quantification of (+)-catechin and (-)-epicatechin in coconut water by LC-MS." Food Chemistry **126**: 710-717.

Chang, E. J., Lee, W. J., et al. (2003). "Proliferative effects of flavan-3-ols and propelargonidins from rhizomes of Drynaria fortunei on MCF-7 and osteoblastic cells." Arch Pharm Res **26**(8): 620-630.

Chang, E. J. L., W. J; Cho, S. H.; Choi, S. W. (2003). "Proliferative Effects of Flavan-3-ols and Propelargonidins from Rhizomes of Drynaria fortunei on MCF-7 and Osteoblastic Cells." Archibes of Pharmacal Research **26**(8): 620-630.

Chen, C. H., Ho, M. L., et al. (2005). "Green tea catechin enhances osteogenesis in a bone marrow mesenchymal stem cell line." Osteoporosis International **16**(12): 2039-2045.

Chen, L., Lee, M. J., et al. (1997). "Absorption, distribution, elimination of tea polyphenols in rats." Drug Metab Dispos **25**(9): 1045-1050.

Chen, L., Lee, M. J., Li, H., Yang, C. S. (1997). "Absorption, Distribution, and Elimination of Tea Polyphenols in Rats." Drug Metab Dispos **25**(9): 1045-1050.

Chen, L. L., Lei, L. H., et al. (2011). "Osteogenic effect of Drynariae rhizoma extracts and Naringin on MC3T3-E1 cells and an induced rat alveolar bone resorption model." Arch Oral Biol.

Chen, L. L., Lei, L. H., et al. (2011). "Osteogenic effect of Drynariae rhizoma extracts and Naringin on MC3T3-E1 cells and an induced rat alveolar bone resorption model." Arch Oral Biol **56**(12): 1655-1662.

Chen LL, L. L., Ding PH, Tang Q, Wu YM. (2011). "Osteogenic effect of Drynariae rhizome extracts and naringin on MC3T3-E1 cells and an induced rat alveolar bone resorption model." Arch Oral Biol **56**: 1655-1662.

Chen, W. F., Huang, M. H., et al. (2003). "Inhibitory actions of genistein in human breast cancer (MCF-7) cells." Biochim Biophys Acta **1638**(2): 187-196.

Chenu, C., Colucci, S., et al. (1994). "Osteocalcin induces chemotaxis, secretion of matrix proteins, and calcium-mediated intracellular signaling in human osteoclast-like cells." J Cell Biol **127**(4): 1149-1158.

Chervenak, J. (2009). "Bioidentical hormones for maturing women." Maturitas **64**(2): 86-89.

Chesnut, C. H., Azria, M., Silverman, S., Engelhardt, M., Olson, M., Mindeholm, L. (2008). "Salmon calcitonin: a review of current and future therapeutic indications " Osteoporosis International **19**(2008).

Cheung, W. M. W., Ng, W. W., et al. (2006). "Dimethyl sulfoxide as an inducer of differentiation in preosteoblast MC3T3-E1 cells." Febs Letters **580**(1): 121-126.

Choi, J. Y., Lee, B. H., et al. (1996). "Expression patterns of bone-related proteins during osteoblastic differentiation in MC3T3-E1 cells." J Cell Biochem **61**(4): 609-618.

Chu, K. O., Wang, C. C., et al. (2006). "Pharmacokinetic studies of green tea catechins in maternal plasma and fetuses in rats." J Pharm Sci **95**(6): 1372-1381.

Chu, K. O., Wang, C. C., et al. (2004). "Determination of catechins and catechin gallates in tissues by liquid chromatography with coulometric array detection and selective solid phase extraction." J Chromatogr B Analyt Technol Biomed Life Sci **810**(2): 187-195.

Cole, R. B. (2010). Electrospray and MALDI Mass Spectrometry. US, Wiley.

Cole, R. B. (2010). Electrospray and MALDI mass spectrometry : fundamentals, instrumentation, practicalities, and biological applications, John Wiley.

Cuetara, B. L., Crotti, T. N., et al. (2006). "Cloning and characterization of osteoclast precursors from the RAW264.7 cell line." In Vitro Cell Dev Biol Anim **42**(7): 182-188.

Cumming, G., Fidler, F., et al. (2007). "Error bars in experimental biology." J Cell Biol **177**(1): 7-11.

Davis, V. L., Couse, J. F., Gray, T. K., Korach, K. S. (1994). "Correlation between low levels of estrogen receptors and estrogen responsiveness in two rat osteoblast-like cell lines." J Bone Miner Res **9**(7): 983-991.

de Villiers, T. J. (2009). "Bone health and osteoporosis in postmenopausal women." Best Pract Res Clin Obstet Gynaecol **23**(1): 73-85.

Del Rio, D., Calani, L., et al. (2010). "Bioavailability and catabolism of green tea flavan-3-ols in humans." Nutrition **26**(11-12): 1110-1116.

Deng, H. W. L., Y. Z. (2005). Current topics in bone biology. Hackensack, NJ, World Scientific.

Dietel, M. (2010). "Hormone replacement therapy (HRT), breast cancer and tumor pathology." Maturitas **65**(3): 183-189.

Dixon, R. A. and Ferreira, D. (2002). "Genistein." Phytochemistry **60**(3): 205-211.

Douglas, D. J., Frank, A. J., et al. (2005). "Linear ion traps in mass spectrometry." Mass Spectrom Rev **24**(1): 1-29.

Ducy, P., Karsenty, G. (1995). "Two distinct osteoblast-specific cis-acting elements control expression of a mouse osteocalcin gene." Mol Cell Biol **15**(4): 1858-1869.

Ducy, P., Zhang, R., et al. (1997). "Osf2/Cbfa1: A transcriptional activator of osteoblast differentiation." Cell **89**(5): 747-754.

Dutertre, M. and Smith, C. L. (2000). "Molecular mechanisms of selective estrogen receptor modulator (SERM) action." J Pharmacol Exp Ther **295**(2): 431-437.

Eastell, R. and Hannon, R. A. (2008). "Biomarkers of bone health and osteoporosis risk." Proc Nutr Soc **67**(2): 157-162.

Ek-Rylander, B., Flores, M., et al. (1994). "Dephosphorylation of osteopontin and bone sialoprotein by osteoclastic tartrate-resistant acid phosphatase. Modulation of osteoclast adhesion in vitro." J Biol Chem **269**(21): 14853-14856.

Enmark, E. and Gustafsson, J. A. (1999). "Oestrogen receptors - an overview." J Intern Med **246**(2): 133-138.

Ermer, J. (2005). Analytical Validation within the Pharmaceutical Environment. Method Validation in Pharmaceutical Analysis. J. E. J. H. M. Miller. UK, Willey-VCH.

Ernst, M., Heath, J. K., et al. (1989). "Estradiol effects on proliferation, messenger ribonucleic acid for collagen and insulin-like growth factor-I, and parathyroid hormone-stimulated adenylate cyclase activity in osteoblastic cells from calvariae and long bones." Endocrinology **125**(2): 825-833.

Ferguson, V. L., Ayers, R. A., et al. (2003). "Bone development and age-related bone loss in male C57BL/6J mice." Bone **33**(3): 387-398.

Franceschi, R. T., Ge, C. X., et al. (2009). "Transcriptional Regulation of Osteoblasts." Cells Tissues Organs **189**(1-4): 144-152.

Fu, T., Liang, J., Han, G., Lv, L., Li, N. (2008). "Simultaneous determination of the major active components of tea polyphenols in rat plasma by a simple and specific HPLC assay." J Chromatogr B Analyt Technol Biomed Life Sci **875**(2): 363-367.

Garnero, P. (2009). "Bone markers in osteoporosis." Current Osteoporosis Reports **7**: 84-90.

Glasier, A. (2006). "HRT and breast cancer." Women's Health Medicine **3**(1): 54.

Goodin, M. G., Fertuck, K. C., et al. (2002). "Estrogen receptor-mediated actions of polyphenolic catechins in vivo and in vitro." Toxicol Sci **69**(2): 354-361.

Gray, T. K., Flynn, T. C., et al. (1987). "17 beta-estradiol acts directly on the clonal osteoblastic cell line UMR106." Proc Natl Acad Sci U S A **84**(17): 6267-6271.

Grier, S. J., Turner, A. S., et al. (1996). "The use of dual-energy x-ray absorptiometry in animals." Investigative Radiology **31**(1): 50-62.

Gross, J. (2011). Chemical Ionization. Mass Spectrometry, Springer-Verlag Berlin Heidelberg.

Gross, J. H. (2011). Practical Aspects of Electron Ionization. Mass Spectrometry, Springer**:** 223-248.

Guo, D., Wang, J., et al. (2011). "Double directional adjusting estrogenic effect of naringin from Rhizoma drynariae (Gusuibu)." J Ethnopharmacol **138**(2): 451-457.

Hadjidakis, D. J. and Androulakis, I. I. (2006). "Bone remodeling." <u>Women's Health and Disease: Gynecologic, Endocrine, and Reproductive Issues</u> **1092**: 385-396.

Harris, H. A., Bapat, A. R., et al. (2002). "The ligand binding profiles of estrogen receptors alpha and beta are species dependent." <u>Steroids</u> **67**(5): 379-384.

Hedaya, M. A. (2012). <u>Basic Pharmacokinetics</u>. US, CRC Press.

Hirata, M. M., C.; Takita, M.; Miyaura, C.; Inada, M. (2009). "Naringin Suppresses Osteoclasts Formation and Enhances bone Mass in Mice." <u>Journal of Health Science</u> **55**(3): 463-467.

Ho, Y., Lee, Y. L., et al. (1995). "Determination of (+)-catechin in plasma by high-performance liquid chromatography using fluorescence detection." <u>J Chromatogr B Biomed Appl</u> **665**(2): 383-389.

Hoang, Q. Q., Sicheri, F., et al. (2003). "Bone recognition mechanism of porcine osteocalcin from crystal structure." <u>Nature</u> **425**(6961): 977-980.

Hofstetter, B., Gamsjaeger, S., et al. (2012). "Effects of alendronate and risedronate on bone material properties in actively forming trabecular bone surfaces." <u>J Bone Miner Res</u> **27**(5): 995-1003.

Howell, A., Osborne, C. K., et al. (2000). "ICI 182,780 (Faslodex): development of a novel, "pure" antiestrogen." <u>Cancer</u> **89**(4): 817-825.

Hsieh, C. Y., Santell, R. C., et al. (1998). "Estrogenic effects of genistein on the growth of estrogen receptor-positive human breast cancer (MCF-7) cells in vitro and in vivo." <u>Cancer Res</u> **58**(17): 3833-3838.

Hsiu, S. L., Huang, T. Y., et al. (2002). "Comparison of metabolic pharmacokinetics of naringin and naringenin in rabbits." <u>Life Sci</u> **70**(13): 1481-1489.

Hsu, H., Lacey, D. L., et al. (1999). "Tumor necrosis factor receptor family member RANK mediates osteoclast differentiation and activation induced by osteoprotegerin ligand." Proc Natl Acad Sci U S A **96**(7): 3540-3545.

Hunter, G. K. and Goldberg, H. A. (1994). "Modulation of crystal formation by bone phosphoproteins: role of glutamic acid-rich sequences in the nucleation of hydroxyapatite by bone sialoprotein." Biochem J **302 (Pt 1)**: 175-179.

Ignar-Trowbridge, D. M., Nelson, K. G., et al. (1992). "Coupling of dual signaling pathways: epidermal growth factor action involves the estrogen receptor." Proc Natl Acad Sci U S A **89**(10): 4658-4662.

Janis, J. A., McCloskey, E. V., Jonansson, H., Oden, A., Strom, O., Borgstrom, F. (2010). "Development and use of FRAX(R) in osteoporosis." Osteoporosis Int. **21**(Supplement 2): 407-413.

Jean-Yves Reginster, N. B. (2006). "Osteoporosis: A still increasing prevalence." Bone **38**(2006): S4-S9.

Jeong, J. C., Lee, J. W., et al. (2004). "Drynariae Rhizoma promotes osteoblast differentiation and mineralization in MC3T3-E1 cells through regulation of bone morphogenetic protein-2, alkaline phosphatase, type I collagen and collagenase-1." Toxicol In Vitro **18**(6): 829-834.

Jeong, J. C., Lee, J. W., et al. (2005). "Stimulative effects of Drynariae Rhizoma extracts on the proliferation and differentiation of osteoblastic MC3T3-E1 cells." J Ethnopharmacol **96**(3): 489-495.

Jilka, R. L. (2003). "Biology of the basic multicellular unit and the pathophysiology of osteoporosis." Med Pediatr Oncol **41**(3): 182-185.

Johnstone, C. G. H. R. A. W. (2003). Mass Spectrometry Basics. US, CRC Press.

Jordan, V. C. and Morrow, M. (1999). "Tamoxifen, raloxifene, and the prevention of breast cancer." Endocr Rev **20**(3): 253-278.

Jozwiak, K. L., W. J. ; Wainer, I. W. (2012). Drug stereochemistry analytical methods and pharmacology, Informa Healthcare.

Kafui Kpegba, A. A., Ana G. Petrovic, Etchri Amouzou, Messanvi Gbeassor, Gloria Proni, and Basri Nesnas (2011). "Epiafzelechin from the Root Bark of Cassia sieberiana: Detection by DART Mass Spectrometry, Spectroscopic Characterization, and Antioxidant Properties." J Nat Prod **74**: 455-459.

Kalervo Vaananen H, Zhao, H.B (2006). Osteoclast Function: Biology and Mechanisms. Principle of Bone Biology. L. G. R. J. P. Bilezikian, T. J. Martin. USA, Academic Press. **1:** 193-209.

Kalu, D. N. (1991). "The ovariectomized rat model of postmenopausal bone loss." Bone Miner **15**(3): 175-191.

Kanellopoulos, A., Lenz, G., et al. (1998). "Stereoselective differences in the vasorelaxing effects of S(+) and R(-) ketamine on rat isolated aorta." Anesthesiology **88**(3): 718-724.

Karsenty, G. (2000). "Role of Cbfa1 in osteoblast differentiation and function." Semin Cell Dev Biol **11**(5): 343-346.

Kartsogiannis, V. and Ng, K. W. (2004). "Cell lines and primary cell cultures in the study of bone cell biology." Mol Cell Endocrinol **228**(1-2): 79-102.

Kasprzyk-Hordern, B. (2010). "Pharmacologically active compounds in the environment and their chirality." Chem Soc Rev. **39**: 4466-4503.

Kato, S., Endoh, H., Masuhiro, Y., Kitamoto, T., Uchiyama, S., Sasaki, H., Masushige, S., Gotoh, Y., Nishida, E., Kawashima, H., Metzger, D., Chambon, P. (1995). "Activation of the estrogen receptor through

phosphorylation by mitogen-activated protein kinase." Science **270**: 1491-1494.

Kazakevich, Y., Lobrutto, R. (2007). HPLC for pharmaceutical Scientists, John Wiley & Sons, Inc.

Kendler, D. L., Palacios, S., et al. (2012). "Arzoxifene versus raloxifene: effect on bone and safety parameters in postmenopausal women with osteoporosis." Osteoporos Int **23**(3): 1091-1101.

Khalid, O., Baniwal, S. K., et al. (2008). "Modulation of Runx2 activity by estrogen receptor-alpha: implications for osteoporosis and breast cancer." Endocrinology **149**(12): 5984-5995.

Khosla, S. (2001). "Minireview: the OPG/RANKL/RANK system." Endocrinology **142**(12): 5050-5055.

King, F. E., Clark-Lewis, J.W., Forbes, W.F. (1955). "The chemistry of extractives from hardwoods. Part XXV.(—)-epiAfzelechin, a new member of the catechin series." J. Chem. Soc: 2948-2956.

Klein-Nulend, J., Bonewald, L.F. (2006). The Osteocyte. Principles of Bone Biology. L. G. R. J. P. Bilezikian, T. J. Martin. USA, Academic Press. **1:** 153-174.

Ko, C. H., Lau, K. M., et al. (2009). "Effects of tea catechins, epigallocatechin, gallocatechin, and gallocatechin gallate, on bone metabolism." J Agric Food Chem **57**(16): 7293-7297.

Kpegba, K. A., A.; Petrovic, A. G.; Amouzou, E.; Gbeassor, M.; Proni, G.; Nesnas, B. (2011). "Epiafzelechin from the Root Bark of Cassia sieberiana: Detection by DART Mass Spectrometry, Spectroscopic Characterization, and Antioxidant Properties." Journal of Natural Products **74**: 455-459.

Kuiper, G. G., Carlsson, B., et al. (1997). "Comparison of the ligand binding specificity and transcript tissue distribution of estrogen receptors alpha and beta." Endocrinology **138**(3): 863-870.

Kuiper, G. G. and Gustafsson, J. A. (1997). "The novel estrogen receptor-beta subtype: potential role in the cell- and promoter-specific actions of estrogens and anti-estrogens." FEBS Lett **410**(1): 87-90.

Kushida, K. T., M; Kawana,K; Inoue, T. (1995). "Comparison of markers for bone formation and resorption in premenopausal and postmenopausal subjects, and osteoporosis patients." J Clin Endocrinol Metab **80**(8): 2447.

La, V. D., Tanabe, S., et al. (2009). "Naringenin inhibits human osteoclastogenesis and osteoclastic bone resorption." J Periodontal Res **44**(2): 193-198.

Lacey DL, T. E., Tan HL, Kelley MJ, Dunstan CR, Burgess T, Elliott R, Colombero A, Elliott G, Scully S, Hsu H, Sullivan J, Hawkins N, Davy E, Capparelli C, Eli A, Qian YX, Kaufman S, Sarosi I, Shalhoub V, Senaldi G, Guo J, Delaney J, Boyle WJ (1998). "Osteoprotegerin ligand is a cytokine that regulates osteoclast differentiation and activation." Cell **93**: 165-176.

Landis-Piwowar, K. R., Huo, C., et al. (2007). "A novel prodrug of the green tea polyphenol (-)-epigallocatechin-3-gallate as a potential anticancer agent." Cancer Res **67**(9): 4303-4310.

Lau, W. S., Chen, W. F., et al. (2009). "Mitogen-activated protein kinase (MAPK) pathway mediates the oestrogen-like activities of ginsenoside Rg1 in human breast cancer (MCF-7) cells." Br J Pharmacol **156**(7): 1136-1146.

Le Bail, J. C., Laroche, T., et al. (1998). "Aromatase and 17 beta-hydroxysteroid dehydrogenase inhibition by flavonoids." Cancer Letters **133**(1): 101-106.

Le Bail, J. C., Varnat, F., et al. (1998). "Estrogenic and antiproliferative activities on MCF-7 human breast cancer cells by flavonoids." <u>Cancer Letters</u> **130**(1-2): 209-216.

Lee, M. J., Prabhu, S., et al. (2000). "An improved method for the determination of green and black tea polyphenols in biomatrices by high-performance liquid chromatography with coulometric array detection." <u>Anal Biochem</u> **279**(2): 164-169.

Lee, M. J., Wang, Z. Y., et al. (1995). "Analysis of plasma and urinary tea polyphenols in human subjects." <u>Cancer Epidemiol Biomarkers Prev</u> **4**(4): 393-399.

Lee, M. S. (2002). <u>LC/MS applications in drug development</u>. New York, J. Wiley & Sones.

Li, X. H. X., .Z. L.; Lu, S.; Zhang, Y.; Li, F. M. (2010). "Pharmacokinetics of Naringin and its Metabolite Naringenin in Rats after Oral Administration of Rhizoma Drynariae Extract Assayed by UPLC-MS/MS." <u>Chinese Journal of Natural Medicines</u> **8(1)**(2010).

Li Xiao-Hong, X. Z.-L., Lu Shan, Zhang Yi, Li Fa-Mei (2010). "Pharmacokinetics of Naringin and its Metabolite Naringenin in Rats after Oral Administration of Rhizoma Drynariae Extract Assayed by UPLC-MS/MS." <u>Chinese Journal of Natural Medicines</u> **8(1)**(2010).

Liang, Y. H., Ye, M., et al. (2011). "Flavan-3-ols from the rhizomes of Drynaria fortunei." <u>Phytochemistry</u> **72**(14-15): 1876-1882.

Lin, R. W., Chen, C. H., et al. (2009). "(-)-Epigallocatechin gallate inhibition of osteoclastic differentiation via NF-kappaB." <u>Biochem Biophys Res Commun</u> **379**(4): 1033-1037.

Liu, S. L. and Lebrun, C. M. (2006). "Effect of oral contraceptives and hormone replacement therapy on bone mineral density in premenopausal and perimenopausal women: a systematic review." Br J Sports Med **40**(1): 11-24.

Lloyd R. Snyder, J. J. K. J. W. D. (2010). Introduction to Modern Liquid Chromatography, John Wiley & Sons, Inc.

Lobrutto, Y. K. R. (2007). HPLC for pharmaceutical Scientists, John Wiley & Sons.

Loizou, K. M. R. C. G. D. (2011). "A work flow for global sensitivity analysis of PBPK models." Frontiers in Pharmacology **2**: 1-22.

Maggi, A. (2011). "Liganded and unliganded activation of estrogen receptor and hormone replacement therapies." Biochim Biophys Acta **1812**(8): 1054-1060.

Manzano, M., Lozano, D., et al. (2011). "Comparison of the osteoblastic activity conferred on Si-doped hydroxyapatite scaffolds by different osteostatin coatings." Acta Biomater **7**(10): 3555-3562.

Martin-Badosa, E., Amblard, D., et al. (2003). "Excised bone structures in mice: Imaging at three-dimensional synchrotron radiation micro CT." Radiology **229**(3): 921-928.

Matuszewski, B. K., Constanzer, M. L., et al. (2003). "Strategies for the assessment of matrix effect in quantitative bioanalytical methods based on HPLC-MS/MS." Anal Chem **75**(13): 3019-3030.

McMaster, M. C. (1994). HPLC - A Practical User's Guide, VCH Publishers, Inc.

McMASTER, M. C. (2005). LC/MS A practical user's guide. US, John Wiley & Sons, Inc.

McNally, K., Cotton, R., et al. (2011). "A Workflow for Global Sensitivity Analysis of PBPK Models." Front Pharmacol **2**: 31.

Merriman, H. L., Vanwijnen, A. J., et al. (1995). "The Tissue-Specific Nuclear Matrix Protein, Nmp-2, Is a Member of the Aml/Cbf/Pebp2/Runt Domain Transcription Factor Family - Interactions with the Osteocalcin Gene Promoter." Biochemistry **34**(40): 13125-13132.

Miksicek, R. J. (1995). "Estrogenic Flavonoids - Structural Requirements for Biological-Activity." Proceedings of the Society for Experimental Biology and Medicine **208**(1): 44-50.

Miller, J. E. J. H. M. (2005). Method Validation in Pharmaceutical Analysis: A Guide to Best Practice, Wiley-VCH.

Mok, S. K., Chen, W. F., et al. (2010). "Icariin protects against bone loss induced by oestrogen deficiency and activates oestrogen receptor-dependent osteoblastic functions in UMR 106 cells." Br J Pharmacol **159**(4): 939-949.

Moonga, B. S., Moss, D. W., et al. (1990). "Intracellular regulation of enzyme secretion from rat osteoclasts and evidence for a functional role in bone resorption." J Physiol **429**: 29-45.

Motrescu, I. O., S.; Rapa, A.; Airinei, A. (2006). "Spectrophotometric Analysis of the Blood Plasma for Different Mammals." Romanian J. Biophys **16**(3): 215-220.

Neffling, M. R., Spoof, L., et al. (2010). "LC-ESI-Q-TOF-MS for faster and accurate determination of microcystins and nodularins in serum." J Chromatogr B Analyt Technol Biomed Life Sci **878**(26): 2433-2441.

Nilsson, S., Makela, S., et al. (2001). "Mechanisms of estrogen action." Physiol Rev **81**(4): 1535-1565.

Oddie, G. W., Schenk, G., et al. (2000). "Structure, function, and regulation of tartrate-resistant acid phosphatase." Bone **27**(5): 575-584.

Pacifici, R. (2008). Mechanisms of Estrogen Action in Bone. <u>Principles of Bone Biology</u>. L. G. R. John P. Bilezikian, T. John Martin. UK, Academic Press. **One:** 921-933.

Pan, H. Y., Liu, D. L., et al. (1991). "[Determination of D-catechin plasma concentration and pharmacokinetic parameters using HPLC method]." <u>Yao Xue Xue Bao</u> **26**(5): 371-374.

Pang, W. Y. (2010). <u>Modern approach to study the osteoprotective effect of Rhizoma Drynariae</u>. Master of Philosophy The Hong Kong Polytechnic University.

Pang, W. Y., Wang, X. L., et al. (2010). "Naringin improves bone properties in ovariectomized mice and exerts oestrogen-like activities in rat osteoblast-like (UMR-106) cells." <u>Br J Pharmacol</u> **159**(8): 1693-1703.

Pang, W. Y., Wang, X.L., Wong, K.C., Leung, P.C., Yao, X.S., Wong, M.S. (2012). " Total flavonoid fraction of Rhizoma Drynaria improves bone properties in ovariectomized mice and exerts estrogen-like activities in rat osteoblast-like (UMR-106) cells." <u>J Food Drug Ana</u> **20**(1): 265-269.

Pang, W. Y., Wang, X.L., Mok, S.K., Lai, W.P., Chow, H.K., Yao, X.S., Leung, P.C., Wong, M.S. (2010). "Naringin activates estrogen receptor ligand-independently in rat osteoblast-like (UMR 106) cells and improves bone properties in ovariectomized mice." <u>Br J Pharmacol</u> **159**: 1693-1703.

Pang WY, W. X., Mok SK, Lai WP, Chow HK, Yao XS, Leung PC, Wong MS. (2010). "Naringin activates estrogen receptor ligand-independently in rat osteoblast-like (UMR 106) cells and improves bone properties in ovariectomized mice." <u>Br J Pharmacol</u> **159**: 1693-1703.

Patel, B. K., Hutt, A. J. (2004). Chirality in Drug Design and Development. Stereoselectivity in Drug Action and Disposition: An Overview. I. K. R. a. R. Mehvar, CRC Press.

Pham-Huy, C., Radenen, B., et al. (1995). "High-performance liquid chromatographic determination of (S)- and (R)-propranolol in human plasma and urine with a chiral beta-cyclodextrin bonded phase." J Chromatogr B Biomed Appl **665**(1): 125-132.

PHARMACOKINETICS, A. w. g. (2004). Collection of terms, symbols, equations, and explanations of common pharmacokinetic and pharmacodynamic parameters and some statistical functions.

Preast, H. X. a. V. (2010). Xie's Chinese Veterinary Herbology. USA, Willey-Blackwell.

Quarles, L. D., Yohay, D. A., et al. (1992). "Distinct proliferative and differentiated stages of murine MC3T3-E1 cells in culture: an in vitro model of osteoblast development." J Bone Miner Res **7**(6): 683-692.

Rahmani, R. M., S. (2009). "Preventation of osteoporosis-related fractures among postmenopausal women and older men." Canadian Medical Association Journal **181**(11).

Rister, R. (1999). Japanese herbal medicine: the healing art of kampo. Avery Publisher.

Rivas, A. L., M.; Olea-Serrano, F.; Laios, I.; Leclercq, G.; Olea, N. (2002). "Estrogenic effect of a series of bisphenol analogues on gene and protein expression in MCF-7 breast cancer cells." J Steroid Biochem Mol Biol **82**(1): 45-53.

Santos, N. C., Figueira-Coelho, J., et al. (2003). "Multidisciplinary utilization of dimethyl sulfoxide: pharmacological, cellular, and molecular aspects." Biochem Pharmacol **65**(7): 1035-1041.

Scheid, V. (2007). "Traditional Chinese medicine - What are we investigating? The case of menopause." Complementary Therapies in Medicine **15**(1): 54-68.

Silberberg, M., Morand, C., et al. (2005). "Co-administration of quercetin and catechin in rats alters their absorption but not their metabolism." Life Sci **77**(25): 3156-3167.

Silverman, S. L. (2001). "Calcitonin." Rheumatic Diseases Clinics of North America **27**(1): 187-196.

Simonet, W. S., Lacey, D. L., et al. (1997). "Osteoprotegerin: a novel secreted protein involved in the regulation of bone density." Cell **89**(2): 309-319.

Siris, E. S., Boonen, S., Mitchell, P. J., Bilezikian, J., Silverman, S. (2012). "what's in a name? What constitutes the clinical diagnosis of osteoporosis?" Osteoporos Int **23**(8): 2093-2097.

Smith, J. C. F. R. B. (1987). "Compartmental Model Analysis in Pharmacokinetics." J Clin Pharmacol **27**(12): 922-926.

Su, B. N., Cuendet, M., et al. (2002). "Constituents of the bark and twigs of Artocarpus dadah with cyclooxygenase inhibitory activity." J Nat Prod **65**(2): 163-169.

Sun, J. S., Dong, G. C., et al. (2003). "The effect of Gu-Sui-Bu (Drynaria fortunei J. Sm) immobilized modified calcium hydrogenphosphate on bone cell activities." Biomaterials **24**(5): 873-882.

Sun, J. S., Lin, C. Y., et al. (2002). "The effect of Gu-Sui-Bu (Drynaria fortunei J. Sm) on bone cell activities." Biomaterials **23**(16): 3377-3385.

Svobaite, R., Solassol, I., et al. (2008). "HPLC with UV or mass spectrometric detection for quantifying endogenous uracil and dihydrouracil in human plasma." Clin Chem **54**(9): 1463-1472.

Szabo, G. K., Browne, H. K., et al. (1994). "Alternatives to least squares linear regression analysis for computation of standard curves for quantitation by high performance liquid chromatography: applications to clinical pharmacology." J Clin Pharmacol **34**(3): 242-249.

Tamir, S., Eizenberg, M., et al. (2000). "Estrogenic and antiproliferative properties of glabridin from licorice in human breast cancer cells." Cancer Research **60**(20): 5704-5709.

Turner, A. S. (2001). "Animal models of osteoporosis--necessity and limitations." Eur Cell Mater **1**: 66-81.

Turner, R. T. R., D. J.; Iwaniec, U. T.; Spelsberg, T. C. (2008). Estrogen and Progestins.

Umegaki, K., Sugisawa, A., et al. (2001). "Analytical method of measuring tea catechins in human plasma by solid-phase extraction and HPLC with electrochemical detection." J Nutr Sci Vitaminol (Tokyo) **47**(6): 402-408.

Vaya, J. and Tamir, S. (2004). "The relation between the chemical structure of flavonoids and their estrogen-like activities." Curr Med Chem **11**(10): 1333-1343.

Vessman, J. (1996). "Selectivity or specificity? Validation of analytical methods from the perspective of an analytical chemist in the pharmaceutical industry." J Pharm Biomed Anal **14**(8-10): 867-869.

Vincent, C., Kogawa, M., Findlay, D. M., Atkins, G. J. (2009). "The generation of osteoclasts from RAW 264.7 precursors in defined, serum-free conditions." J Bone Miner Metab **27**(1): 114-119.

Wakeling, A. E., Dukes, M., et al. (1991). "A potent specific pure antiestrogen with clinical potential." Cancer Res **51**(15): 3867-3873.

Wan, S. B. and Chan, T. H. (2004). "Enantioselective synthesis of afzelechin and epiafzelechin." Tetrahedron **60**(37): 8207-8211.

Wang, C. Y., Li, Q. S., Han, G. Z., Zou, L. L., Li, L.V., Zhou, Q. , Li, N. (2010). "LC-MS/MS for Simultaneous Determination of Four Major Active Catechins of Tea Polyphenols in Rat Plasma and Its Application to Pharmacokinetics." Chinese Herbal Medicines **2**(4): 289-296.

Wang, D., Christensen, K., et al. (1999). "Isolation and characterization of MC3T3-E1 preosteoblast subclones with distinct in vitro and in vivo differentiation/mineralization potential." J Bone Miner Res **14**(6): 893-903.

Wang, X., Zhen, L., et al. (2011). "Osteogenic effects of flavonoid aglycones from an osteoprotective fraction of Drynaria fortunei--an in vitro efficacy study." Phytomedicine **18**(10): 868-872.

Wang, X. L., Wang, N. L., et al. (2008). "Effects of eleven flavonoids from the osteoprotective fraction of Drynaria fortunei (KUNZE) J. SM. on osteoblastic proliferation using an osteoblast-like cell line." Chem Pharm Bull (Tokyo) **56**(1): 46-51.

Wei, Y. J., Tsai, K. S., et al. (2011). "Catechin stimulates osteogenesis by enhancing PP2A activity in human mesenchymal stem cells." Osteoporos Int **22**(5): 1469-1479.

Wermuth, C. G. (2008). Optical Isomerism in Drugs. <u>The practice of medicinal chemistry</u>. C. G. Wermuth, Academic Press.

Westendorf, J. J., Kahler, R. A., et al. (2004). "Wnt signaling in osteoblasts and bone diseases." <u>Gene</u> **341**: 19-39.

Wong, K. C. P., W.Y.; Wang, X.L.; Mok, S.K.; Lai, W.P.; Chow, H.K.; Leung, P.C.; Yao, X.S; Wong, M.S. (2013). "Drynaria fortunei derived total flavonoid fraction and isolated compounds exert oestrogen-like protective effects in bone." <u>Br J Nutr</u> **10**: 1-11.

Wong, R. W. and Rabie, A. B. (2006). "Effect of naringin collagen graft on bone formation." <u>Biomaterials</u> **27**(9): 1824-1831.

Xiao, G., Jiang, D., et al. (2000). "MAPK pathways activate and phosphorylate the osteoblast-specific transcription factor, Cbfa1." <u>J Biol Chem</u> **275**(6): 4453-4459.

Xie, Y. (2004). Drynaria Extractions for Treating Osteoporosis and their Extraction Process. <u>Patent Application Publication</u>. **US2004/0048811 A1**.

Xing, L. and Remick, D. G. (2005). "Mechanisms of dimethyl sulfoxide augmentation of IL-1 beta production." <u>Journal of Immunology</u> **174**(10): 6195-6202.

Yanquan, P. Z. (2003). "Understanding Kidney Yin and Kidney Yang." Retrieved 10Jan, 2012, from http://www.shen-nong.com/eng/principles/kidneyyinyang.html.

Yin, P. W. (2007). <u>Modern approach to study the osteoprotectie effect of Rhizoma Drynariae</u>. Master of Philosophy, The Hong Kong Polytechnic University.

Yuan, C. S. B., E. J.; Bauer, B. A. (2011). <u>Traditional Chinese medicine</u>. London, Informa Healthcare.

Zhang, P., Dai, K. R., et al. (2009). "Effects of naringin on the proliferation and osteogenic differentiation of human bone mesenchymal stem cell." Eur J Pharmacol **607**(1-3): 1-5.

Zhang, Q. H., Wang, W. B., et al. (2012). "Simultaneous determination of catechin, epicatechin and epicatechin gallate in rat plasma by LC-ESI-MS/MS for pharmacokinetic studies after oral administration of Cynomorium songaricum extract." J Chromatogr B Analyt Technol Biomed Life Sci **880**(1): 168-171.

Zhang, Y. W., M. S.; Wu, C. F. (2006). "Anti-osteoporotic Effects of Medicinal Herbs and their Mechanisms of Action." Asian Journal of Traditional Medicines **1**: 3-4.

Zuo, C., Huang, Y., et al. (2012). "Osteoblastogenesis regulation signals in bone remodeling." Osteoporos Int **23**(6): 1653-1663.